



**Flanders**  
State of  
the Art

14\_024\_11  
FHR reports

# Agenda for the future - Hydrodynamics and Sediment Dynamics in the Schelde Estuary

Sub report 11  
Factual data report for frame-measurements at  
Drepel van Frederik in December 2015 and January 2016

DEPARTMENT  
MOBILITY &  
PUBLIC  
WORKS

[www.flandershydraulicsresearch.be](http://www.flandershydraulicsresearch.be)

# Agenda for the future - Hydrodynamics and Sediment Dynamics in the Schelde Estuary

Sub report 11 - Factual data report for frame-measurements at Drempeel van Frederik in December 2015 and January 2016

Vandebroek, E.; Claeys, S.; Plancke, Y.; Verwaest, T.; Mostaert, F.

Legal notice

Flanders Hydraulics Research is of the opinion that the information and positions in this report are substantiated by the available data and knowledge at the time of writing.  
 The positions taken in this report are those of Flanders Hydraulics Research and do not reflect necessarily the opinion of the Government of Flanders or any of its institutions.  
 Flanders Hydraulics Research nor any person or company acting on behalf of Flanders Hydraulics Research is responsible for any loss or damage arising from the use of the information in this report.

Copyright and citation

© The Government of Flanders, Department of Mobility and Public Works, Flanders Hydraulics Research 2017  
 D/2017/3241/256

This publication should be cited as follows:

**Vandebroek, E.; Claeys, S.; Plancke, Y.; Verwaest, T.; Mostaert, F.** (2017). Agenda for the future - Hydrodynamics and Sediment Dynamics in the Schelde Estuary: Sub report 11 - Factual data report for frame-measurements at Drempeel van Frederik in December 2015 and January 2016. Version 3.0. FHR Reports, 14\_024\_11. Flanders Hydraulics Research & Antea Group: Antwerp.

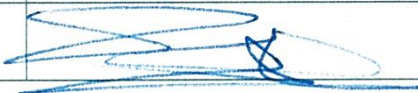
Reproduction of and reference to this publication is authorised provided the source is acknowledged correctly.

Document identification

Customer:	Vlaams Nederlandse Scheldec commissie (VNSC)	Ref.:	WL2017R14_024_11
Keywords (3-5):	Schelde estuary, hydrodynamics, sediment transport, monitoring		
Text (p.):	75	Appendices (p.):	5
Confidentiality:	<input checked="" type="checkbox"/> No	<input checked="" type="checkbox"/> Available online	

Author(s):	Vandebroek, E.; Plancke, Y.
------------	-----------------------------

Control

	Name	Signature
Reviser(s):	Claeys, S.	
Project leader:	Plancke, Y.	

Approval

Coordinator research group:	Verwaest, T.	
Head of Division:	Mostaert, F.	

## Abstract

Within the framework of the cross-border Flemish-Dutch research program, Agenda for the Future (Agenda voor de Toekomst), field measurements were performed at a number of strategic locations along the Schelde. This report describes a December 2015/January 2016 field campaign to measure hydrodynamics and sediment transport near the sill of Frederik (Drempel van Frederik).

Two measurement frames consisting of a down-looking Aquadopp, up-looking AWAC, OBS 3+ and a YSI were placed on the bed and left to measure currents and sediment concentrations over a period of six weeks. In order to estimate sediment transport rates using the acoustic backscatter of the ADCP's and the optical backscatter, two 6-hour calibration campaigns were conducted on January 29<sup>th</sup> and February 5<sup>th</sup>. During the calibration, currents, suspended sediment concentration, sediment transport, and grain size were measured using two Aquadopps, a LISST-100X, both OBS 3+ sensors, the YSI, and by collecting water samples for lab analysis.

The Aquadopp and AWAC data were calibrated and combined (using interpolation in the gap between) to produce a time series of currents and sediment transport for the six week period. This report presents the measurement techniques, calibration methods, and summary of results (including ambient conditions). Accompanying this report are time series of hydrodynamic and sediment transport measurements from the two frames. The results from this campaign (and others) are being used to calibrate and validate numerical models, the results of which will be described in a later report.



# Contents

Abstract .....	III
Contents .....	V
List of tables.....	VII
List of figures .....	VIII
1 Introduction.....	1
1.1 Report Organization .....	1
1.2 Acknowledgements .....	1
2 Overview of the Measurement Campaign .....	2
2.1 Ambient Conditions .....	2
2.2 Measurement Frames.....	4
2.2.1 Frame Locations and Set-up .....	4
2.2.2 Aquadopp Profilers (ADP) .....	4
2.2.3 Acoustic Wave and Current Profiler (AWAC).....	7
2.2.4 Turbidity Sensor (OBS 3+) .....	8
2.2.5 YSI.....	9
2.3 6-Hour Calibration Measurements.....	10
2.3.1 Configuration .....	11
2.3.2 Currents .....	13
2.3.3 Suspended sediment concentrations (SSC) .....	13
2.3.4 Grain size distribution.....	15
3 Post-Processing.....	16
3.1 Locating instruments relative to each other based on water depth.....	16
3.2 Sediment Concentration from Acoustic Backscatter.....	18
3.2.1 Step 1: Convert internal units to a linear or log scale.....	18
3.2.2 Step 2: Range normalization .....	18
3.2.3 Step 3: Develop calibration curve relating ABS to SSC .....	21
3.2.4 Step 4: Apply the calibration curve to the long-term measurement frames .....	21
3.3 Calibrating the AWAC using Aquadopp data .....	22
3.3.1 Method 1: Apply the Aquadopp calibration to the AWAC (with a shift).....	22
3.3.2 Method 2: Estimate SSC in AWAC cell 1 by applying a Rouse profile to the Aquadopp SSC.....	24
3.3.3 Apply the calibration curve to the long-term measurement frames .....	31

3.4	Sediment Concentration from YSI and OBS 3+ sensors.....	31
3.5	Sediment Concentration from LISST-100X Volume Concentration.....	33
3.6	Combining AWAC and Aquadopp profiles.....	34
3.6.1	Aquadopp Profilers (ADP).....	<b>Fout! Bladwijzer niet gedefinieerd.</b>
3.6.2	Velocity magnitude and direction.....	35
3.6.3	Suspended sediment concentration (SSC).....	37
3.7	Sediment Transport Rate.....	37
4	Results: Stationary 6-hr Calibration Campaigns.....	38
4.1	Water levels.....	38
4.2	Currents.....	38
4.3	Suspended sediment concentration (SSC).....	41
4.4	Grain size distribution.....	42
5	Results: Measurement Frames.....	45
5.1	Ambient Conditions.....	45
5.1.1	Wind.....	45
5.1.2	Water Levels.....	46
5.2	Currents.....	46
5.3	Sediment Transport.....	61
6	References.....	75
7	Appendices.....	1
7.1	Appendix A – Aquadopp Profiler Technical Specifications.....	1
7.2	Appendix B – AWAC Technical Specifications.....	2
7.3	Appendix C – OBS 3+ Technical Specifications.....	3
7.4	Appendix D – LISST-100X Technical Specifications.....	4
7.5	Appendix E – YSI Technical Specifications.....	5

## List of tables

Table 1. Tidal datums at the Bath station (nearest to the present campaign) .....	3
Table 2. Summary of monitoring equipment for campaign 1 at Drempel van Frederik .....	4
Table 3. Aquadopp Current Profiler technical specifications from the manufacturer (Nortek) .....	6
Table 4. AWAC technical specifications from the manufacturer (Nortek).....	8
Table 5. OBS 3+-3+ technical specifications from the manufacturer (Campbell Scientific).....	9
Table 6. YSI 6-Series technical specifications from the manufacturer. ....	10
Table 7. Summary of calibration campaigns .....	10
Table 8. Number of water samples (and grain size) analyzed during calibration campaigns .....	14
Table 9. Aquadopp and AWAC parameters used to develop Rouse profile.....	25
Table 10. Calibration coefficients for AWAC SSC to ABS exponential relationship.....	26

## List of figures

Figure 1. Map of measurement frame and calibration campaign locations at Drempeel van Frederik. Location for HYLAS I is approximate. Map on the right also shows active dredge and disposal zones.....	2
Figure 2. Rijkswaterstaat water level monitoring locations in the Westerschelde. Wind and water level data are available at the PROS station .....	3
Figure 3. Drawing of HYLAS I measurement frame with instrument heights above the bed. HYLAS I had the vertical Aquadopp .....	5
Figure 4. Photo of HYLAS II measurement frame. HYLAS II had the horizontal Aquadopp.....	5
Figure 5. Aquadopp Profiler dimensions (left, mm), conceptual diagram (middle), and reference coordinate system (right).....	7
Figure 6. AWAC dimensions (top, mm), conceptual diagram (bottom left), and reference coordinate system (bottom right).....	7
Figure 7. OBS 3+-3+ dimensions (left), conceptual diagram (right) .....	9
Figure 8. Dredging data for day 2 of the calibration campaign.....	11
• Figure 9. Calibration frame set-up with measurements .....	12
Figure 10. Calibration setup .....	12
Figure 11. Photos of (left) Aquadopp and (right) LISST-100X calibration frames .....	13
Figure 12. Left) Overview LISST-100X, Middle) detail of the transmit and receive windows for the light beam, Right) example of a PRM .....	14
Figure 13. Malvern Mastersizer 2000.....	15
Figure 14. Instrument depth below water surface, calibration day 1.....	17
Figure 15. Instrument depth below water surface, calibration day 2.....	17
Figure 16. Absorption in water vs. frequency for fresh and salt water.....	19
Figure 17. Absorption of sound in the water column for various frequencies.....	19
Figure 18. Normalized acoustic backscatter (in dB) and LISST-100X volume concentration (in $\mu\text{l/l}$ ) during day 1 (29/1/2016) of the calibration campaign .....	20
Figure 19. Normalized acoustic backscatter (in dB) and LISST-100X volume concentration (in $\mu\text{l/l}$ ) during day 2 (5/2/2016) of the calibration campaign .....	20
Figure 20. Aquadopp acoustic backscatter (from both Aquadopps) calibration to suspended sediment concentration .....	21
Figure 21. Comparison of cell 1 of the down-facing Aquadopp and up-facing AWAC for HYLAS I and II .....	23
Figure 22. Rouse profiles for various N (z in the figure) values.....	24
Figure 23. Histogram of Rouse numbers estimated for each timestep of the Aquadopp data. Median N = 0,042.....	26
Figure 24. Calibration between range-normalized ABS in cell 1 of the AWAC and SSC predicted using a Rouse profile (HYLAS I) .....	27

Figure 25. Calibration between range-normalized ABS in cell 1 of the AWAC and SSC predicted using a Rouse profile (HYLAS II) ..... 27

Figure 26. Calibration between range-normalized ABS in cell 1 of the AWAC and SSC predicted using a Rouse profile (HYLAS I) ..... 28

Figure 27. Calibration between range-normalized ABS in cell 1 of the AWAC and SSC predicted using a Rouse profile (HYLAS I) ..... 28

Figure 28. Calibration between range-normalized ABS in cell 1 of the AWAC and SSC predicted using a Rouse profile (HYLAS II) ..... 29

Figure 29. Calibration between range-normalized ABS in cell 1 of the AWAC and SSC predicted using a Rouse profile (HYLAS II) ..... 29

Figure 30. Colors indicate how ebb/flood and above/below threshold elevation (top) and depth-averaged velocity (bottom) were identified based on the water level and depth-averaged velocity..... 30

Figure 31. Threshold depth-averaged velocity to initiate movement, by particle size and water depth, according to Jarocki 1963..... 30

Figure 32. Comparison of SSC in cell 1 of the AWAC derived from Method 1 and Method 2 (HYLAS I)..... 31

Figure 33. Calibration fit for OBS 3+ counts to sample suspended sediment concentrations (HYLAS I and II) ..... 32

Figure 34. Calibration fit for YSI turbidity to sample suspended sediment concentrations (HYLAS II only) ... 32

Figure 35. Calibration fit for LISST-100X volume concentration to sample suspended sediment concentration ..... 33

Figure 36. Sediment grain size as related to suspended sediment concentration ..... 34

Figure 37. Examples of (left) log interpolation between measured AWAC and Aquadopp velocity, (middle) Rouse profile extrapolation of Aquadopp velocities, and (right) transport rate calculation in the gap (black circles) based on the magnitude and SSC..... 36

Figure 38. Example of velocity profile over time. (top) velocity magnitude, including interpolated area. (bottom) velocity direction, with gap. Velocity magnitude varies much more than direction over the vertical profile ..... 36

Figure 39. Water levels during the two days of 6-hour calibration measurements ..... 38

Figure 40. Depth-averaged currents as measured by the up-looking Aquadopp during the first calibration campaign on 29-1-2016..... 39

Figure 41. Instrument orientation recorded by the Aquadopp during the first calibration campaign on 29-1-2016..... 40

Figure 42. Depth-averaged currents as measured by the up-looking Aquadopp during the second calibration campaign on 5-2-2016..... 40

Figure 43. Suspended sediment concentrations as measured by the LISST-100X, Aquadopp, OBSs, and YSI during day 1 (29/1/2016), calibrated using the intermittent water samples (black circles/Xs). Aquadopp measurements are for the first cell of the down-looking Aquadopp..... 41

Figure 44. Suspended sediment concentrations as measured by the LISST-100X, Aquadopp, and OBSs during day 2 (5/2/2016), calibrated using the intermittent water samples (black circles/Xs). No YSI data was recorded on day 2. Aquadopp measurements are for the first cell of the down-looking Aquadopp..... 42

Figure 45. Median grain size (D50) and sand fraction (% >63  $\mu\text{m}$ ) in time as measured by water samples and the LISST-100X on day 1 of the calibration campaign ..... 43

Figure 46. Median grain size (D50) and sand fraction (% >63 $\mu\text{m}$ ) in time as measured by water samples and the LISST-100X on day 2 of the calibration campaign .....	44
Figure 47. Median grain size (D50) and sand fraction (% >63 $\mu\text{m}$ ) in time as measured by water samples and the LISST-100X on day 2 of the calibration campaign, zoomed into 120 to 200 minutes after high water ...	44
Figure 48. Wind conditions at the PROS station during campaign #1 at Schaar Ouden Doel (top: December 2015, bottom: January 2016) .....	45
Figure 49. Water levels at the PROS station during campaign #1 at Schaar Ouden Doel.....	46
Figure 50. Depth averaged magnitude, direction, and water levels (as measured by the ADCP) for frame HYLAS I, weeks 1 and 2 .....	47
Figure 51. Depth averaged magnitude, direction, and water levels (as measured by the ADCP) for frame HYLAS I, weeks 3 and 4.....	48
Figure 52. Depth averaged magnitude, direction, and water levels (as measured by the ADCP) for frame HYLAS I, weeks 5 and 6.....	49
Figure 53. Depth averaged magnitude, direction, and water levels (as measured by the ADCP) for frame HYLAS II, weeks 1 and 2.....	50
Figure 54. Depth averaged magnitude, direction, and water levels (as measured by the ADCP) for frame HYLAS II, weeks 3 and 4.....	51
Figure 55. Depth averaged magnitude, direction, and water levels (as measured by the ADCP) for frame HYLAS II, weeks 5 and 6.....	52
Figure 56. Current magnitude and direction for frame HYLAS I, weeks 1 and 2.....	53
Figure 57. Current magnitude and direction for frame HYLAS I, weeks 3 and 4.....	54
Figure 58. Current magnitude and direction for frame HYLAS I, weeks 5 and 6.....	55
Figure 59. Current magnitude and direction for frame HYLAS II, weeks 1 and 2.....	56
Figure 60. Current magnitude and direction for frame HYLAS II, weeks 3 and 4.....	57
Figure 61. Current magnitude and direction for frame HYLAS II, weeks 5 and 6.....	58
Figure 62. Depth averaged current magnitude for both frames HYLAS I & II, weeks 1 through 4 .....	59
Figure 63. Depth averaged current magnitude for both frames HYLAS I & II, weeks 5 and 6 .....	60
Figure 64. Suspended sediment concentration and sediment transport rate profiles and total sediment transport rate for HYLAS I frame, week 1.....	62
Figure 65. Suspended sediment concentration and sediment transport rate profiles and total sediment transport rate for HYLAS I frame, week 2.....	63
Figure 66. Suspended sediment concentration and sediment transport rate profiles and total sediment transport rate for HYLAS I frame, week 3.....	64
Figure 67. Suspended sediment concentration and sediment transport rate profiles and total sediment transport rate for HYLAS I frame, week 4.....	65
Figure 68. Suspended sediment concentration and sediment transport rate profiles and total sediment transport rate for HYLAS I frame, week 5.....	66
Figure 69. Suspended sediment concentration and sediment transport rate profiles and total sediment transport rate for HYLAS I frame, week 6.....	67
Figure 70. Suspended sediment concentration and sediment transport rate profiles and total sediment transport rate for HYLAS II frame, week 1.....	68

Figure 71. Suspended sediment concentration and sediment transport rate profiles and total sediment transport rate for HYLAS II frame, week 2..... 69

Figure 72. Suspended sediment concentration and sediment transport rate profiles and total sediment transport rate for HYLAS II frame, week 3..... 70

Figure 73. Suspended sediment concentration and sediment transport rate profiles and total sediment transport rate for HYLAS II frame, week 4..... 71

Figure 74. Suspended sediment concentration and sediment transport rate profiles and total sediment transport rate for HYLAS II frame, week 5..... 72

Figure 75. Suspended sediment concentration and sediment transport rate profiles and total sediment transport rate for HYLAS II frame, week 6..... 73



# 1 Introduction

One component of the 4-year collaborative research program “Agenda for the Future,” between Flanders and the Netherlands, is to improve hydrodynamic and sediment transport numerical models. Within the “mesoscale morphology” project, numerical models will be used to reproduce both sedimentation patterns at dredging locations (“sills”) and sediment transport patterns of disposed sediments at deeper parts of the navigation channels. Field measurements are necessary in order to calibrate and validate the improved models. Two field measurement campaigns were conducted in 2015-2016 at strategic locations in order to validate the numerical models.

This report describes measurements collected at Drempeel van Frederik in December 2015 and January 2016, including the data collection methods, post-processing, and brief interpretation of the results. Vandebroek et al. (2017) reports similar measurements carried out at Drempeel van Hansweert in April and May 2016.

## 1.1 Report Organization

Section 2 provides an overview of the data and methods used to describe ambient conditions (2.1), for the long-term frame measurements (2.2) and during the calibration campaigns (2.3). Section 3 describes how the data were post-processed, including how the 6-hour campaigns were used to calibrate the frame data. Section 4 presents time-series of the post-processed data collected during the 6-hour calibration campaigns. Section 5 presents the resulting time series of data from the measurement frames.

## 1.2 Acknowledgements

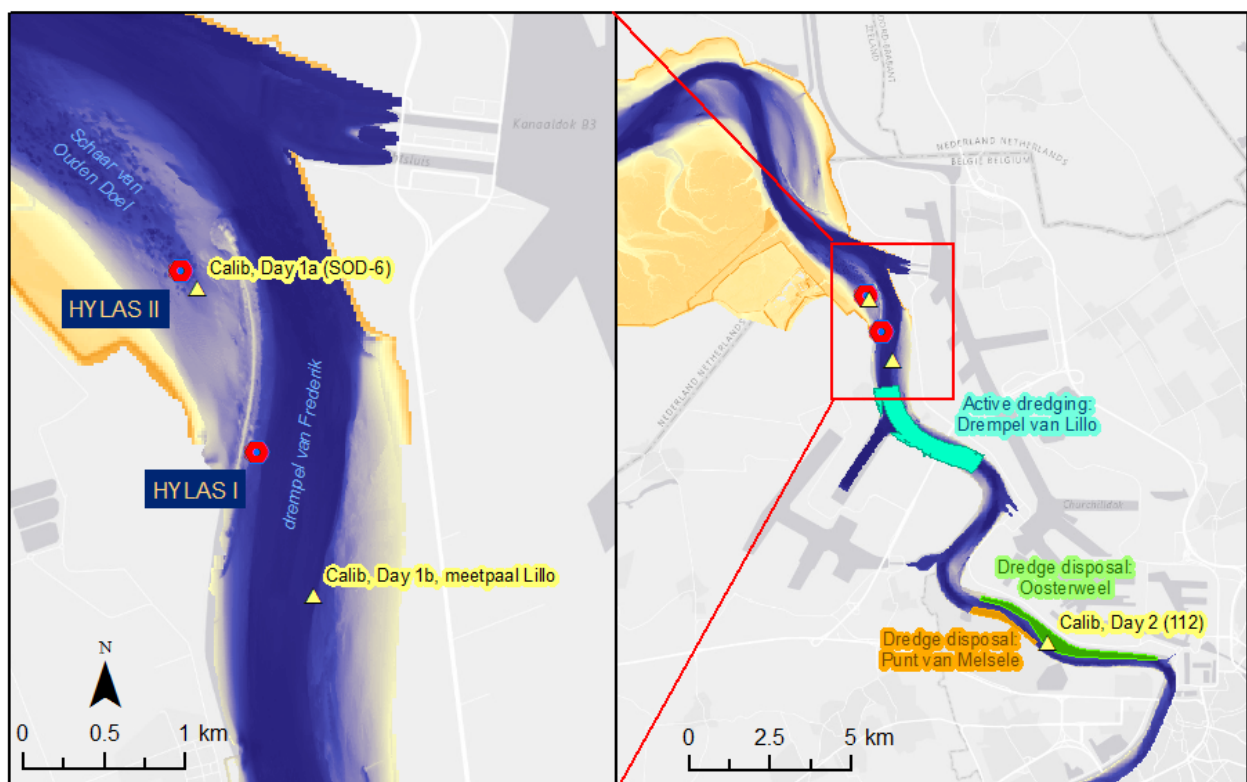
The authors and reviewers would like to thank the following contributors to this project:

- Field technicians who deployed the long-term measurement frames and collected the calibration data.
- Captain and crew of the MS Hondius who assisted during the calibration campaigns.
- Sediment lab for analyzing sediment samples.

## 2 Overview of the Measurement Campaign

The measurement campaign included month-long measurement frames (HYLAS I and II) and two 6-hour calibration campaigns. Locations are shown in Figure 1. This section describes the various datasets used to describe ambient conditions (section 2.1), the instruments/methods used during the long-term frame deployment (section 2.2) and the two 6-hour calibration campaigns (section 2.3).

Figure 1. Map of measurement frame and calibration campaign locations at Drempeel van Frederik. Location for HYLAS I is approximate. Map on the right also shows active dredge and disposal zones

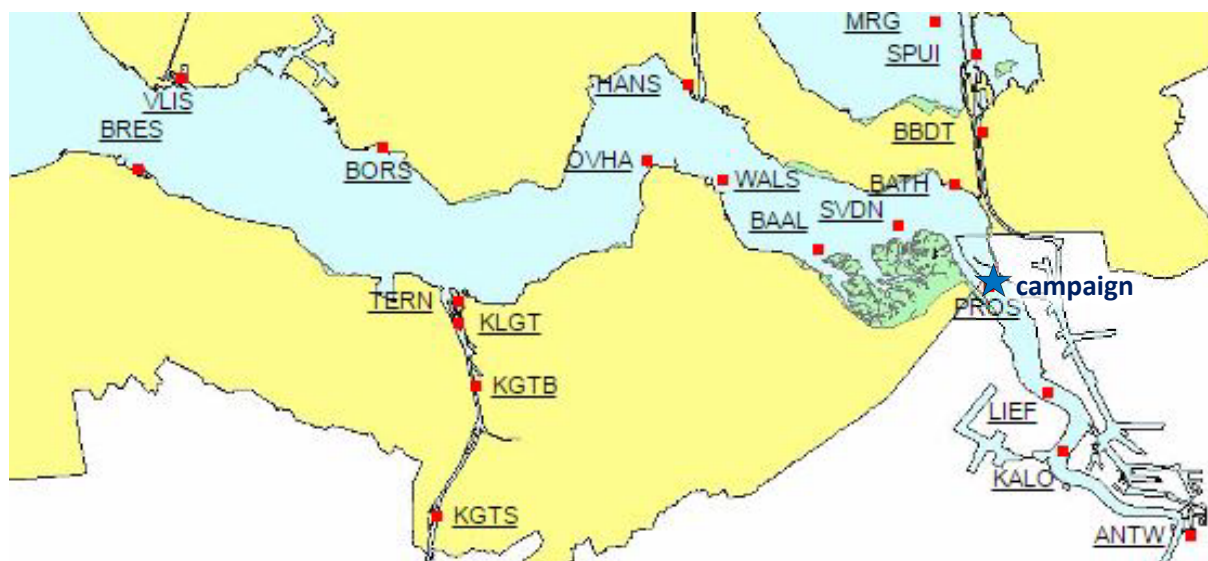


### 2.1 Ambient Conditions

Water levels, wind, and waves are measured by Rijkswaterstaat (Westerschelde) and Flanders Hydraulics (Zeeschelde) at many locations. The Dutch data are available for download from the Hydro Meteo Centrum Zeeland<sup>1</sup> and were used in this report. The water levels are measured using a Digital Level Meter and an analog Metrawatt. Wind and water level data are available in 10-minute increments while wave data in 30-minute increments. Water levels from the Prosperpolder (PROS) station were downloaded for the duration of the present monitoring campaign. Wind data were also downloaded from the PROS. No wave data is available in the vicinity of this campaign.

<sup>1</sup> [http://waterberichtgeving.rws.nl/nl/water-en-weer\\_dataleveringen\\_ophalen-opgetreden-data.htm](http://waterberichtgeving.rws.nl/nl/water-en-weer_dataleveringen_ophalen-opgetreden-data.htm)

Figure 2. Rijkswaterstaat water level monitoring locations in the Westerschelde.  
 Wind and water level data are available at the PROS station



For comparison, 10-year tidal datums at Bath are also reported, including mean high water (MHW), mean low water (MLW), mean sea level (MSL), mean tide rage (MTR), and the mean spring tide range and mean neap tide range.

Table 1. Tidal datums at the Bath station (nearest to the present campaign)<sup>2</sup>

Water Level (cm NAP <sup>3</sup> )	Bath
Mean High Water Spring	313
Mean High Water	272
Mean High Water Neap	219
Mean Sea Level	14
Mean Low Water Neap	-178
Mean Low Water	-211
Mean Low Water Spring	-232
Spring Tide Range (m)	5.45
Average Tide Range (m)	4.83
Neap Tide Range (m)	3.97

<sup>2</sup> [https://staticresources.rijkswaterstaat.nl/binaries/Referentiewaarden%20waterstanden\\_tcm174-326696\\_tcm21-24223.pdf](https://staticresources.rijkswaterstaat.nl/binaries/Referentiewaarden%20waterstanden_tcm174-326696_tcm21-24223.pdf)

<sup>3</sup> NAP reference plane is 2,33 m above TAW reference plane (0 m TAW = -2,33 m NAP).

## 2.2 Measurement Frames

### 2.2.1 Frame Locations and Set-up

Two measurement frames were installed by Flanders Hydraulics on the bed in the vicinity of Drempeel van Frederik. The locations of the monitoring frames are shown in Figure 1. Table 2 reports the coordinates, durations, and relevant data files for each frame.

Each frame contained one upward-looking AWAC, one downward looking Aquadopp (AQD), a YSI, and an OBS 3+. Figure 3 shows a diagram of the HYLAS I frame, which contained the vertical downward-facing Aquadopp. Figure 4 shows a photograph of the HYLAS II frame, which contained the horizontal downward-facing Aquadopp. Since the Aquadopp and AWAC have blanking distances of 30 cm and 90 cm, respectively, there was still a gap in the vertical velocity profile. The following sections describe each of the instruments in more detail.

Table 2. Summary of monitoring equipment for campaign 1 at Drempeel van Frederik

	Measurement Frame	
	HYLAS I	HYLAS II
Northing (m RD)	371466	372578
Easting (m RD)	77077	76607
Elevation (m NAP), derived from PROS water levels and depth sensors	-12.3	-8.2
Start Time	10/12/2015 00:00	10/12/2015 00:00
Time of Last Readable Ensemble	21/01/2016 11:10	21/01/2016 14:40
Duration (days)	42.5	42.6
AWAC File Name	659401	660602
Aquadopp File Name	1196801 (vertical)	847902 (horizontal)
Distance between AWAC and Aquadopp sensors, derived from depth measurements	AWAC 0.38 m higher than AQD	AWAC 0.10 m lower than AQD
YSI File Name	<i>None – failed</i>	14024-N9.txt
OBS 3+ File Name	OBS 3+ t8857 hylas I_counts.txt	OBS 3+ t8860 hylas II_counts.txt

For current profile calculations we assume that the frame sunk 25 cm into the bed. This is based on looking at the Aqd current profiles.

### 2.2.2 Aquadopp Profilers (ADP)

Acoustic Doppler current profilers (ADCPs) measure the current profile on the basis of acoustic Doppler technology. This monitoring campaign used two Aquadopp Profilers<sup>4</sup> manufactured by Nortek (one horizontal and one vertical). The instrument is capable of being deployed for long time frames using an internal battery and datalogger with sufficient data capacity. The dimensions and technical specifications of the Aquadopp Profiler are shown in Figure 5 and in Table 3, respectively. More details can be found in Appendix A.

<sup>4</sup> <http://www.nortek-as.com/en/products/current-profilers/aquadopp-profiler>

Figure 3. Drawing of HYLAS I measurement frame with instrument heights above the bed. HYLAS I had the vertical Aquadopp

---

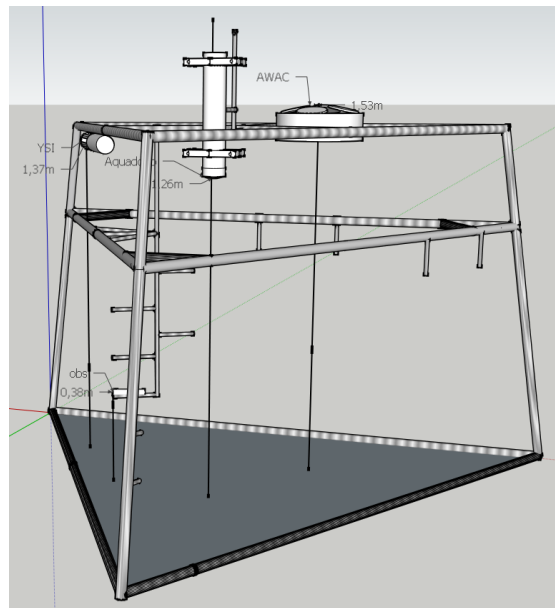
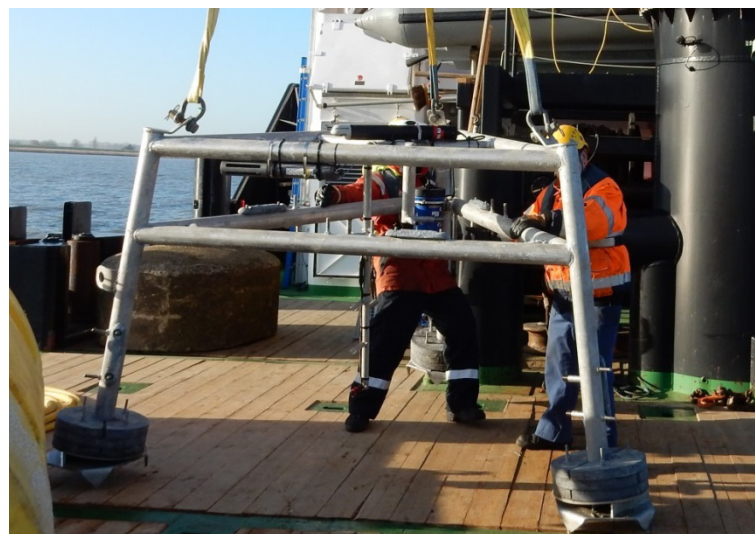


Figure 4. Photo of HYLAS II measurement frame. HYLAS II had the horizontal Aquadopp

---



ADCPs use the Doppler effect to measure current velocities by sending out a short sound wave and listening to the echo that returns when soundwaves reflect off particles in the water. The ADCP measures the difference in frequency between the two signals (sent/detected). This principle can be expressed as:

$$V = \frac{F_{Doppler}}{F_{Source}} \cdot \frac{C}{2}$$

Where:

V = current velocity in one direction (along the axis of the sound wave)

F<sub>Doppler</sub> = difference in frequency, also known as the Doppler shift

F<sub>Source</sub> = frequency of the sent signal

C = speed of sound

The Aquadopp Profiler measures the current velocity along 3 axes (Figure 5, middle), but reports the data in East, North, and Up coordinates (ENU coordinates). The measured data are converted to XYZ coordinates (Figure 5, right). Then, the instrument uses an internal magnetometer and tilt measurement to convert the XYZ coordinates to ENU coordinates. The profiler can be configured to be “upward facing” or “downward facing”. During the long-term frame deployments, the profilers were set up in the “downward facing” configuration.

The Aquadopp Profile also measures the strength of the return signal, or acoustic backscatter. The strength of the backscatter depends in part on the level of suspended sediments in the water column. Comparing the backscatter values with water samples allows the data to be calibrated with sediment concentration, as described in section 3.2.

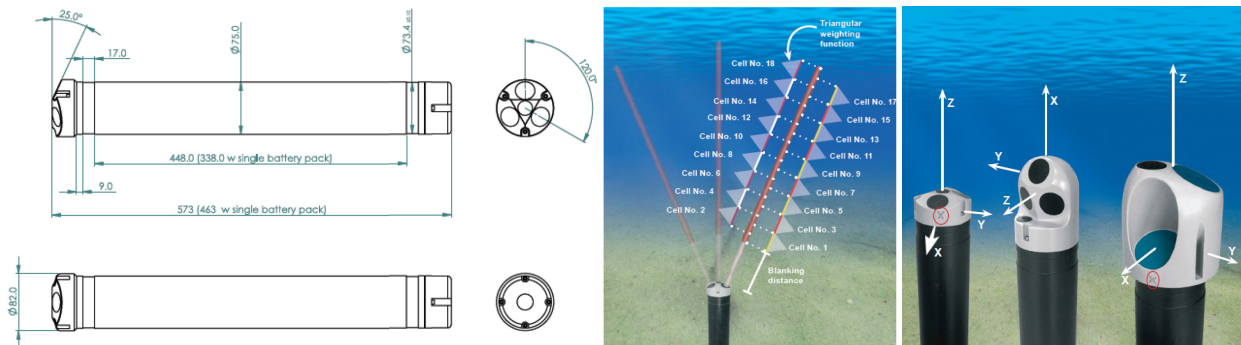
Table 3. Aquadopp Current Profiler technical specifications from the manufacturer (Nortek)

<b>Water velocity measurement</b>	
Acoustic frequency	2.0 MHz
Maximum profiling range	4–10 m
Cell size	0.1–2 m
Beam width	1.7°
Minimum blanking	0.05 m
Number of beams	3
Maximum number of cells	128
Velocity Range	±10 m/s
Accuracy	1% of measured value ±0.5cm/s
Maximum sampling rate:	1 Hz
<b>Standard sensors</b>	
<b>Temperature</b>	<i>Thermistor embedded</i>
Range	–4°C to 30°C
Accuracy/resolution	0.1°C/0.01°C
Time response	10 min
<b>Compass</b>	<i>Magnetometer</i>
Accuracy/resolution	2°/0.1° for tilt <20°
<b>Tilt</b>	<i>Liquid level</i>
Accuracy/resolution	0.2°/0.1°
Maximum tilt	30°
Up or down	Automatic detect
<b>Pressure</b>	<i>Piezoresistive</i>
Range	0–100m (standard)
Accuracy/resolution	0.5%/0.005% of full scale

For the long-term deployment, the two Aquadopps were programmed to collect velocity data as follows, in order to capture the portion of the current (and sediment transport) profile close to the bed:

Bin size	0.1 m
Middle of bin 1 (blanking distance)	0.3 m
Ensemble interval	600 sec
Measurement period per ensemble	60 sec

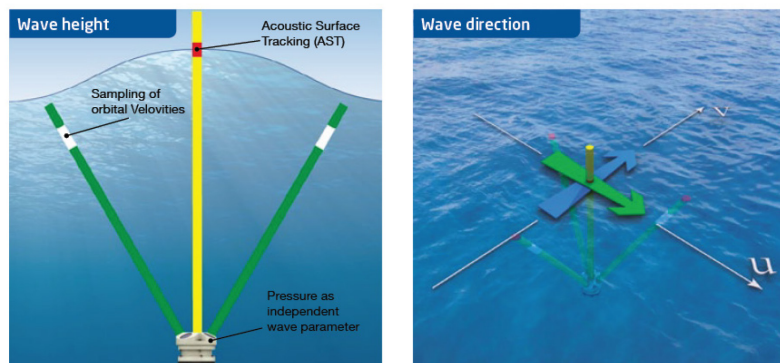
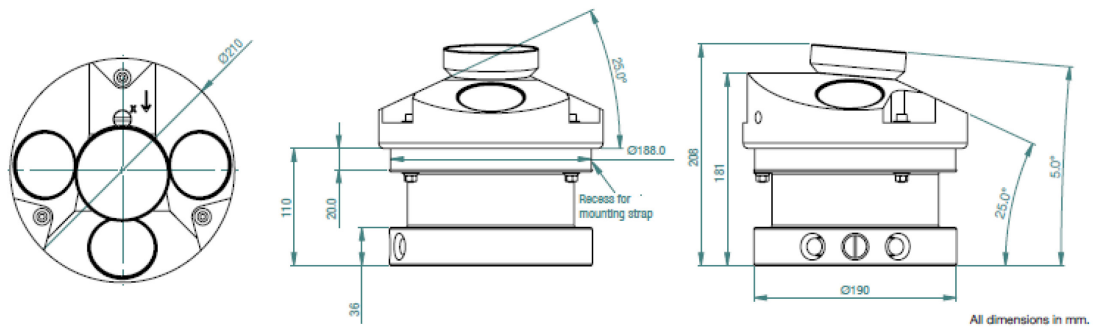
Figure 5. Aquadopp Profiler dimensions (left, mm), conceptual diagram (middle), and reference coordinate system (right)



### 2.2.3 Acoustic Wave and Current Profiler (AWAC)

The Acoustic Wave and Current Profiler<sup>5</sup> (AWAC), made by Nortek, measures wave height, wave direction, tidal elevation, and current profile in a single instrument. Like an ADCP, it measures current speed and direction along a row of cells radiating from the top of the instrument using the Doppler effect. Additionally, it can measure different types of waves (long waves, storm waves, short wind waves, and even ship waves) using pressure sensors and a technology called Acoustic Surface Tracking (AST). The instrument is usually deployed on a frame at the bottom of the water column. The dimensions and technical specifications of the Aquadopp Profiler are shown in Figure 6 and in Table 4, respectively.

Figure 6. AWAC dimensions (top, mm), conceptual diagram (bottom left), and reference coordinate system (bottom right).



<sup>5</sup> <http://www.nortek-as.com/en/products/wave-systems/awac>

Table 4. AWAC technical specifications from the manufacturer (Nortek)

<b>Weight and Dimensions</b>	
Weight in air	5.6 kg
Weight in water	2.5 kg
Height	0.17 m
Diameter	0.21 m
<b>Sensors</b>	
Compass maximum tilt	30°
Compass Accuracy/Resolution	2°/0.1°
Tilt Accuracy/Resolution	-0.2°/0.1°
Tilt Up or down	Automatic detect
Pressure Range	0–50 m (standard)
<b>System</b>	
Acoustic frequency	1MHz
Acoustic beams	4 beams, one vertical, three slanted at 25°
Vertical beam opening angle	1.7°
<b>Wave measurements</b>	
Maximum depth	35 m
Data types	Pressure, one velocity along each beam, AST*
<b>Wave estimates</b>	
Accuracy	1% of measured value ±0.5 cm/s
Range	-15 to +15 m
Accuracy/resolution (Hs)	<1% of measured value/1 cm
Accuracy/resolution (Dir):	2° / 0.1°
Period range:	0.5-100s
<b>Current Profile</b>	
Maximum range	20–30 m (depends on local conditions)
Depth cell size	0.4–2.0 m
Internal sampling rate	6 Hz

The two AWACs were programmed to observe the majority of the velocity profile (excluding the lowest portion, which was measured by the Aquadopps) as follows:

Bin size	0.5 m
Middle of bin 1 (blanking distance)	0.9 m
Ensemble interval	600 sec

#### 2.2.4 Turbidity Sensor (OBS 3+)

The OBS 3+-3+ Turbidity Sensor<sup>6</sup> (OBS 3+) by Campbell Scientific measures optical backscatter to monitor suspended sediment concentrations. The sensor monitors backscatter along a beam parallel to the instrument axis. At the centre of the instrument is a near infrared laser and photodiode to detect the intensity of backscattered light reflected from particles in suspension. Turbidity is reported in units of NTUs. The working assumption is that the turbidity increases as the concentration of suspended solids (and therefore also sediment) increases in the water. As with all optical sensors, the OBS 3+ is sensitive to the size, shape, and composition of the suspended particles. Calibration with in-situ material

<sup>6</sup> <https://www.campbellsci.com/obs-3plus>

is highly recommended. The main technical specifications are given in Figure 7 and Table 5. Additional technical specifications can be found in Appendix C.

Figure 7. OBS 3+-3+ dimensions (left), conceptual diagram (right)

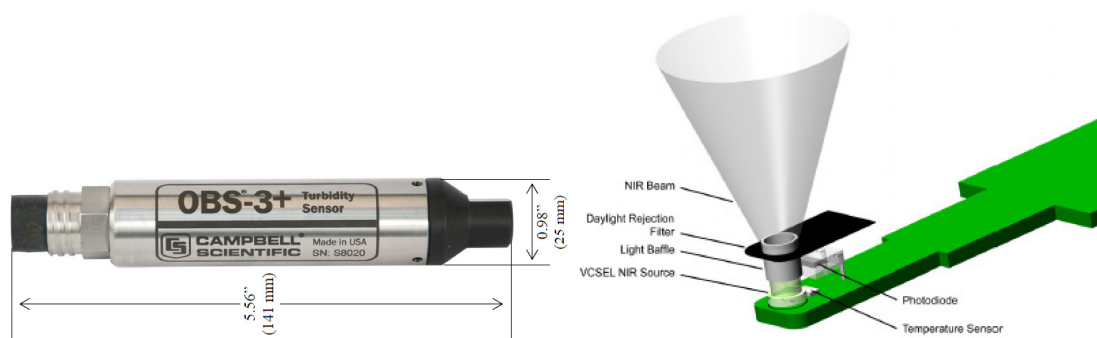


Table 5. OBS 3+-3+ technical specifications from the manufacturer (Campbell Scientific)

Turbidity Range	Up to 4000 NTU
Characteristics	Compact Compatible with Campbell Scientific dataloggers Titanium housing allowing measurements at great depths.
Operating Temperature	0 to 40C
Weight	181.4 g
<b>Measurement Range</b>	
Turbidity (Low/High)	250/1000, 500/2000, 1000/4000 NTU
Silt	5000 to 10000 mg/L
Sand	50000 to 100000 mg/L
<b>Accuracy</b>	
Turbidity	2% of value or 0.5 NTU
Silt	2% of value or 1 mg/L
Sand	2% of value or 10 mg/L

The OBS 3+ was programmed to collect with a 10 minute averaging interval.

### 2.2.5 YSI

The 6-Series Environmental Monitoring Systems from YSI are multi-parameter, water quality measurement, and data collection systems. A YSI was deployed on both measurement frames, but only the instrument on HYLAS II successfully collected data. A standard YSI is equipped with a conductivity, pressure and temperature sensor. For this measurement campaign, a turbidity sensor was also added. The YSI was programmed to collect one data point every 10 minutes.

Table 6. YSI 6-Series technical specifications from the manufacturer.

Sensor	Range	Resolution	Accuracy
6136 Turbidity Sensor	0 to 1000 NTU	0.1 NTU	+/-2% of reading or 0,3 NTU, whichever is greater
Conductivity	0 to 100 mS/cm	0.001 mS/cm to 0.1 mS/cm (range dependent)	+/- 0.5% of reading + 0.001 mS/cm
Temperature thermistor	-5 to 50 °C	0.01 °C	+/- 0.15 °C

## 2.3 6-Hour Calibration Measurements

After the long-term frames (HYLAS I and II) were retrieved, two days of calibration measurements were conducted at various locations, as summarized in Table 7 and Figure 1.

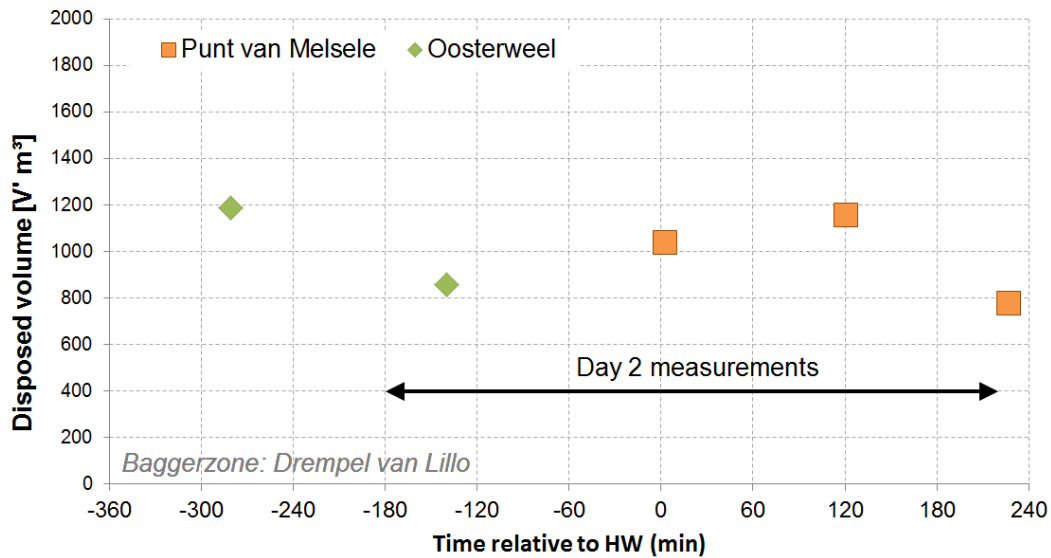
The first day of calibration measurements, January 29<sup>th</sup> 2016, took place in two locations: first near the HYLAS II frame location at Schaar Ouden Doel and then at the Lillo measurement station (“meetpaal Lillo”). The first location was chosen because there was a discrepancy between OBS 3+/ABS sensors at HYLAS II during initial phase of the ebb, and the goal was to better understand this discrepancy. In order to measure higher transport rates, the measurements were then moved to meetpaal Lillo (Figure 1). The HYLAS I location was not measured during calibration due to its vicinity to the navigation channel, preventing the presence of an extra vessel for calibration.

A second day of calibrations were conducted at Oosterweel on February 5<sup>th</sup> 2016 because the SSC concentrations measured during Day 1 of the calibration were not high enough. The Oosterweel location is located between two dredge disposal sites, both of which were actively in use (Figure 8).

Table 7. Summary of calibration campaigns

	Calibration Date		
	29/1/2016 (part 1)	29/1/2016 (part 2)	5/2/2016
Location Name	SOD06	Meetpaal Lillo	Oosterweel
Northing (m RD)	372474	370580	361895
Easting (m RD)	76710	77422	82186
Aquadopp + OBS 3+ File Name	6550ca01 (vert, HYLAS I) 8479ca01 (horz, HYLAS II)		1196802 (vert) 847903 (horz)
YSI File Name	CAL14024.txt (HYLAS II) <i>No YSI calibrated for HYLAS I because the YSI on HYLAS I failed during long-term measurements.</i>		<i>No data - failed</i>

Figure 8. Dredging data for day 2 of the calibration campaign



The next section describes how the various instruments were mounted and deployed during the calibration. The subsequent sections describe the methods associated with each of the measurements listed above.

### 2.3.1 Configuration

The calibration measurements were done from a boat using two measurement frames, each suspended from one side of the boat (Figure 10). One frame, pictured on the left in Figure 11, held the two Aquadopps (one up-facing and one down-facing), both OBS 3+ sensors, the YSI, and an inlet pump for water samples. The other frame, pictured on the right in Figure 11, held the LISST-100X and a second inlet pump for water samples. Figure 9 presents a sketch of the frame with dimensions. The following list summarizes the various types of calibration measurements:

- Currents
  - Downward facing velocity profile measured using the vertical **Aquadopp** that was also deployed on the HYLAS I frame.
  - Upward facing velocity profile measured using the horizontal **Aquadopp** that was also deployed on the HYLAS II frame.
  - Note: The two AWACs deployed on the long-term frames were not calibrated during the calibration campaigns. Section 3.3 describes how the AWAC backscatter was calibrated to SSC, and section 3.6 explains how the AWAC and Aquadopp data were combined to see a complete profile.
- Suspended sediment concentrations (SSC)
  - **Water samples** were collected intermittently during the calibration and analysed for suspended sediment concentration. One inlet was attached to the Aquadopp frame, calibration of the first cell of the downlooking Aquadopp. A second inlet was attached to the LISST-100X frame, intended for the calibration of the up-looking Aquadopp.
  - The acoustic backscatter measured by the two **Aquadopps** is an indicator of sediment concentration in the water column.
  - Sediment volume concentrations measured using the **LISST-100X**. The LISST-100X was deployed on a separate hanging frame from the AQD, but was kept at a height such that the water samples could be used to calibrate the horizontal up-looking AQD.
  - The turbidity measured by the **YSI** (data only available on the first day of calibration) and the optical backscatter measured by the two **OBS 3+** sensors are indicators of

suspended sediment concentration. Both devices were attached to the Aquadopp frame at the same length as the first cell of the downlooking Aquadopp and pump inlet.

- Grain size distributions
  - Grain size distribution was measured using optical methods with the *LISST-100X*.
  - **Water samples** were collected intermittently and analysed for grain size distribution (half of the water samples that were analysed for SSC).

• Figure 9. Calibration frame set-up with measurements

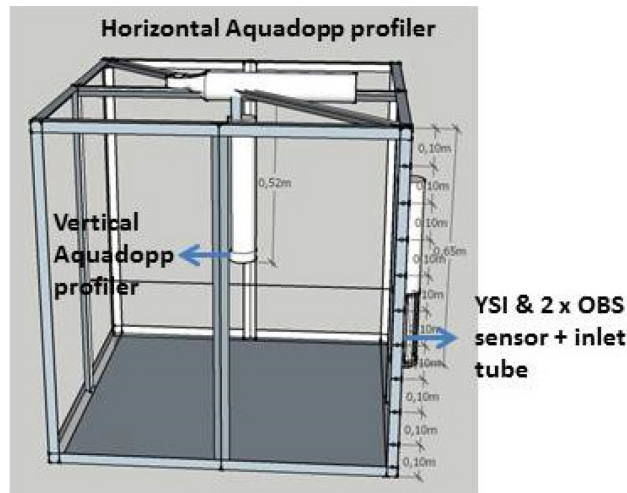


Figure 10. Calibration setup

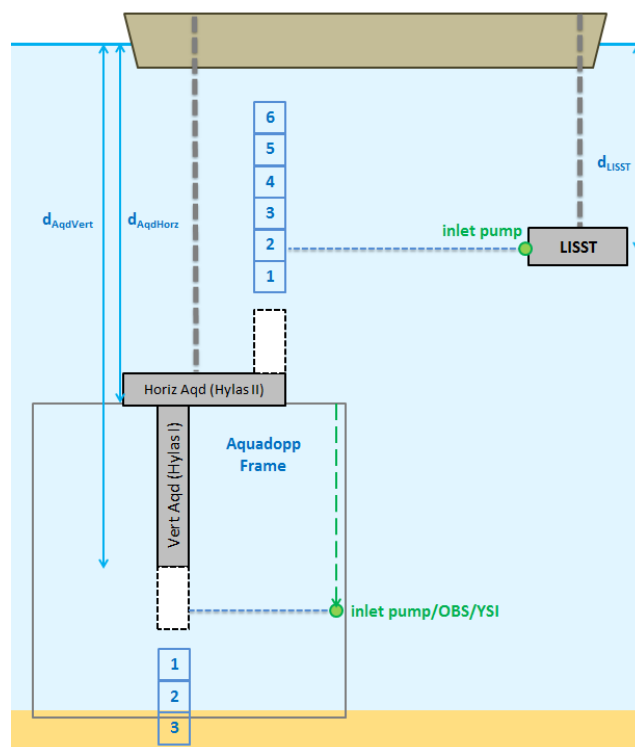
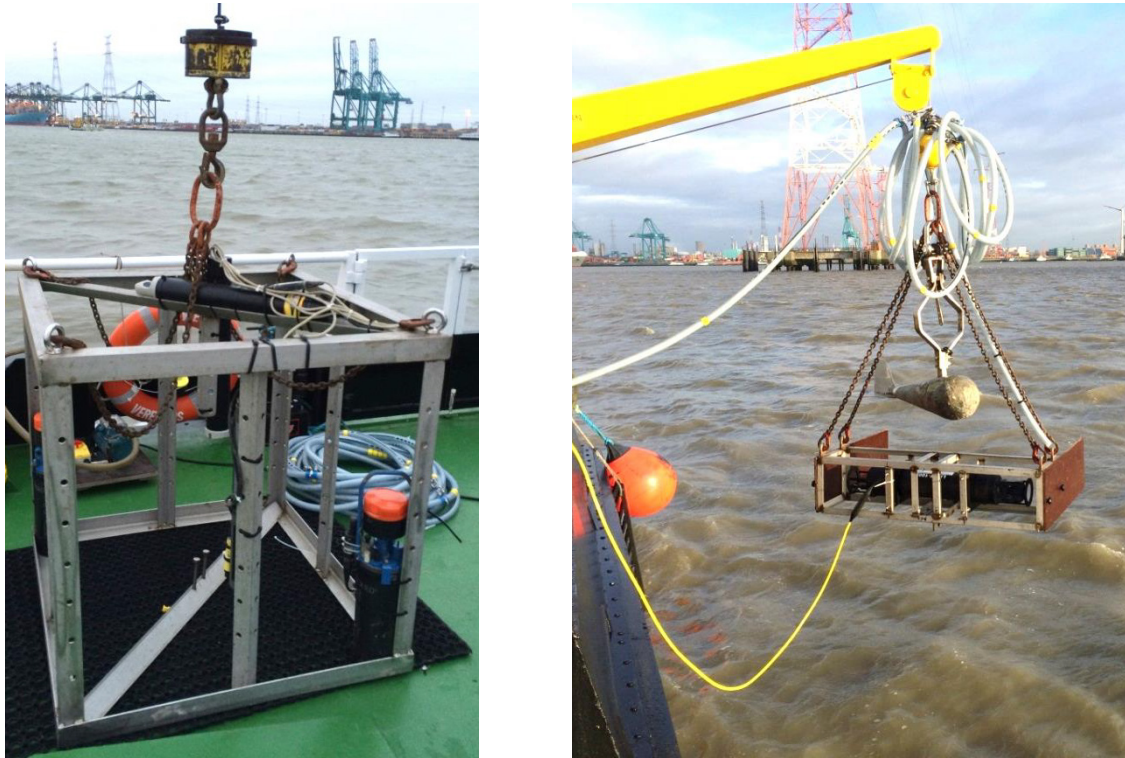


Figure 11. Photos of (left) Aquadopp and (right) LISST-100X calibration frames

---



### 2.3.2 Currents

The two 2 MHz Nortek Aquadopps that were deployed for the long-term frame measurements were mounted on the calibration frame, with one facing up (the horizontal Aquadopp used on HYLAS II) and one facing down (the vertical Aquadopp used on HYLAS I). The same settings used during the long-term measurements (described in section 2.2.2) were used during the calibration campaigns, with the exception that the ensemble interval was reduced to 10 seconds for the calibration compared to 600 seconds for the long-term deployment.

While the Aquadopps were both deployed in downward-facing configurations during the long-term deployment, they were configured this way (one up, one down) during the calibration to avoid interference that would occur if they both pointed the same direction. For the same reason the AWACs were not used during the calibration campaign, so these had to be calibrated using the data collected by the Aquadopps (see section 3.2 for an explanation of how this was done).

### 2.3.3 Suspended sediment concentrations (SSC)

#### **Water samples**

Water samples (161 total, Table 8) were collected intermittently at the same vertical location as the LISST-100X and downfacing Aquadopp. and sent to the lab to be analysed for suspended sediment concentration (SSC). Samples were filtered through 0.45  $\mu\text{m}$  filter paper, dried, and weighed to estimate the suspended sediment concentration.

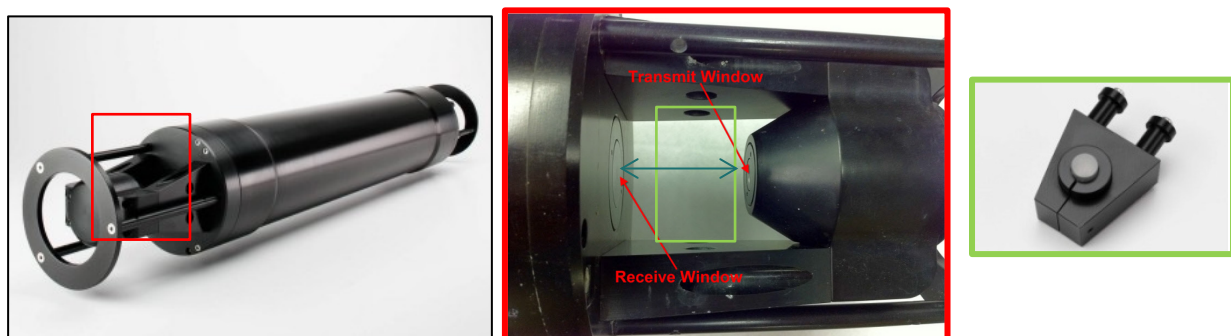
Table 8. Number of water samples (and grain size) analyzed during calibration campaigns

	Day 1 (29/1/2016)	Day 2 (5/2/2016)	Total
Frame with Aquadopps	38 (18)	61 (31)	99 (49)
Frame with LISST-100X	24 (12)	38 (19)	62 (31)
Total	62 (30)	99 (50)	<b>161 (80)</b>

### LISST-100X

A Laser In-Situ Scattering and Transmissometry (LISST-100X) instrument was used to measure in-situ suspended sediment volume concentration and particle size. The LISST-100X uses laser diffraction (forward scattering) to measure the size of suspended sediment particles at one point in the water column (Figure 12). The manufacturer technical specifications are reported in Appendix B. A set of ring detectors, each of a different width and representing a different range of scattering angles, detect scattering from different angles. There are 32 detector rings covering 32 different angles over which light scattering is measured. When multiple grain sizes are present, the detected scattering is reflective of the combined scattering of all particles in suspension. From this combined scattering pattern it is possible to derive the concentrations of particles in 32 different size classes. The exact shape of the light scattering off a spherical particle of any size, colour, or composition can be computed, and conversely, the size of the particle can be derived from light scattering pattern. No two particles of different size or composition will have the same scattering patterns. The result is a detailed time series (1 to 2 second interval) of volume concentration ( $\mu\text{l/l}$ ) by grain size, a total volume concentration, and a D50 estimate. The volume concentration is an indicator of sediment concentration, and can be calibrated using water samples assuming that the sediment density is constant. See section 3.2 for a description and the nuances of this post-processing step.

Figure 12. Left) Overview LISST-100X, Middle) detail of the transmit and receive windows for the light beam, Right) example of a PRM



The double blue arrow indicates the length of the optical path.

The green box indicates the place where a PRM should be installed if needed.

### Aquadopp

Another indicator of sediment concentration in the water column is the acoustic backscatter (ABS) measured by the Aquadopp. Each flow velocity measurement by the Aquadopp is accompanied by the ABS (also known as the Echo Amplitude) measured along each of the 3 Aquadopp beams. The higher the sediment concentration, the higher the ABS, except when the concentration is too high, causing

multiple scattering of the acoustic signal. Section 3.2 describes how the Aquadopp ABS can be range-normalized and calibrated using water samples.

### **OBS 3+**

Two OBS 3+ sensors were deployed on the same frame as the Aquadopps, with the sensors close to the inlet pump for the water samples. They measured optical backscatter (in counts) over time, which is an indicator of suspended sediment concentration. The OBS 3+ sensors were programmed to collect data at the same sampling interval as the Aquadopps, every 10 seconds during the calibration campaign.

### **YSI**

A YSI was deployed on the same frame as the Aquadopps and measured temperature, pressure, depth, and turbidity. The turbidity (in NTUs) is an indicator of suspended sediment concentration and was used to validate the SSC derived from the LISST-100X and Aquadopps. The YSI was programmed to collect data every 10 seconds during the calibration campaign.

## 2.3.4 Grain size distribution

### **LISST-100X**

The grain size was measured in-situ using the LISST-100X, as described in section 2.3.3. The result is a detailed time series (1 to 2 second interval) of volume concentration by grain size, total volume concentration, and a D50 estimate.

### **Water samples**

Additionally, half the water samples collected for SSC (Table 8, 80 in total) were sent to the lab to be analysed for grain size distributions. The grain size is analysed in the lab using a Malvern Mastersizer 2000 (Figure 13), which uses laser diffraction to analyse samples up to 2000  $\mu\text{m}$  in diameter. The water samples were first filtered and then incinerated to remove the filter paper, leaving behind only inorganic material. The samples are first filtered through a sieve with a mesh size of 2000  $\mu\text{m}$ . The device can be used to analyse very small sediment samples (e.g. volumes of 1  $\text{cm}^3$ ). The analysis results in a complete grain size distribution, and the D10, D20, D35, D50, D65, D80, and D90 grainsize is reported. Fractions of sand is also derived using a grain size cut-off of 63  $\mu\text{m}$ . However, pre-treatment (sonication, mixing, pumping) of the samples can alter the original (in-situ) grain size (flocs, organo-mineral structures...). Additionally, the sediment can flocculate, consolidate, or otherwise change during transit time between sampling and analysis, resulting in a different grain size. Therefore, results must be interpreted with this in mind.

---

Figure 13. Malvern Mastersizer 2000

---



## 3 Post-Processing

The following sections describe various analyses performed, conducted using measurements from both the calibration campaigns and long-term deployments.

### 3.1 Locating instruments relative to each other based on water depth

This processing step was applied to the calibration campaigns. One of the first steps in post-processing the calibration measurements is to identify the vertical location of each instrument relative to the others (in particular, the LISST-100X samples relative to the Aquadopps), so the data can be properly compared. This step is also important for checking that timestamps on all datasets are correctly aligned.

The depths measured by both Aquadopps, the LISST-100X, and the YSI (day 1 only) on day 1 and day 2 are presented in Figure 14 and Figure 15, respectively. The time and depth of water samples collected on the Aquadopp and LISST-100X frames are also marked. Two sets of water depths are shown for the LISST-100X samples: once using the depths recorded by the LISST-100X and once using the depths recorded in the logbook (based on the crane counter). The recorded water depth on day 1 is on average 1,25 m less than the measured water depth, which cannot be explained by the LISST-100X frame dimensions. One explanation for this discrepancy could be that the current pushed the LISST-100X frame far enough in the direction of the current that it lifted it up. However, on day 2 the recorded depth is greater than the measured depth. Since it is not possible to identify which of the measured or written depth is “more correct,” both sets of depths were considered when developing the SSC-ABS calibration curves, as described in section 3.2.

It is possible to use the relative distance between the Aquadopp and LISST-100X in order to assign the correct Aquadopp bin to each SSC sample collected near the LISST-100X. This was done for both the measured and written depths:

$$Bin = \frac{Dist_{LISST\ to\ Aquadopp} - blanking\ distance}{bin\ size}$$

When the LISST-100X water sample was collected beyond reach of the up-looking Aquadopp, the farthest (15<sup>th</sup>) cell was used. When the LISST-100X water sample was collected too close or below the up-looking Aquadopp, the first cell was used.

The absolute elevation of the bed at the location of the instruments was estimated by assuming the water level at the HYLAS I and HYLAS II frames was equal to that measured and reported at the PROS water level gage. Then, it is possible to back-calculate an average bed elevation by subtracting the depth measured by the instrument and the height of the instrument above the bed. The approximate bed elevation at HYLAS I and HYLAS II was -12.3 and -8.2 m NAP, respectively.

The sampling height and the estimated position are measured by the cable length. This length is displayed at the rear part of the bridge of the vessel. In our experience, the cable length is not always correct, and drift of the instrument caused by current will result in a greater depth than is correct.

Figure 14. Instrument depth below water surface, calibration day 1

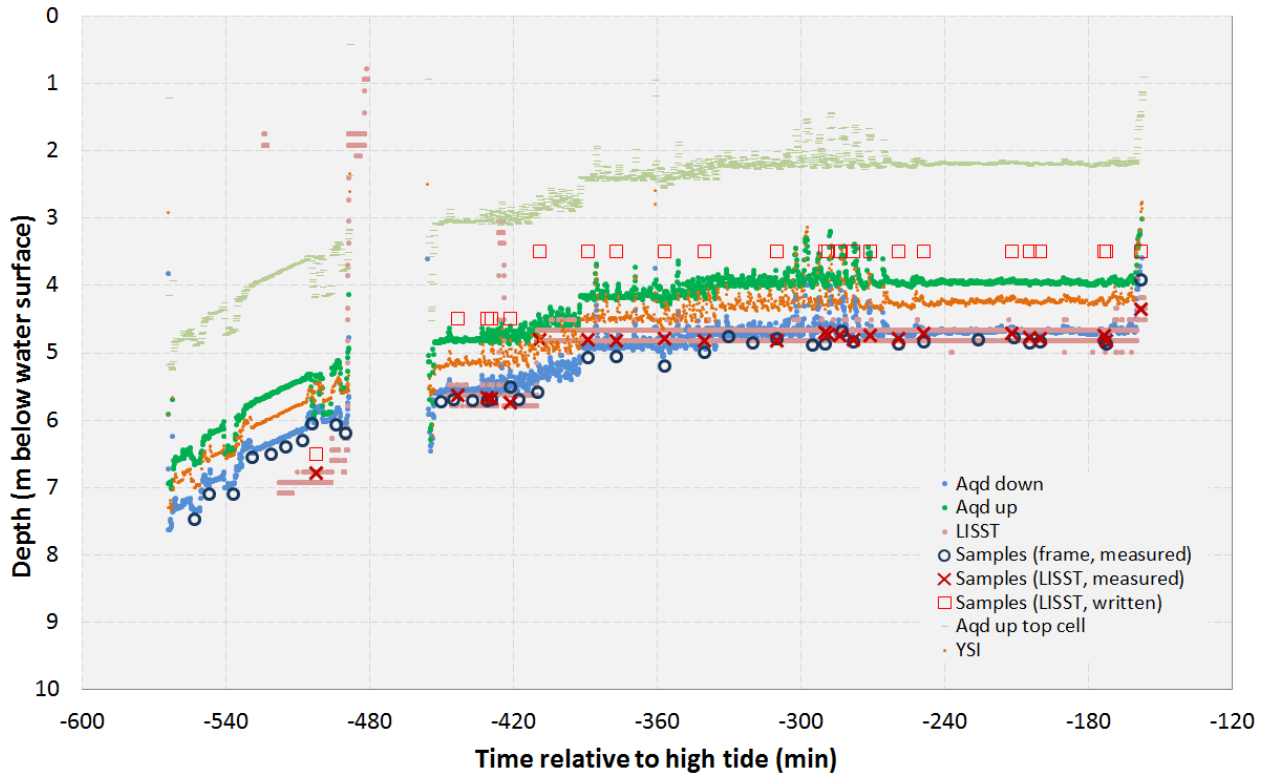
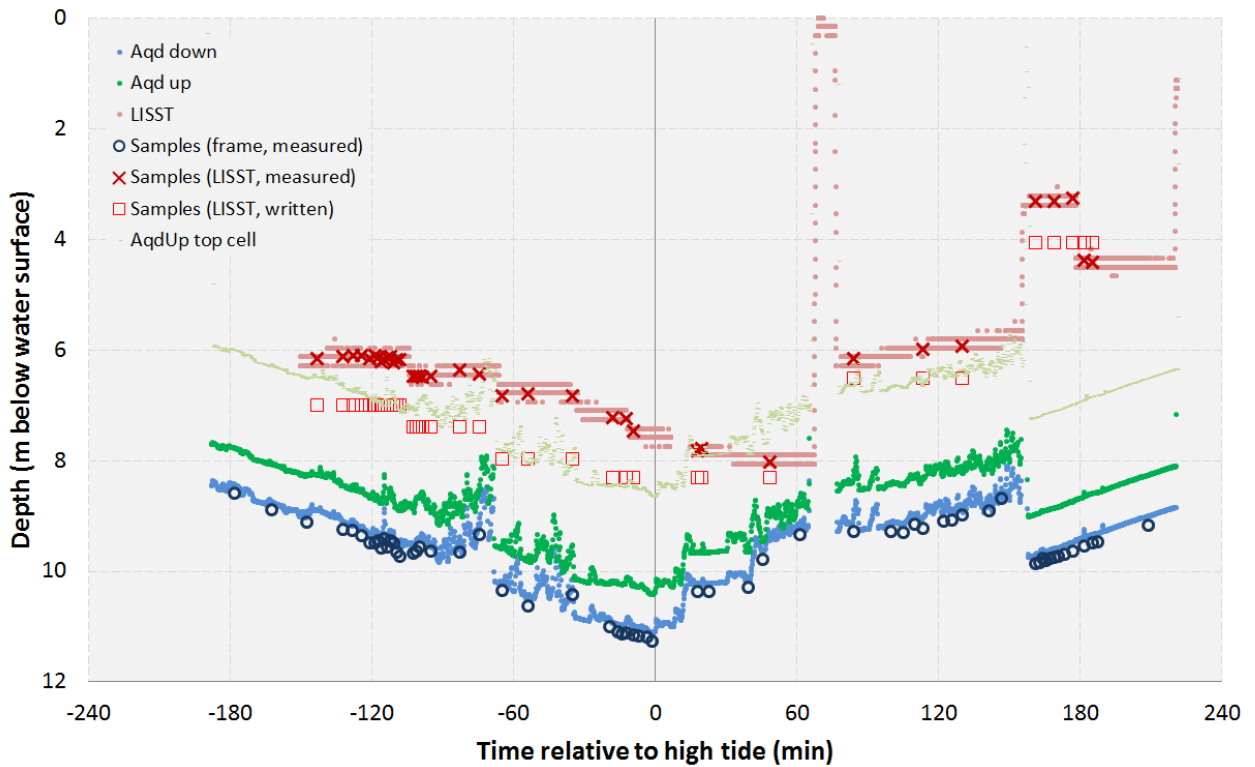


Figure 15. Instrument depth below water surface, calibration day 2



## 3.2 Sediment Concentration from Acoustic Backscatter

Acoustic backscatter (ABS) intensities can be used to estimate sediment concentration in the water column (e.g. Lohrmann 2001, Gartner 2004, Aardoom 2005). This section describes how the water samples collected during the calibration campaign were used to calibrate the two Aquadopps.

The following steps, based on Lohrmann 2001, can be taken to make this conversion and are explained in more detail in this section:

1. Convert internal units (counts) to a linear or log scale (dB)
2. Range normalization - correct backscatter intensity (dB) for sound absorption in water
3. Develop calibration curve relating ABS (dB) to measured SSC (mg/l)
4. Convert ABS (dB) to SSC (mg/l)

Step 1 and Step 2 were also applied to the long-term AWAC data. Section 3.3 describes how the AWAC backscatter was calibrated using the long-term calibrated Aquadopp data.

### 3.2.1 Step 1: Convert internal units to a linear or log scale

According to Lohrmann 2001, the internal units (counts) can be converted to decibels (dB) linearly over a range of 70 dB. Inside this range the scaling factor is approximately  $K_c = 0.43$  counts/dB (range 0.40 to 0.47). Beyond the linear range (which corresponds to roughly 1 to 10,000 mg/L), the conversion is non-linear and values should not be used for sediment analysis.

$$K_c = 0.43 \text{ dB/count}$$

### 3.2.2 Step 2: Range normalization

The second step involves correcting the ABS for acoustic loss terms, which increase with distance from the sensor and is independent of sediment in the water column. The three terms to correct for include acoustic spreading, water absorption, and particle attenuation. More explanation of each of these terms can be found in Lohrmann 2001.

$$\text{acoustic spreading} = 20 \log_{10} R$$

$$\text{water absorption} = 2\alpha_w R \quad \left( \alpha_w = \text{water absorption in } \frac{\text{dB}}{\text{m}} \right)$$

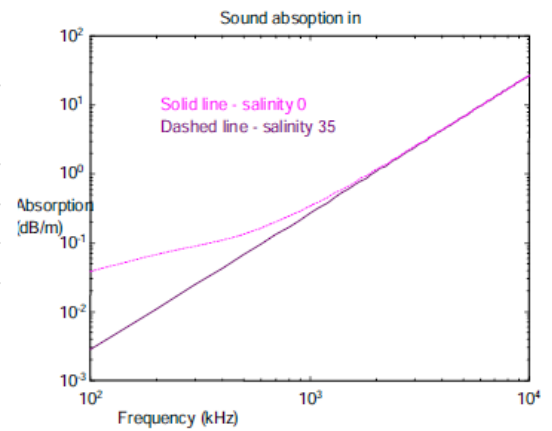
$$\text{particle attenuation} = 20R \int \alpha_p dr \quad \left( \alpha_p = \text{particle attenuation in } \frac{\text{dB}}{\text{m}} \right)$$

$$R = \text{range} = z / \cos(\text{beam angle}, 25^\circ \text{ for Aquadopp/AWAC})$$

The water absorption is dependent on the water density, pressure, and the transmitted frequency. Figure 16 shows how absorption in water varies with frequency and salinity.

Figure 16. Absorption in water vs. frequency for fresh and salt water

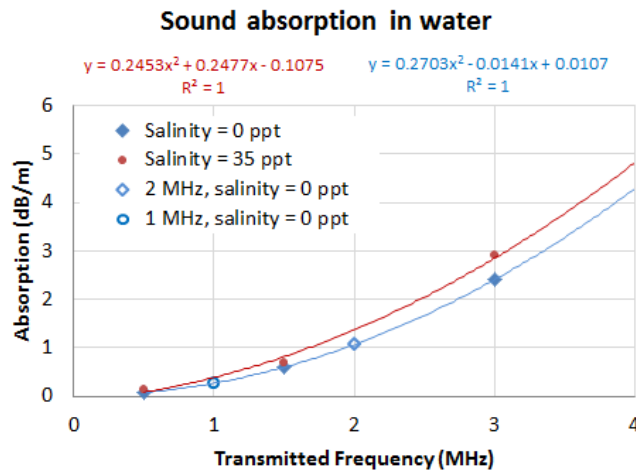
Frequency (MHz)	$\alpha$ (dB / meter) Salinity = 0 ppt	$\alpha$ (dB / meter) Salinity = 35 ppt
10	26.9	26.9
3.0	2.4	2.9
1.5	0.6	0.7
0.50	0.07	0.14



Source: Lohrmann 2001.

Figure 17 estimates the absorption for the 2 MHz Aquadopp and 1 MHz AWAC (hollow blue points) for low salinity conditions based on the rates reported in Figure 16 (solid points) using a second order polynomial. Since this location is relatively low salinity, an absorption of 1.0637 dB/m was used for the Aquadopp (2 MHz) and 0.2669 dB/m for the AWAC (1 MHz).

Figure 17. Absorption of sound in the water column for various frequencies



The last term, particle attenuation, is estimated to be small at low concentrations and is assumed here to be zero. The present method ignores particle attenuation. The resulting complete equation (which already takes into account that the correction must be made twice, since the signal passes through the water column twice) is:

$$ABS_{norm} = Amp * K_c + acoustic\ spreading + water\ absorption$$

Figure 18 and Figure 19 plot the normalized acoustic backscatter measured near the down-looking Aquadopp for day 1 and day 2 of the calibration campaign, respectively. The moments when water samples were collected near the Aquadopp are also marked. The LISST-100X volume concentrations and water samples are discussed later, in section 3.4, but presented on the figures below in order to compare trends between the LISST-100X and Aquadopps.

Figure 18. Normalized acoustic backscatter (in dB) and LISST-100X volume concentration (in  $\mu\text{l/l}$ ) during day 1 (29/1/2016) of the calibration campaign

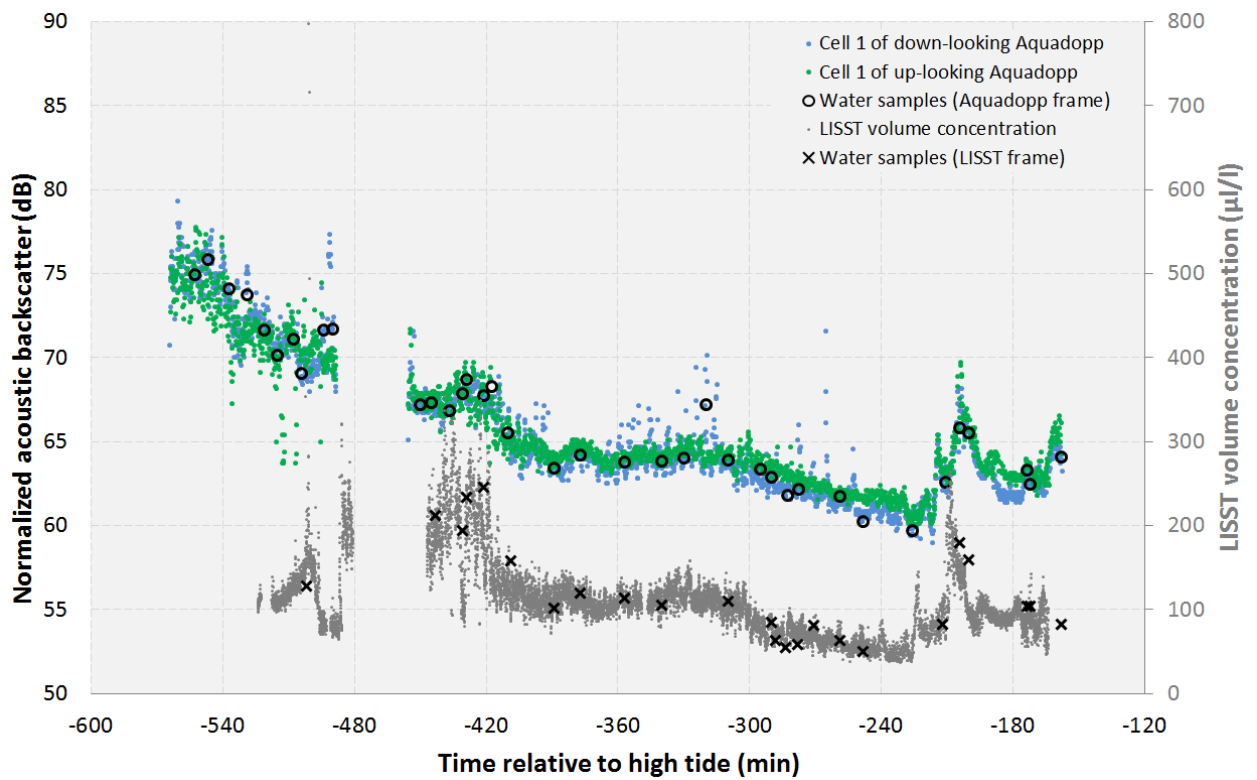
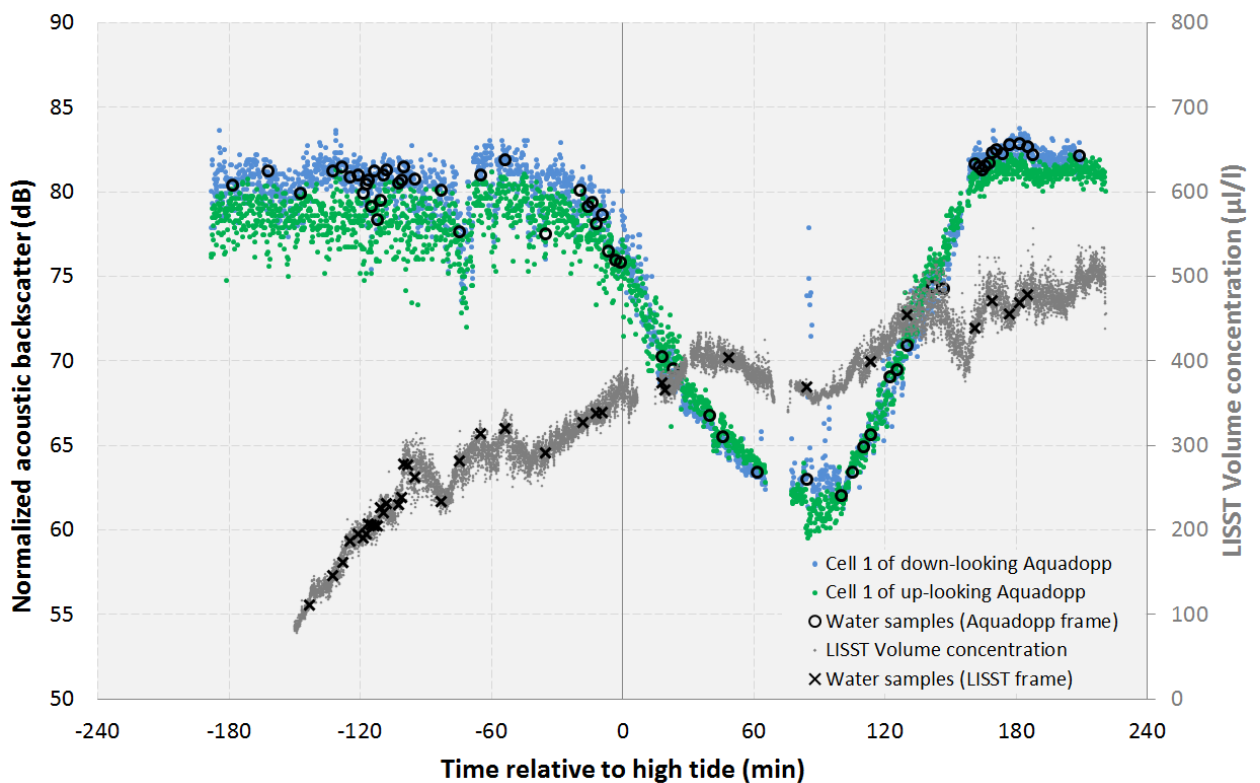


Figure 19. Normalized acoustic backscatter (in dB) and LISST-100X volume concentration (in  $\mu\text{l/l}$ ) during day 2 (5/2/2016) of the calibration campaign



### 3.2.3 Step 3: Develop calibration curve relating ABS to SSC

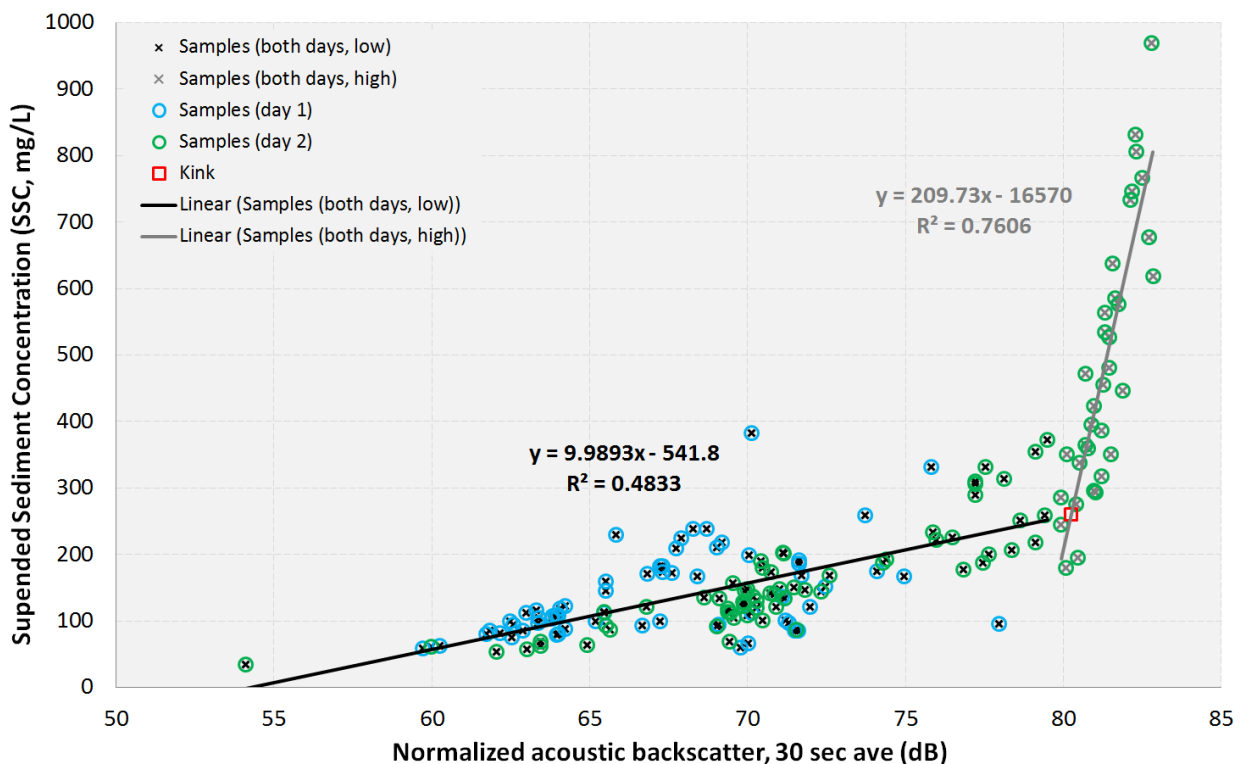
The next step is to correlate the range-normalized ABS from the Aquadopps with measured SSC from the water samples. Over the course of the two 6-hour calibration campaigns, 310 water samples were collected and analysed for SSC (overview in Table 8). These samples were used to calibrate the Aquadopp ABS with SSC. The samples were taken via tube/pump from both the hanging Aquadopp and LISST-100X frames.

#### 6-hour calibration campaign

The SSC from the water samples can be compared to the acoustic backscatter measured in the corresponding bin of the Aquadopps. For the water samples collected on the Aquadopp frame, simply the first cell of the vertical, down-facing Aquadopp was used. For the water samples collected on the LISST-100X, the correct cell of the up-looking Aquadopp was selected by comparing the water depths of the two frames (described more in section 3.1). The water depth as documented in the log book for the LISST-100X (rather than as measured by the LISST-100X) was used, as this was considered more reliable.

Ideally, only the backscatter from the beam nearest the water sample would be used. However, the precise orientation of the ADCP relative to the sampling tube is not known, so an average  $ABS_{norm}$  of all three beams is used instead.

Figure 20. Aquadopp acoustic backscatter (from both Aquadopps) calibration to suspended sediment concentration



### 3.2.4 Step 4: Apply the calibration curve to the long-term measurement frames

The next step is to apply the calibration curves developed during the 6-hour campaigns to the long-term measurement frames on the bed. The calibration described in the previous section was simply applied to both long-term Aquadopp datasets. The AWAC was calibrated using the calibrated Aquadopp data, as described in the next section.

### 3.3 Calibrating the AWAC using Aquadopp data

Since the AWACs were not calibrated during the two calibration campaigns, it was necessary to find an alternative method for calibrating the AWAC backscatter to estimate SSC over time. A few approaches were taken and compared:

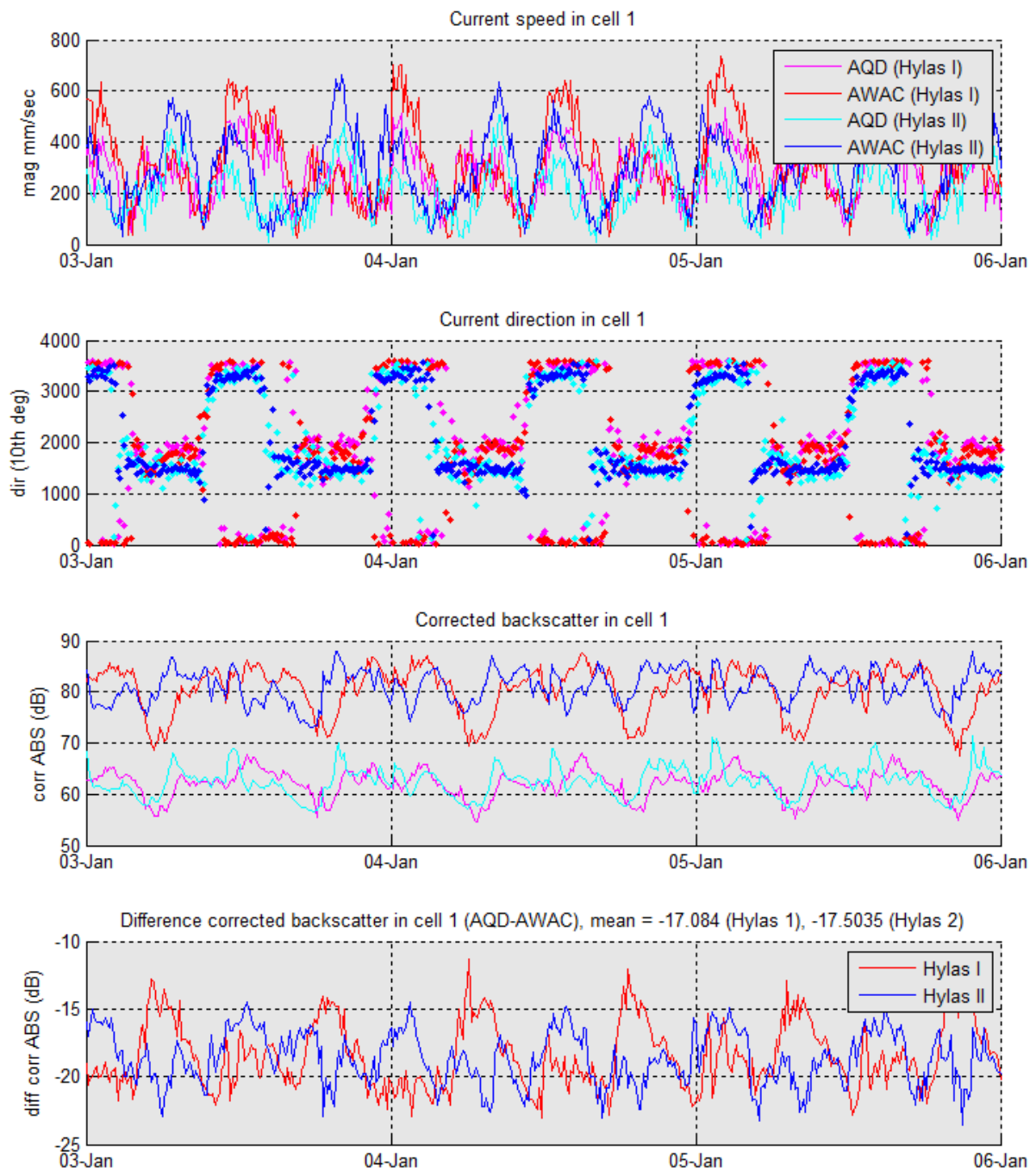
1. Apply the calibration developed for the Aquadopps to the normalized ABS from the AWACs. This approach inherently assumes that the vertical variation in SSC is small at this height above the bed (that the SSC would be the same at 1<sup>st</sup> cell of both instruments).
2. Estimate the SSC in cell 1 of the AWAC by applying a Rouse profile fit to the vertical SSC profile from the Aquadopp. Then, develop a calibration curve for the AWAC relating the AWAC ABS to the predicted SSC in cell 1, that can then be applied to all cells of the AWAC.

The following sections describe each of these methods in more detail.

#### 3.3.1 Method 1: Apply the Aquadopp calibration to the AWAC (with a shift)

This method would simply apply the Aquadopp calibration curve identified in section 3.2.3 to the normalized ABS of the AWAC. Before using this method, the first cell of the down-looking Aquadopp and the first cell of the up-looking AWAC (the two cells closest to each other) were compared (Figure 21). As would be expected, the current magnitude measured by the Aquadopps (which are lower in the water column) are lower than those measured by the AWAC. The current directions are in close agreement. However, a comparison of the range-normalized backscatter shows that the ABS measured by the AWACs is generally higher than that measured by the Aquadopps (average of 17 dB). Since the backscatter has already been range-normalized, any difference would normally be related to differences in SSC at different heights in the water column. However, the results contradict the understanding that SSC is normally lower further from the bed. It is possible that this difference could also be explained by the different frequencies of the instruments (Aquadopp 2 MHz, AWAC 1 MHz), leading the higher frequency Aquadopp to be more sensitive to finer particles than AWAC. Since there is no way to correct for this difference in backscatter caused by grain size/frequency, a simple approach was taken. A shift of ~17 dB (-17.1 for HYLAS I, -17.5 for HYLAS II) was applied to the AWAC before applying the Aquadopp calibration to estimate SSC. As described later in section 3.3.3, this method was not chosen as method 2 was more statistically defensible and better constrained.

Figure 21. Comparison of cell 1 of the down-facing Aquadopp and up-facing AWAC for HYLAS I and II



### 3.3.2 Method 2: Estimate SSC in AWAC cell 1 by applying a Rouse profile to the Aquadopp SSC

Another approach is to develop a calibration specific to the AWAC by predicting the SSC in the first cell of the AWAC using the Aquadopp data (see schematic on the right of Figure 22), and develop a calibration with the measured AWAC. One method to predict SSC at different heights above the bed is the Rouse (1937) profile (Figure 22). Rouse (1937) defines a simple equation for the vertical sediment concentration profile based on one measurement of the concentration at height  $a$  above the bed:

$$\frac{C(z)}{C(a)} = \left[ \left( \frac{h-z}{z} \right) \left( \frac{a}{h-a} \right) \right]^N$$

and

$$N = \frac{w_0}{ku_*}$$

Where:

$C(z)$  = concentration at height  $z$  above the bed

$C(a)$  = reference concentration at height  $z = a$  of the saltation layer (generally  $\sim 0.05h^7$ )

$h$  = water depth

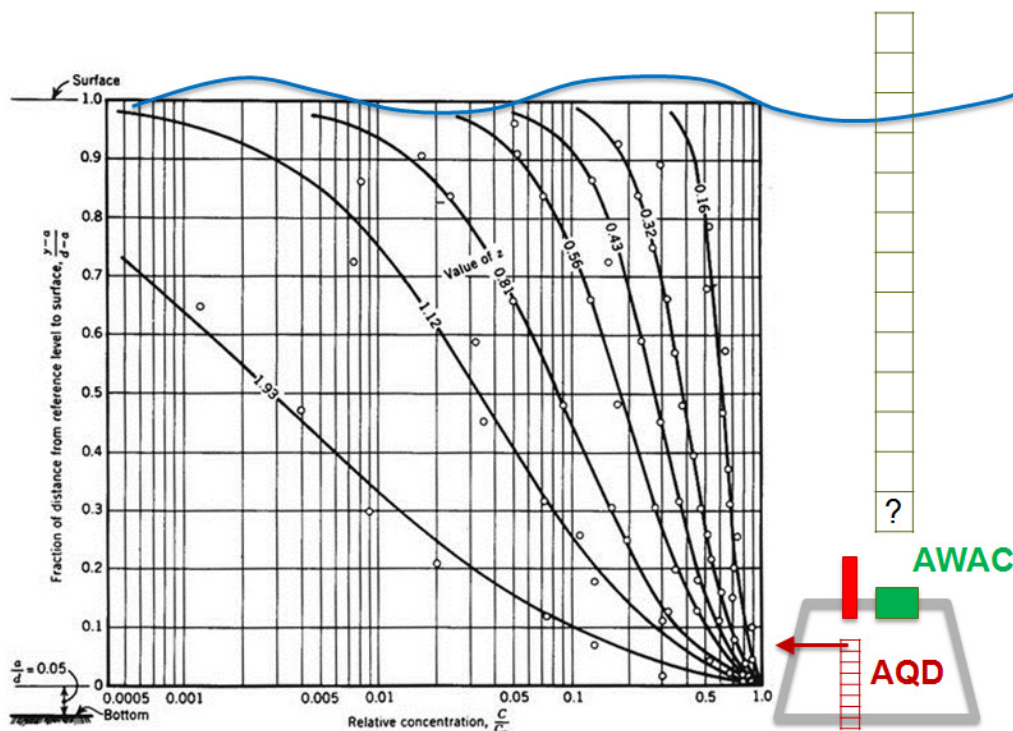
$N$  = Rouse number

$w_0$  = settling velocity

$k$  = von Karman constant (0.4)

$u_*$  = bed shead velocity

Figure 22. Rouse profiles for various  $N$  ( $z$  in the figure) values



<sup>7</sup> [http://www.ics2011.pl/artic/SP64\\_2079-2083\\_K.%20Udo.pdf](http://www.ics2011.pl/artic/SP64_2079-2083_K.%20Udo.pdf)

Graph from [http://apo.sdsu.edu/cive530\\_lecture\\_17b.html](http://apo.sdsu.edu/cive530_lecture_17b.html)

For the current project, the calibrated SSC of the Aquadopp was used to estimate the SSC in the first cell of the AWAC. Table 9 lists the relevant values of  $a$  and  $z$  for HYLAS I and HYLAS II. This table also reports the Aquadopp cell that should be used if assuming that  $a = 0,05 h$ . However, this calculation was done only to check that using the first cell of the Aquadopp was reasonable, since the first cell of the Aquadopp is the one that is best calibrated using water samples. All subsequent calculations use the first cell of the Aquadopp.

Table 9. Aquadopp and AWAC parameters used to develop Rouse profile

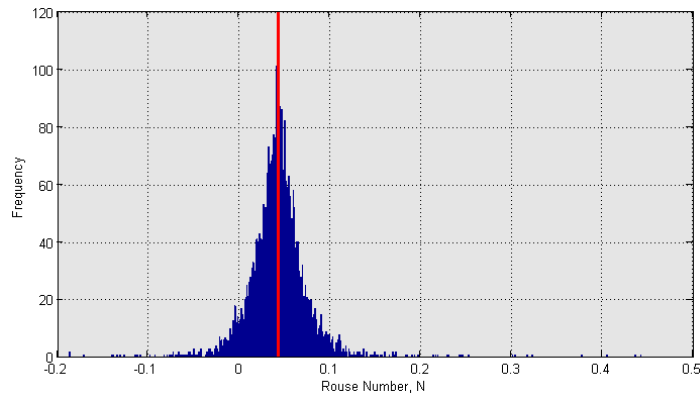
	HYLAS I	HYLAS II
Aquadopp height above bed (m)	1.01	1.26
Median depth above Aquadopp (m)	11.4	7.0
Median water depth, h (m)	12.4	8.26
a, if assuming 0.05 h (m)	0.62	0.41
Aquadopp cell corresponding to a	2	6 or 7
AWAC height above bed (m)	1.39	1.16
Height of cell 1 of AWAC, z (m)	2.29	2.06
Height of cell 1 of Aquadopp, a (m)	0.71 (0.06h)	0.96 (0.11h)

Before the Rouse equation can be applied to estimate SSC for the AWAC, it was necessary to estimate the Rouse number,  $N$ . Since an entire time series of vertical profiles of SSC is available via the Aquadopp, this was used to estimate an average  $N$  value. The Rouse number was solved-for by reorganizing the Rouse equation as follows:

$$\ln\left(\frac{C(z)}{C(a)}\right) = N * \log\left[\left(\frac{h-z}{z}\right)\left(\frac{a}{h-a}\right)\right]$$

Then, the left term was plotted (using  $a$  = first cell of Aquadopp) vs. the right term. A linear fit through the origin gives an estimate of the Rouse number,  $N$ , for each timestep. Figure 23 presents a histogram of the Rouse numbers estimated in this way. The median value is 0.042. A Rouse number less than 0.8 is normally associated with entirely wash load flow (all transported sediments in suspension, normally consists of very fine particles), while a value greater than 2.5 is almost entirely bedload transport. Since the vast majority of the sediment collected in the water samples consisted of fine material (see Figure 45 and Figure 46), a low Rouse number appears appropriate. A negative Rouse number in the histogram occurs in situations when the SSC is higher at the top of the Aquadopp profile than at the bottom.

Figure 23. Histogram of Rouse numbers estimated for each timestep of the Aquadopp data. Median N = 0,042



Since the Rouse number predicted in this way is quite noisy, the median Rouse number was used to predict the SSC in the first cell of the AWAC for the complete time series. From this it is possible to make a calibration between the range-normalized ABS in cell 1 of the AWAC with the predicted SSC in cell 1, as shown in Figure 24 and Figure 25. This calibration shows a similar shape to that developed for the Aquadopp (Figure 20), with a flatter slope for lower ABS that steepens at higher ABS values. Since a “kink” point is much harder to define due to the large number of points, an exponential regression was fit to the point cloud:

$$SSC(ABS) = Ae^{B*ABS}$$

Where:

- SSC(ABS) = the SSC calibrated as a function of range-normalized acoustic backscatter
- ABS = range-normalized acoustic backscatter measured by the AWAC
- A = first calibration constant
- B = second calibration constant

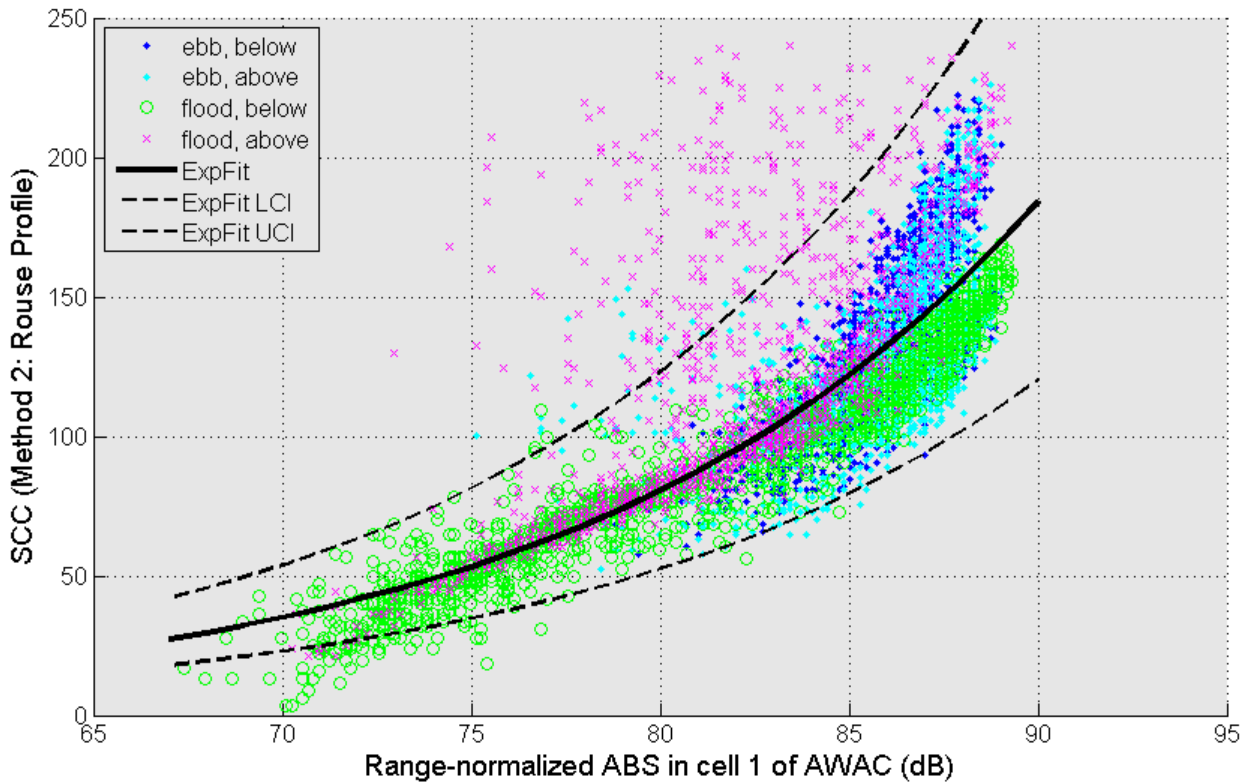
In order to understand the uncertainty associated with this calibration, 95% confidence intervals were derived together with the exponential fit. Table 10 presents the calibration coefficients for the exponential fit and lower and upper confidence intervals. The exponential fits are also plotted on Figure 24 and Figure 25.

Table 10. Calibration coefficients for AWAC SSC to ABS exponential relationship.

Curve	Coeff	HYLAS I	HYLAS II
Fit	A	0.10642440	0.01574259
	B	0.08284983	0.10495120
Lower confidence interval	A	0.06942107	0.01122888
	B	0.08286042	0.10495730
Upper confidence interval	A	0.16315140	0.02207068
	B	0.08283923	0.10494520

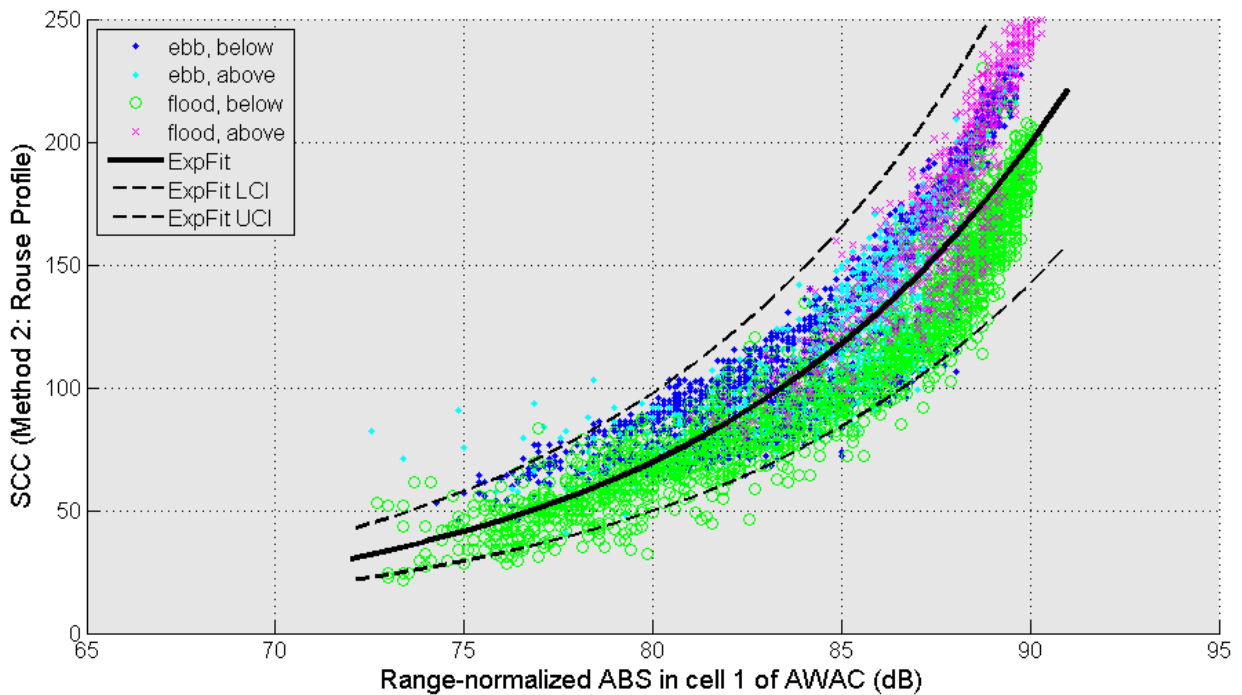
To better understand the jointed and bifurcated nature of the scatterplot, we separate the points into different categories based on whether they are during ebb/flood and above or below a threshold elevation and depth-averaged velocity (Figure 30). The different groupings show clear differences in the relationship between SSC and ABS, which is thought to be related to the type of sediment being transported (see for example Figure 31). This should be investigated further in a subsequent research effort.

Figure 24. Calibration between range-normalized ABS in cell 1 of the AWAC and SSC predicted using a Rouse profile (HYLAS I)



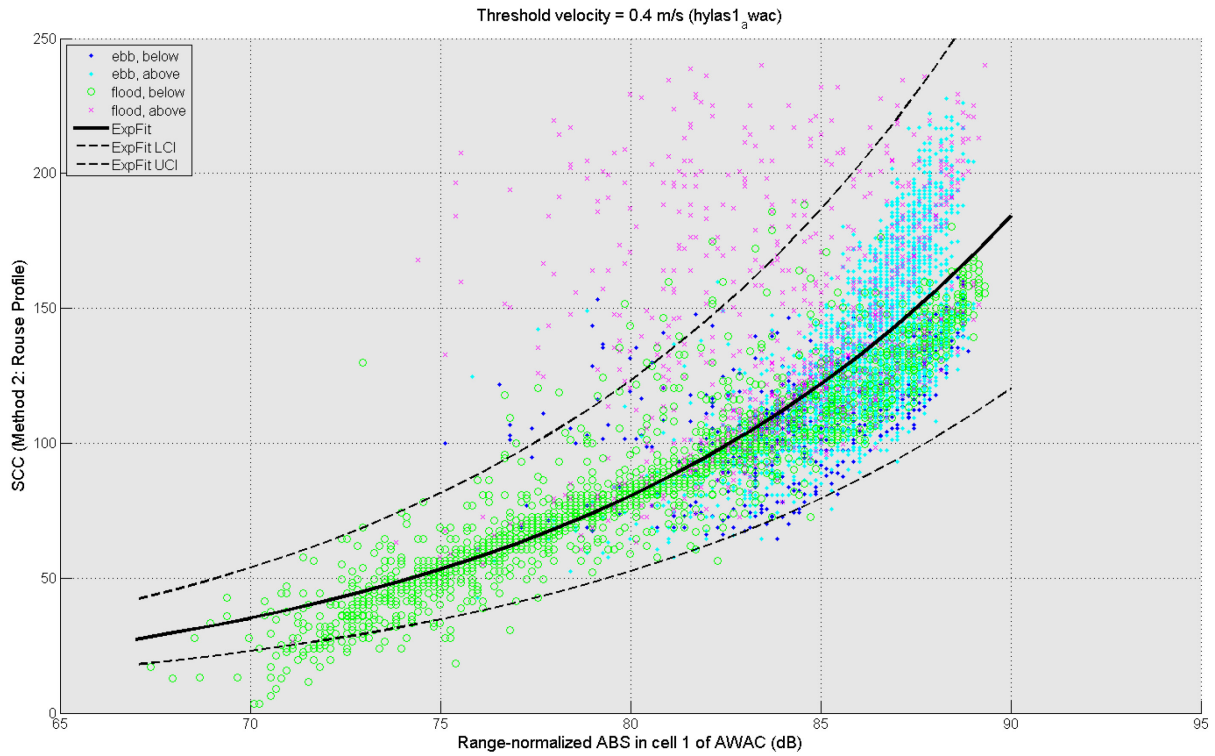
Points are coloured based on ebb/flood and above/below the reference water level of 1 m NAP

Figure 25. Calibration between range-normalized ABS in cell 1 of the AWAC and SSC predicted using a Rouse profile (HYLAS II)



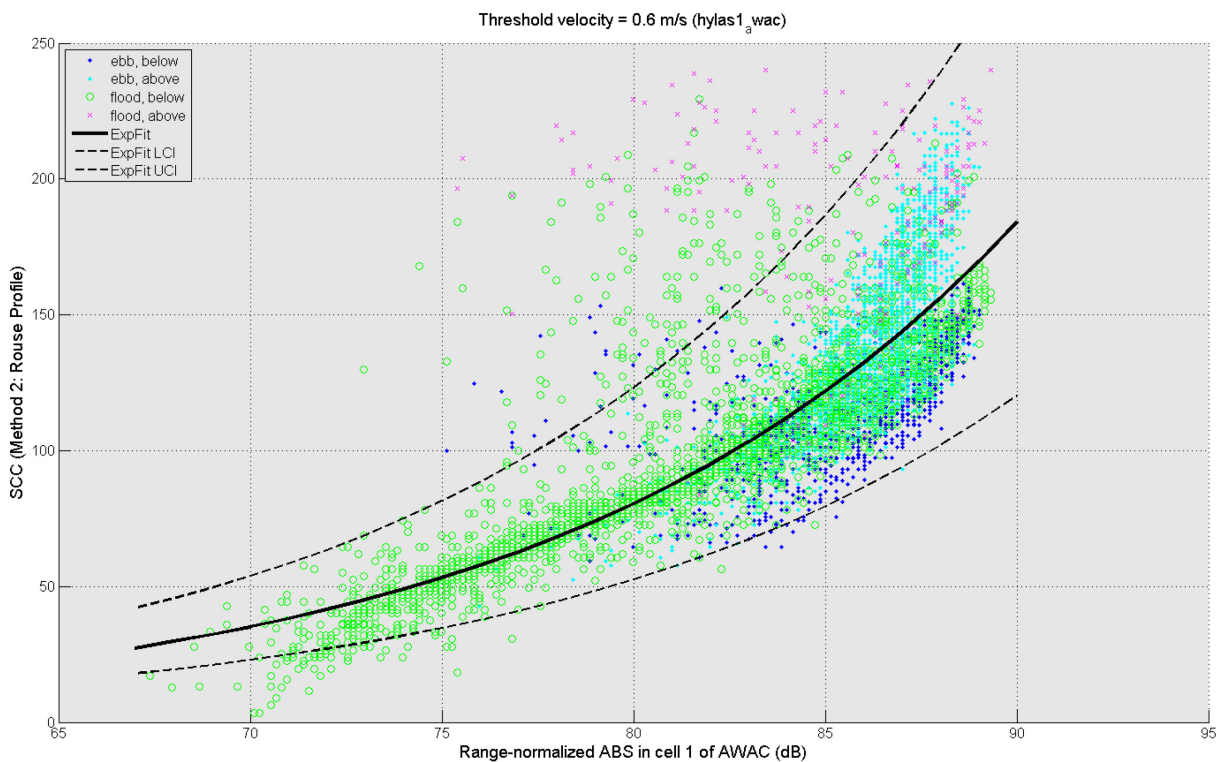
Points are coloured based on ebb/flood and above/below the reference water level of 1 m NAP

Figure 26. Calibration between range-normalized ABS in cell 1 of the AWAC and SSC predicted using a Rouse profile (HYLAS I)



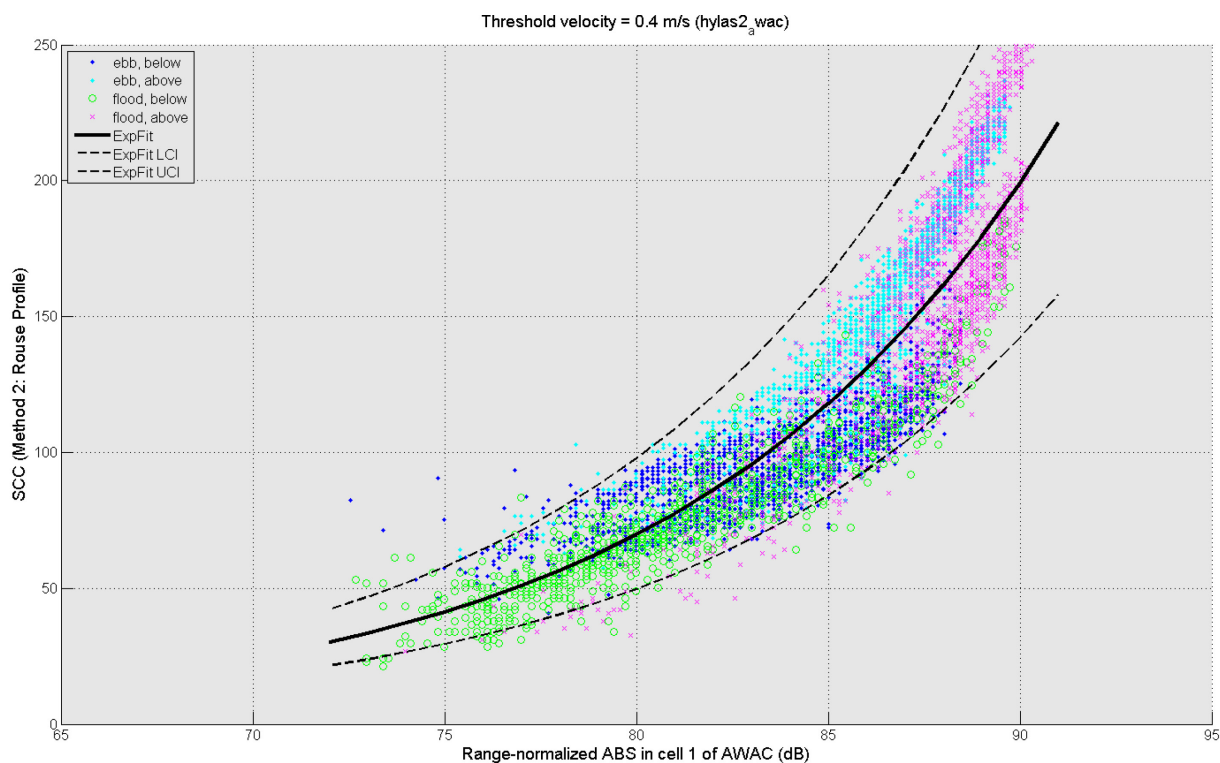
Points are coloured based on ebb/flood and above/below a depth-averaged velocity of 0,4 m/s.

Figure 27. Calibration between range-normalized ABS in cell 1 of the AWAC and SSC predicted using a Rouse profile (HYLAS I)



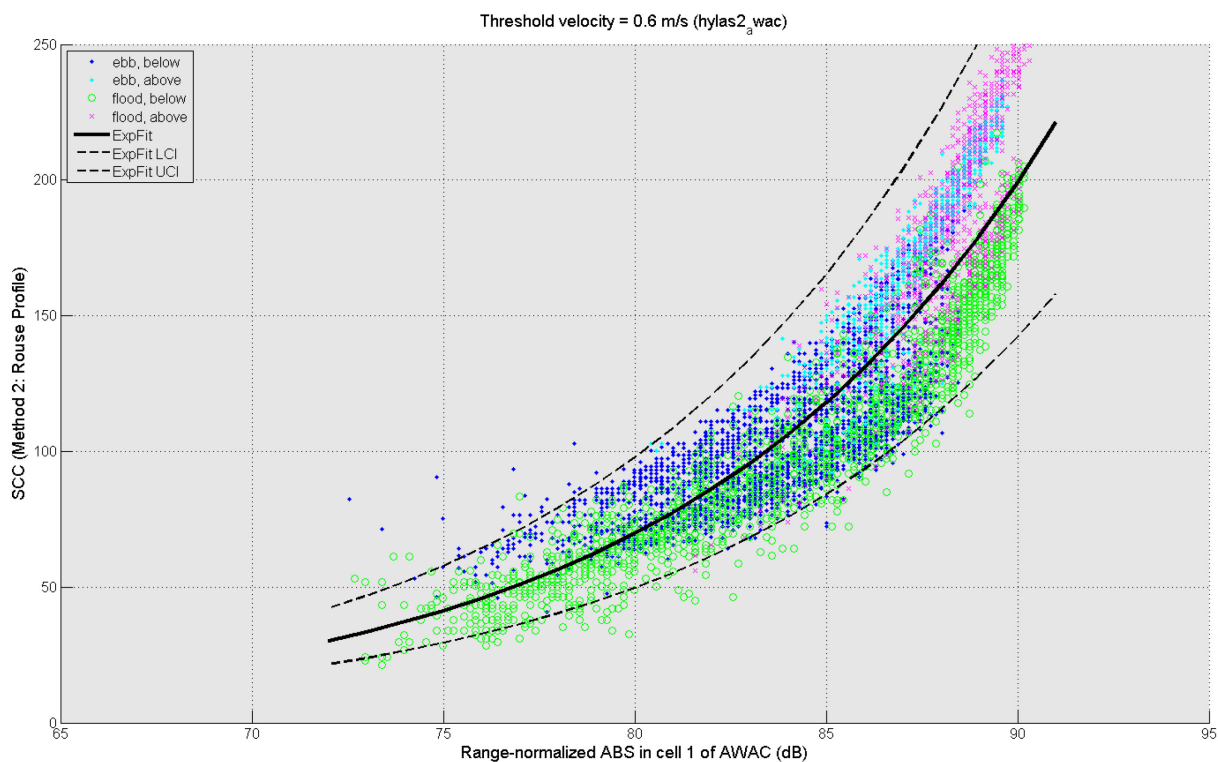
Points are coloured based on ebb/flood and above/below a depth-averaged velocity of 0,6 m/s.

Figure 28. Calibration between range-normalized ABS in cell 1 of the AWAC and SSC predicted using a Rouse profile (HYLAS II)



Points are coloured based on ebb/flood and above/below a depth-averaged velocity of 0,4 m/s.

Figure 29. Calibration between range-normalized ABS in cell 1 of the AWAC and SSC predicted using a Rouse profile (HYLAS II)



Points are coloured based on ebb/flood and above/below a depth-averaged velocity of 0,6 m/s.

Figure 30. Colors indicate how ebb/flood and above/below threshold elevation (top) and depth-averaged velocity (bottom) were identified based on the water level and depth-averaged velocity

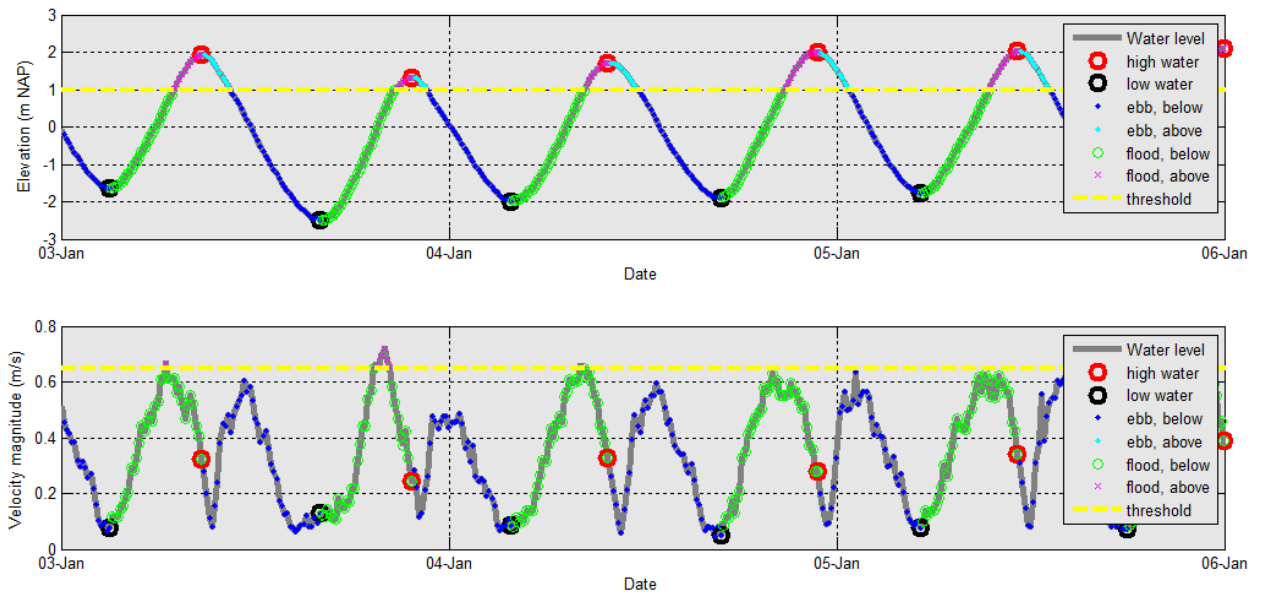
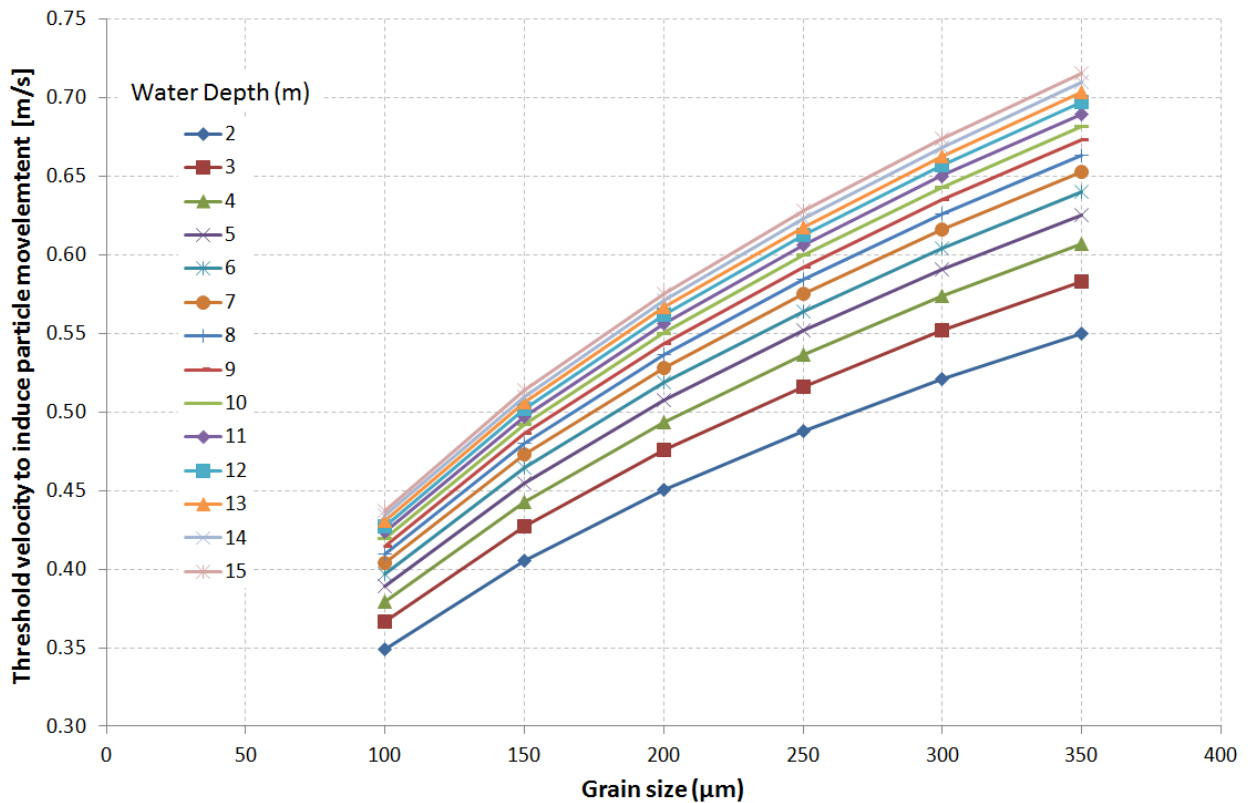


Figure 31. Threshold depth-averaged velocity to initiate movement, by particle size and water depth, according to Jarocki 1963



### 3.3.3 Apply the calibration curve to the long-term measurement frames

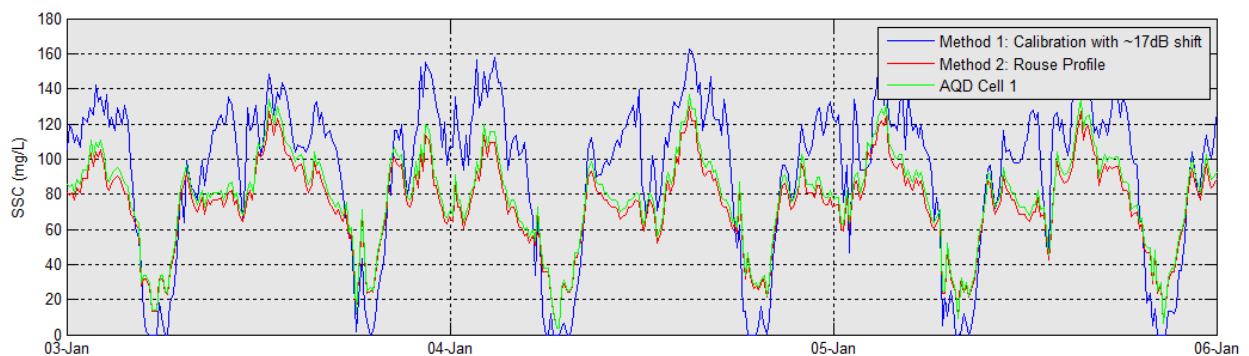
Figure 32 compares the SSC calculated in cell 1 of the AWAC using the two methods described above for the same 3 days show in Figure 21. With a few exceptions, the Rouse Profile method appears to estimate SSCs lower than Method 1. Finally, Method 2 was chosen as the results are constrained to be more realistic (i.e. lower than the values in cell 1 of the Aquadopp) and can be described using 95% confidence intervals, which can be carried through to the total sediment transport calculations.

The exponential calibration curves developed in section 3.3.2 were applied to the complete time series and vertical profiles of range-normalized ABS collected by the AWAC, resulting in a profile time series of SSC over time.

---

Figure 32. Comparison of SSC in cell 1 of the AWAC derived from Method 1 and Method 2 (HYLAS I)

---



## 3.4 Sediment Concentration from YSI and OBS 3+ sensors

The optical backscatter and turbidity measured by the OBS 3+ and YSI sensors, respectively, were converted to suspended sediment concentration (SSC in mg/L) using a calibration curve developed using measurements collected during the two-day calibration campaign. Both OBS 3+ sensors were calibrated on both days, and the calibration fits are shown in Figure 33. Since near-field measurements are considered more accurate, and since the maximum count limit was not reached, the near-field calibration will be applied to the long-term near-field frame measurements. Since only one YSI sensor was functioning during the long-term measurements (on HYLAS II), only that sensor was used during the calibration campaign. The YSI only successfully collected data during the first day of the calibration campaign. Figure 34 shows the calibration fit for the YSI. This fit was applied to the long-term measurements.

Figure 33. Calibration fit for OBS 3+ counts to sample suspended sediment concentrations (HYLAS I and II)

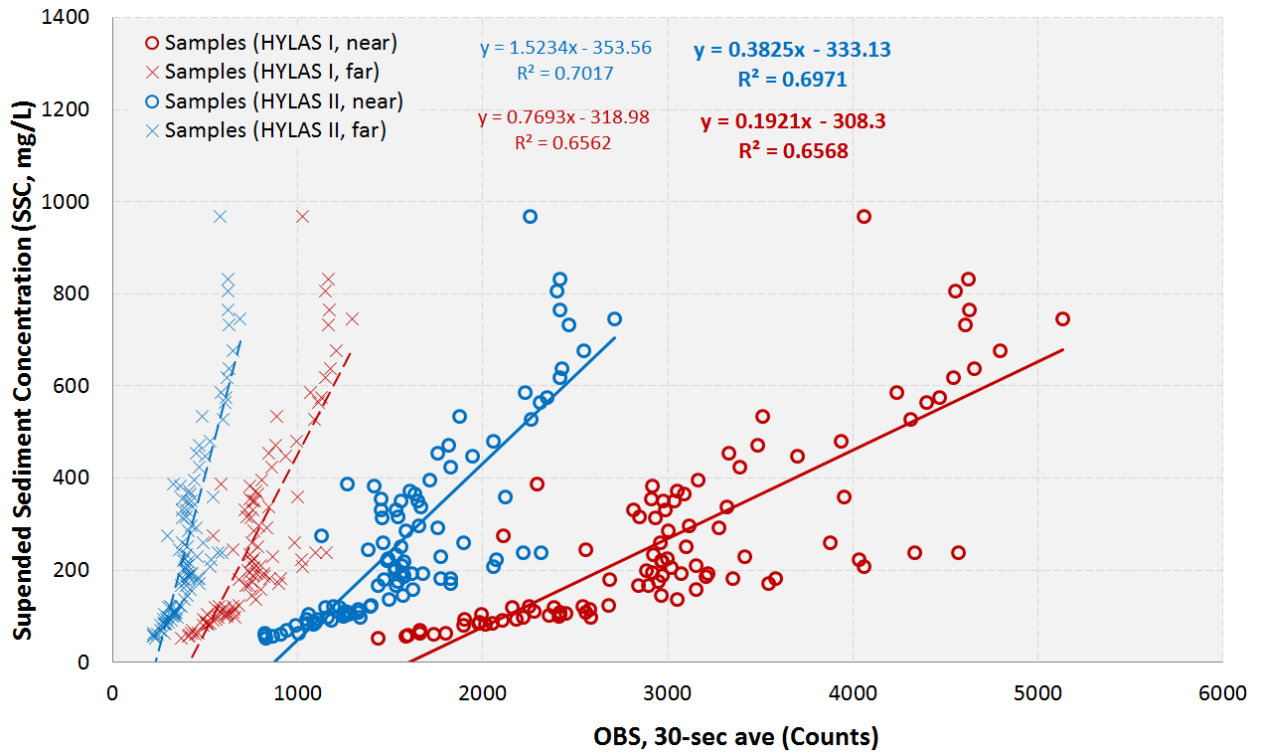
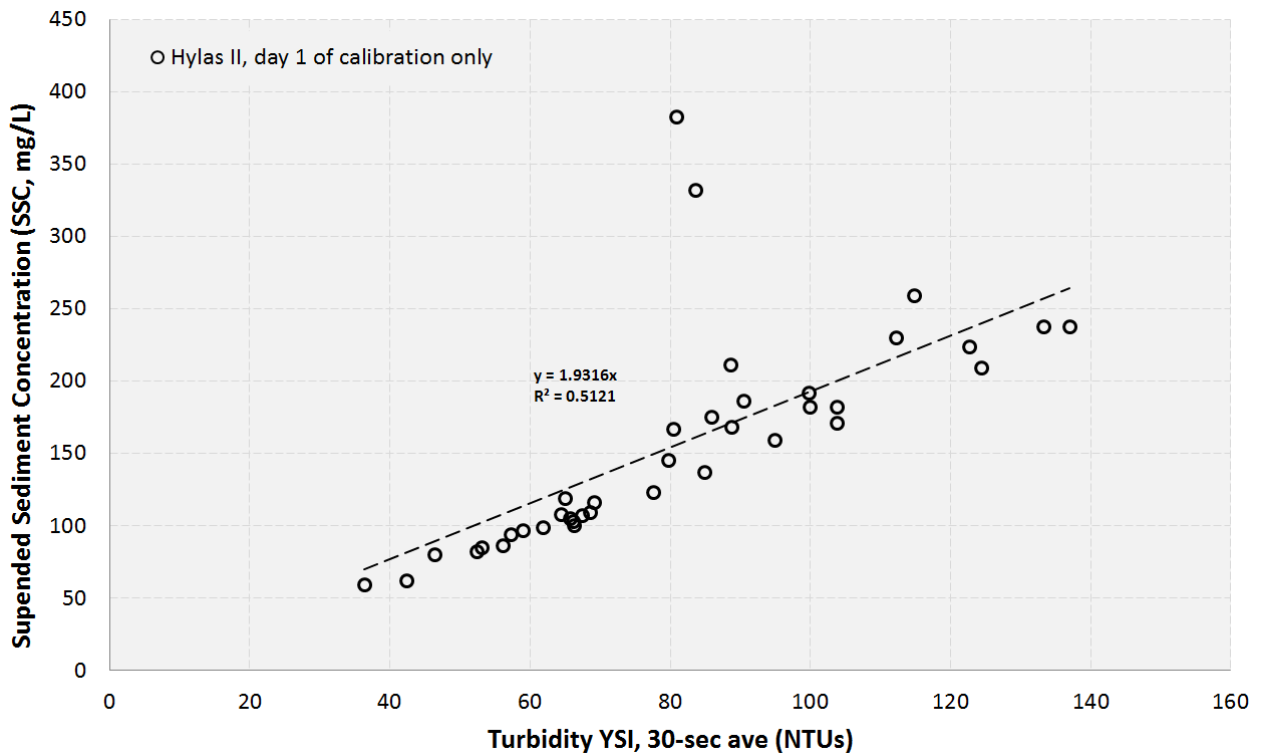


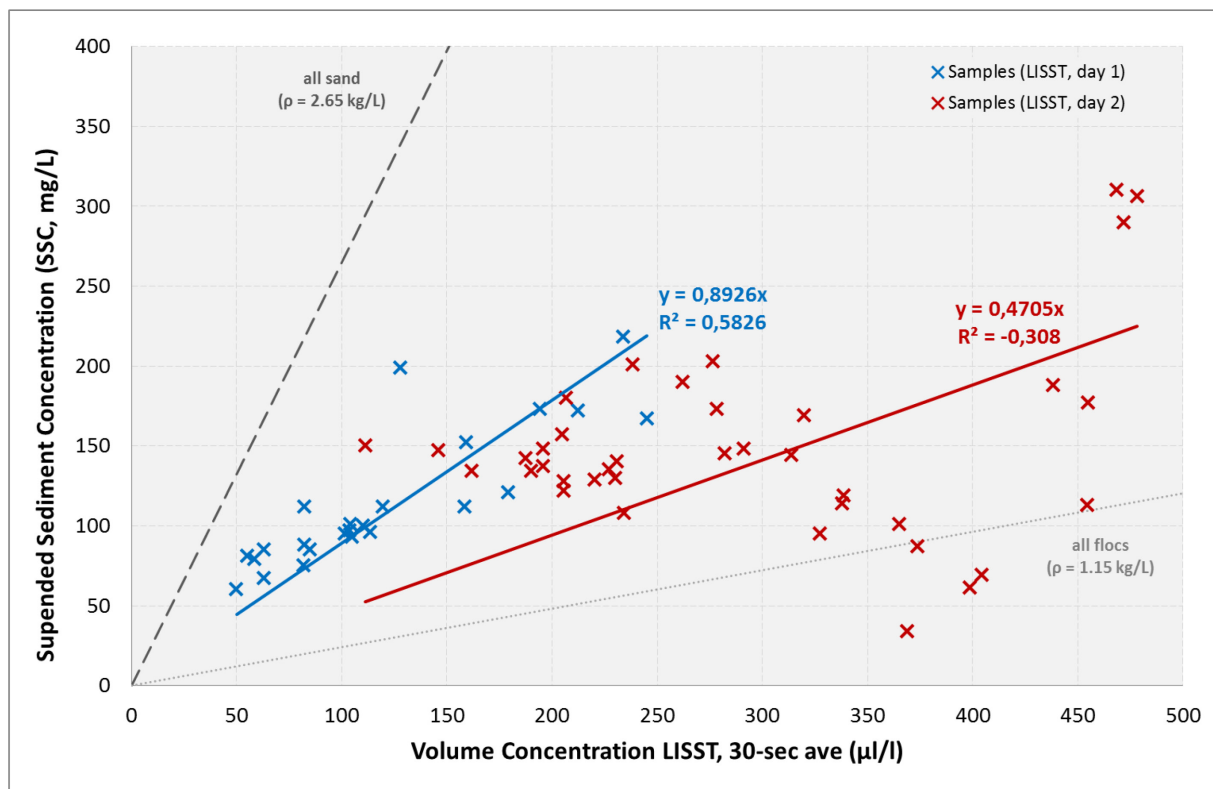
Figure 34. Calibration fit for YSI turbidity to sample suspended sediment concentrations (HYLAS II only)



### 3.5 Sediment Concentration from LISST-100X Volume Concentration

The volume concentrations reported by the LISST-100X (in  $\mu\text{g/L}$ ) were converted to suspended sediment concentration (SSC in  $\text{mg/L}$ ) using a calibration curve developed by comparing the LISST-100X concentration to water samples collected over the courses of both survey days. Figure 18 and Figure 19 plot the LISST-100X volume concentration over time for day 1 and day 2, respectively. Figure 35 presents a scatterplot of the SSC in the water samples collected at the LISST-100X versus the coincident (1-minute averaged) LISST-100X volume concentration. A linear fit (with a zero-intercept) was applied to each measurement day separately, and applied to the LISST-100X volume concentration to develop a continuous time series of SSC over the full 6-hour measurement campaign (see Plancke and Paridaens 2012 for similar analysis). The results are presented in section 4.3. Day 1 and Day 2 show very different calibration results. Day 1 shows a reasonable correlation between volume concentration and suspended sediment concentrations. Figure 18 shows that the general trend in volume concentration matches that of the acoustic backscatter (also an indicator of SSC) from the Aquadopps. However, Figure 19 shows that this is not the case for day 2. The volume concentration measured by the LISST-100X increases almost continuously throughout the day, while the Aquadopp backscatter shows a temporary but substantial drop after high tide. The water samples agree with the Aquadopp trends. The fact that this is not measured by the LISST-100X may be an issue with the LISST-100X on day 2. LISST-100X and ABS measurements collected at Oosterweel show a similar divergence of LISST-100X volume concentration from ABS and water samples (Thant and Plancke, 2016). That study suggested that this may be related to grain size, but is not able to verify this hypothesis. Fortunately, since the LISST-100X calibration is not used in calibrating the long-term measurements, this issue does not directly affect the long-term sediment transport rates derived in the current study.

Figure 35. Calibration fit for LISST-100X volume concentration to sample suspended sediment concentration



The link between volume concentration and suspended sediment concentration (a.k.a. “mass concentration”) is the density of the suspended particles. Two dashed grey lines are added to Figure 35

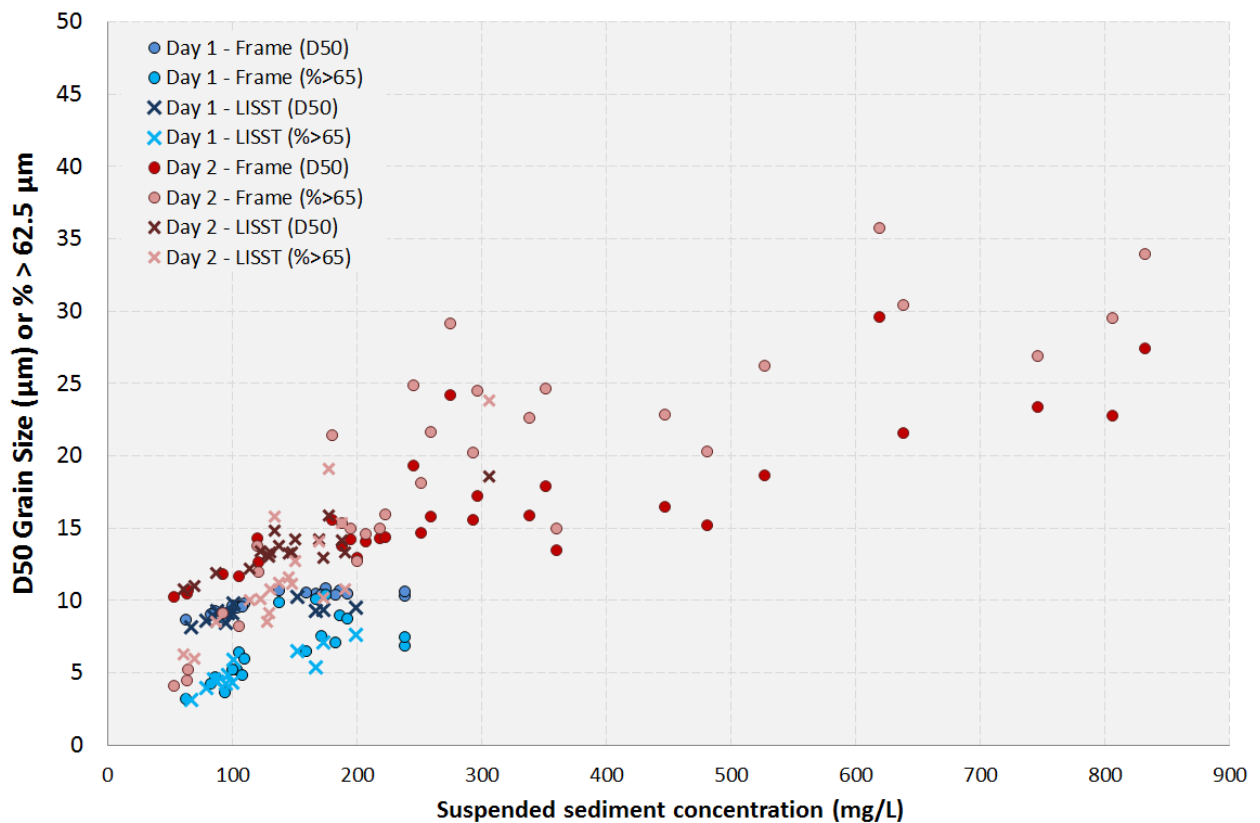
to show what the fit would be if the material was perfectly sandy (with a sediment density of 2,65 kg/l) or floc-dominated (with a representative “floc” density of 1.15 kg/l, Gartner et al 2001, IMDC 2007). The SSC was calculated by multiplying the volume concentration by assumed particle (pure sediment or floc) density:

$$SSC \left( \frac{mg}{l} \right) = VC \left( \frac{\mu l}{l} \right) * \rho_{sediment} \left( \frac{kg}{l} \right) * \frac{1l}{10^6 \mu l} * \frac{10^6 mg}{1kg} * \left( 1 - \frac{\rho_{sediment} - \rho_{floc}}{\rho_{sediment} - \rho_{water}} \right)$$

The density of the particles can also indirectly be related to grain size. Generally, larger grain sizes (i.e. sandier material) will result in a lower volume concentration with a higher SSC, falling above the regression line.

Figure 36 shows the resulting relationship between suspended sediment concentration and grain size. Grain size (both D50 and % of sediment that is considered sand) and SSC are directly correlated.

Figure 36. Sediment grain size as related to suspended sediment concentration



### 3.6 Combining AWAC and Aquadopp profiles

The AWAC data measured the current profile above the long-term frame, while the Aquadopp measured the current profile near the bed (see frame set-ups in For current profile calculations we assume that the frame sunk 25 cm into the bed. This is based on looking at the Aqd current profiles.

#### 3.6.1 Aquadopp Profilers (ADP)

Acoustic Doppler current profilers (ADCPs) measure the current profile on the basis of acoustic Doppler technology. This monitoring campaign used two Aquadopp Profilers manufactured by Nortek (one

horizontal and one vertical). The instrument is capable of being deployed for long time frames using an internal battery and datalogger with sufficient data capacity. The dimensions and technical specifications of the Aquadopp Profiler are shown in Figure 5 and in Table 3, respectively. More details can be found in Appendix A.

Figure 3 and Figure 4). The following post-processing steps combine the two into a single profile that captures the complete vertical velocity, SSC, and sediment transport profiles.

Due to the blanking distance of the two instruments, gaps of 1.5 meters (HYLAS I) and 1,1 meters (HYLAS II) exist between the AWAC and Aquadopp data, so the vertical profile must be interpolated in order to estimate water and sediment transport at these heights. The method used to interpolate depends on the type of data (velocity, SSC, sediment transport). The various methods are described in the sections below.

As described in section 2.3, both instruments were set to collect data at the exact same timesteps, so no interpolation was required to align the timesteps. A new bin structure was set up with the (smaller) bin resolution of the Aquadopp (0.1 m), onto which the Aquadopp and AWAC data were resampled before applying the following interpolations.

### 3.6.2 Velocity magnitude and direction

The velocity magnitude was estimated using the log-law for turbulent boundary layers. For each timestep, the following log profile was applied to the measured vertical velocity data to obtain a best fit:

$$U = \frac{u^*}{\kappa} \ln(z) + C$$

Where:

U = velocity magnitude (*input*)

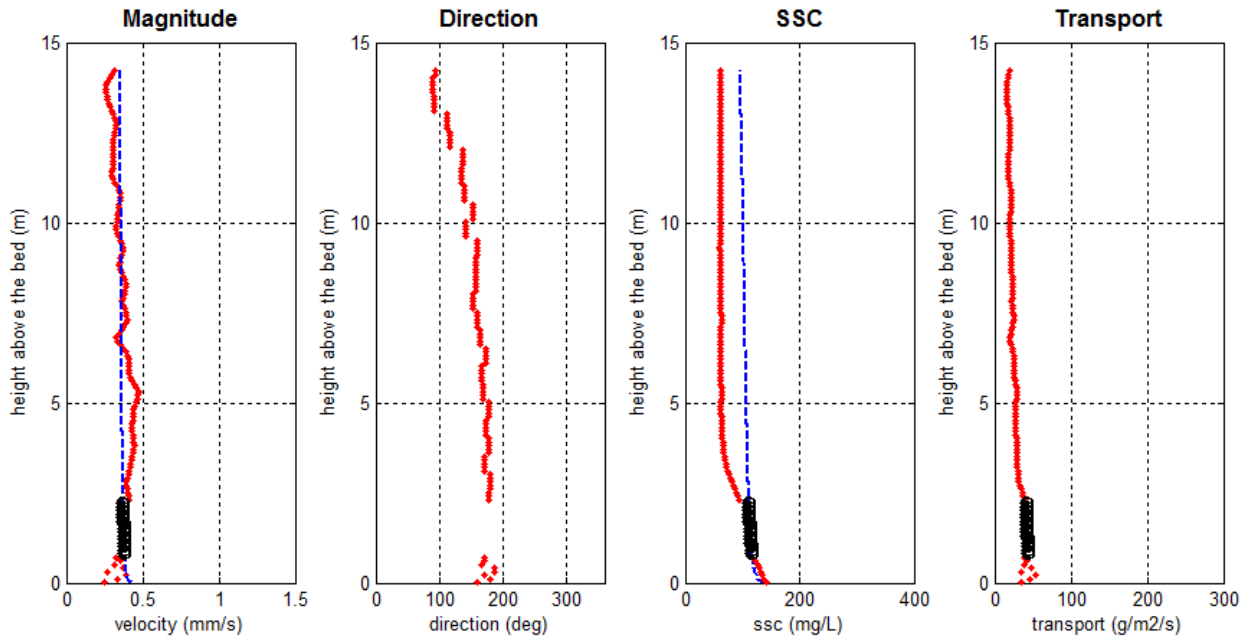
$u^*/\kappa$  = shear velocity/Von Karman constant (*solved for*)

z = height above the bed (*input*)

C = constant (*solved for*)

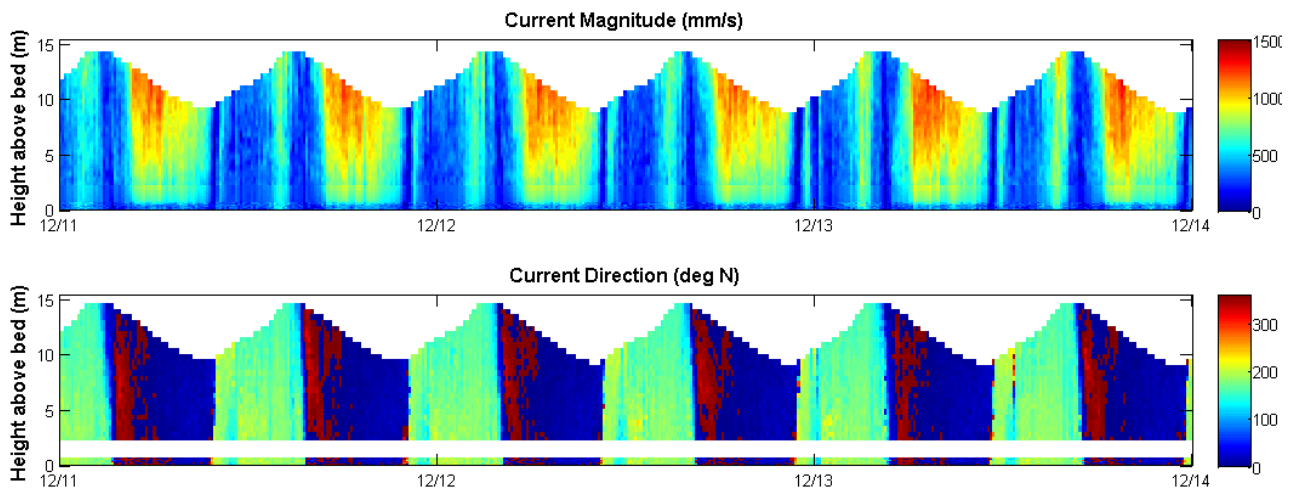
The best fit equation was then applied to z-values corresponding to the bins between the measured Aquadopp and AWAC data. An example of such a fit is shown in Figure 37.

Figure 37. Examples of (left) log interpolation between measured AWAC and Aquadopp velocity, (middle) Rouse profile extrapolation of Aquadopp velocities, and (right) transport rate calculation in the gap (black circles) based on the magnitude and SSC



Interpolating the direction data is more complicated, as the direction sometimes jumps between 0 and 360 degrees, so an assumption was made that the gap could be ignored. This assumption can be made given that the direction does not vary significantly in the vertical direction (see example in Figure 38, left).

Figure 38. Example of velocity profile over time. (top) velocity magnitude, including interpolated area. (bottom) velocity direction, with gap. Velocity magnitude varies much more than direction over the vertical profile



### 3.6.3 Suspended sediment concentration (SSC)

The suspended sediment concentration in the gap between the AWAC and Aquadopp was calculated using the same Rouse profile ( $N = 0.041$ ) described in section 3.3. An example is shown in Figure 37 (middle).

## 3.7 Sediment Transport Rate

The sediment transport rate in each bin ( $\text{g/m}^2/\text{s}$ ) was calculated by multiplying the bin SSC by the bin velocity magnitude, resulting in a vertical and temporal grid of sediment transport rates. Finally, a time series of total sediment transport rates ( $\text{g/m/s}$ ) was calculated by summing the sediment transport rates over all the vertical bins and multiplying by the bin size.

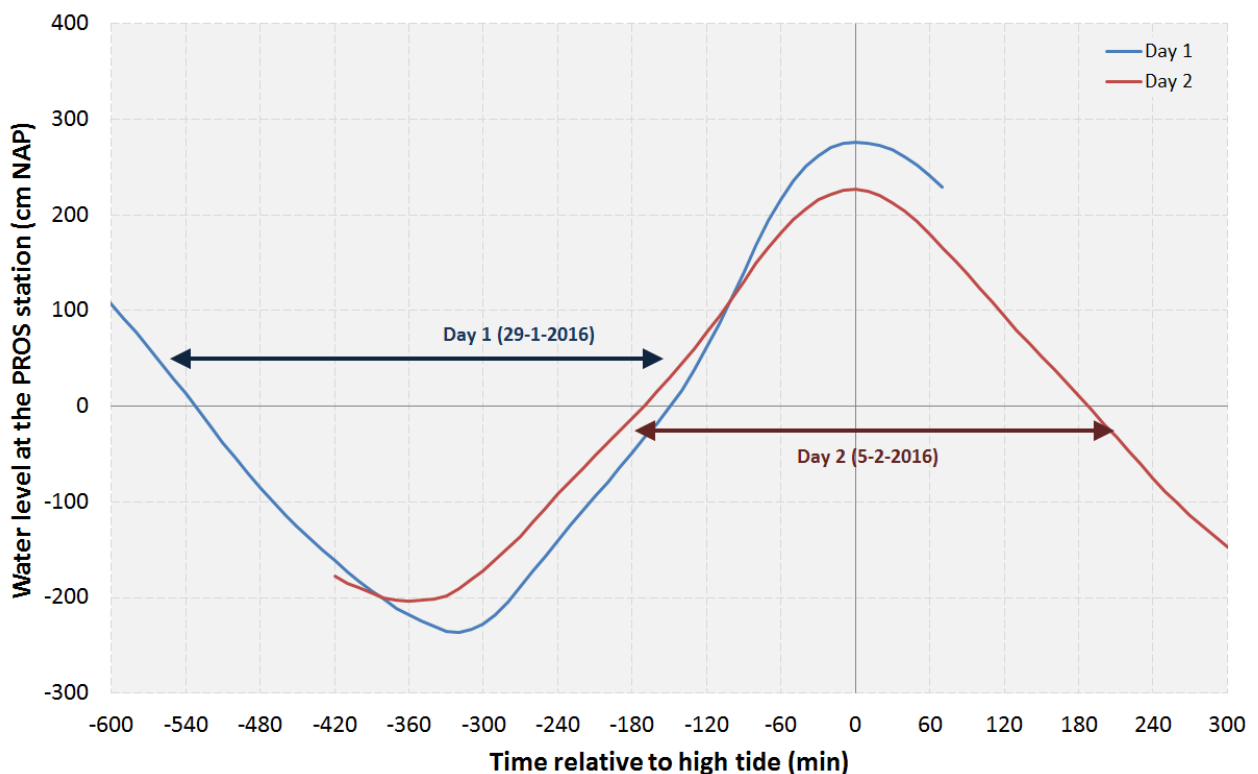
## 4 Results: Stationary 6-hr Calibration Campaigns

The following sections present the measurements collected during the two 6-hour calibration campaigns, after post-processing as described in section 3.

### 4.1 Water levels

Figure 39 describes the tidal conditions during the 6-hour measurements, as measured at the PROS water level station (location shown in Figure 2). Both campaigns started just before slack tide, and ended at the next slack tide, with the first and second campaigns measuring during a low and high tide, respectively. The low tide was -2.36 m NAP on the first day, and the high tide was 2.27 m NAP on the second day. For average tidal datums, please refer to Table 1.

Figure 39. Water levels during the two days of 6-hour calibration measurements



### 4.2 Currents

Figure 40 and Figure 42 present the depth-averaged currents as measured by the up-looking Aquadopp during the stationary 6-hour measurements day 1 (January 29<sup>th</sup>, 2016) and day 2 (February 5<sup>th</sup>, 2016), respectively. Since the Aquadopp was deployed using the same settings as used during the long-term campaign, only 1.5 m of the water column was measured (see Figure 14 and Figure 15 for a visualization

of which part of the water column was measured by the up-looking Aquadopp at a given moment), so the “depth-averaged” values here should only be used as an indicator of the relative changes in current velocity. The gap on Day 1 that occur between approximately -490 and -450 minutes is when the boat was moved from SOD6 to Lillo, causing all instruments to be brought on board.

On day 1, the current magnitude was slightly stronger (around 0.8 m/s) at the start of the measurements and at slack tide. The lowest currents (about 0.4 m/s) were measured in the middle of the campaign, around low later. From the start of the measurement campaign, the direction slowly turned, starting around -30 degrees and increasing to about 160 degrees at the end of the campaign. In the middle both the directions and currents are very noisy. This can probably be explained by the calibration campaign not sitting completely on the bed. A comparison of Figure 14 and Figure 49 shows that after low water (around HW -320'), the water depth above the frame stayed constant. That means that the frame was no longer sitting on the bed. This can also be seen in the instrument orientation as recorded by the Aquadopp (Figure 41), which shows that the frame was moving almost constantly between 2 and 5 hours of the measurement campaign. The current direction and magnitude are not used directly in calibration of the long-term instruments, so this hopefully will not affect the results. However, if the backscatter (which does not rely on the instruments' internal compasses) was also affected by this motion, it may have an effect on the quality of the calibration.

On day 2, the strongest currents were measured around HW-70 minutes, during the flood-phase of the tide, just before high water. The depth-averaged magnitude reached 1.1 m/s. The lowest currents measured were approximately 0.1 m/s, about 1 hour after high water. During these low flows, the measured current direction is quite variable, due to difficulty of estimating the mean flow direction at such low flows. For the three hours before high water the direction is relatively stable, around 120 degrees. About an hour after high water it turns 180 degrees and stabilizes again around 300 degrees for the rest of the campaign.

Figure 40. Depth-averaged currents as measured by the up-looking Aquadopp during the first calibration campaign on 29-1-2016

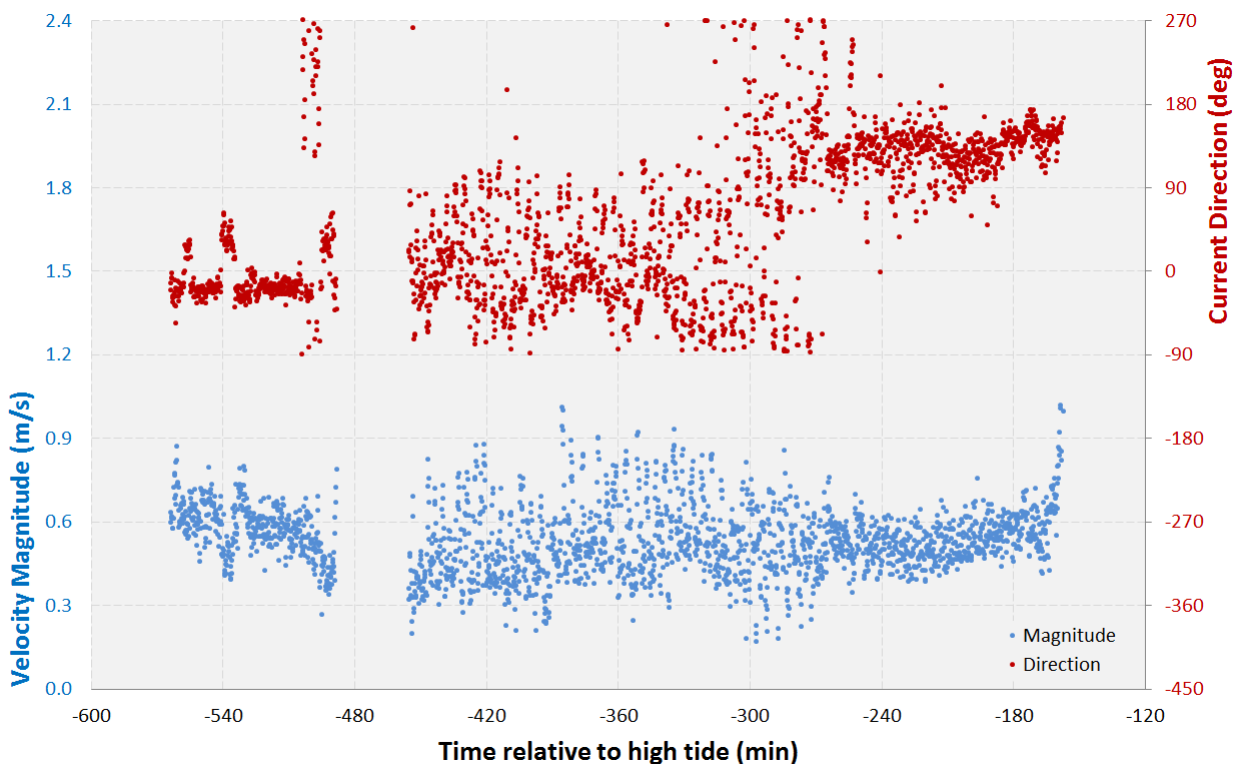


Figure 41. Instrument orientation recorded by the Aquadopp during the first calibration campaign on 29-1-2016

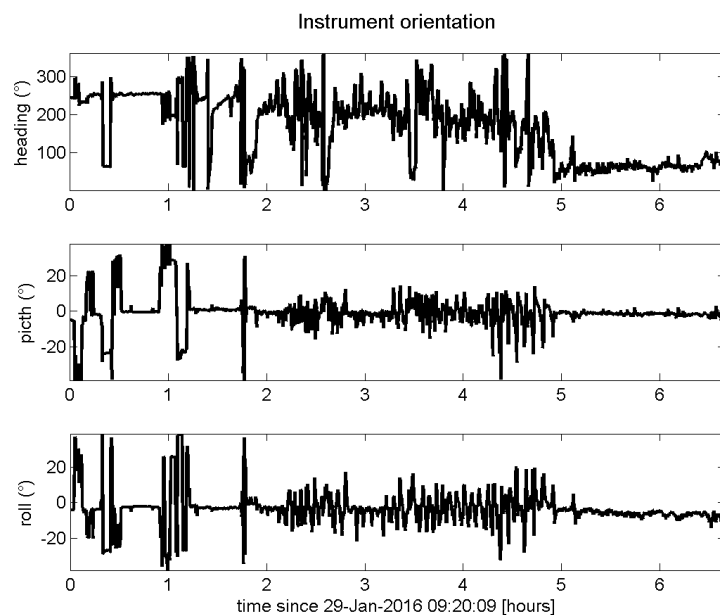
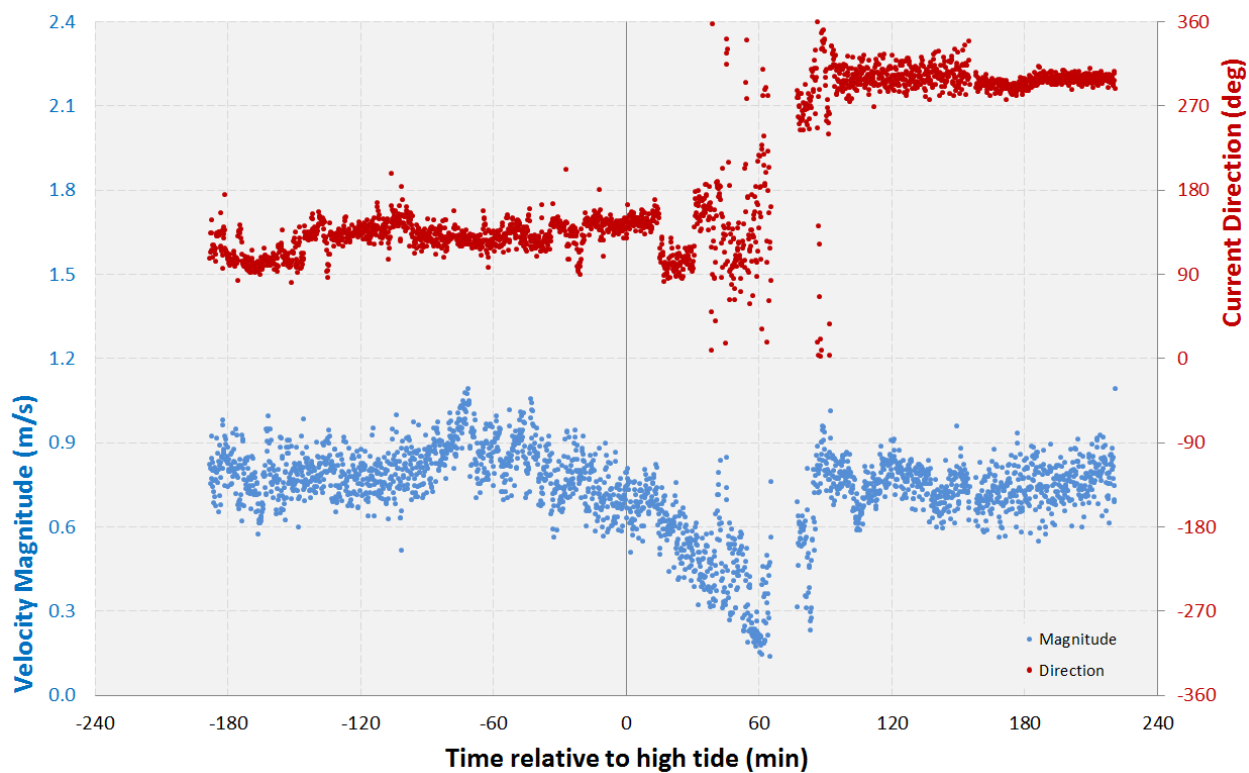


Figure 42. Depth-averaged currents as measured by the up-looking Aquadopp during the second calibration campaign on 5-2-2016

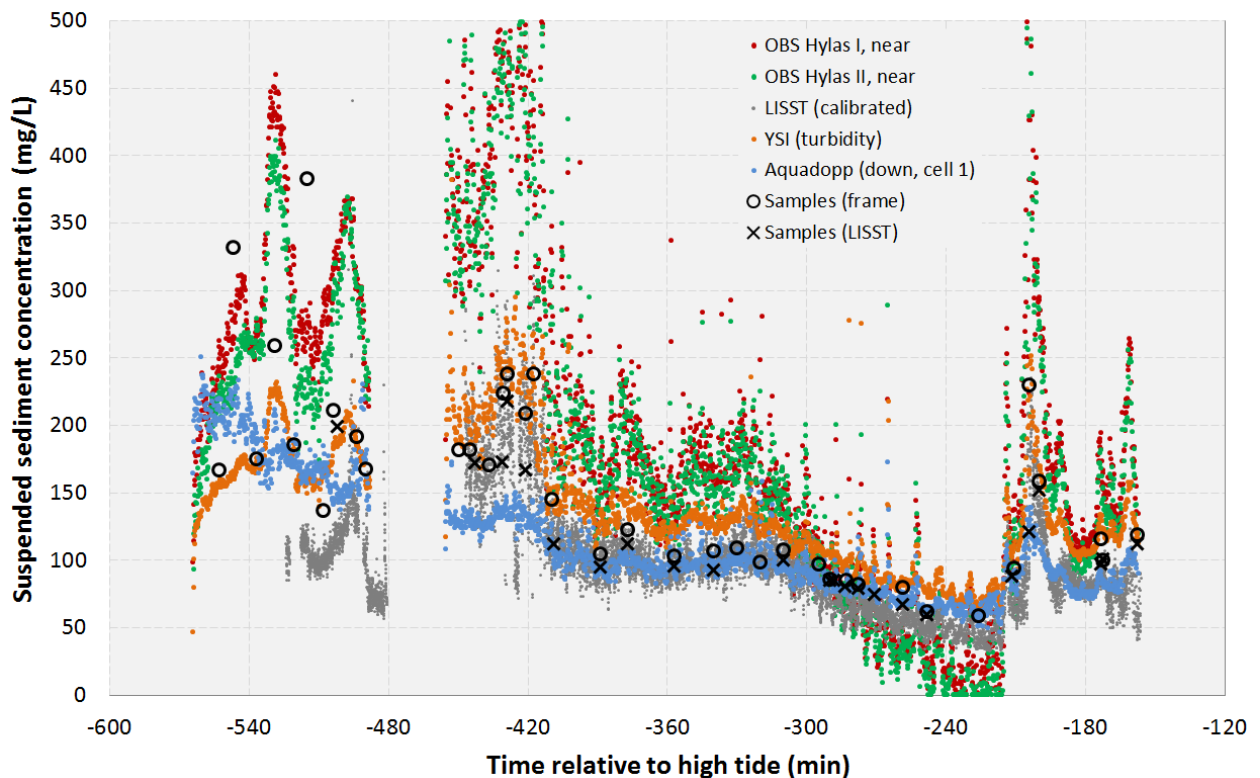


### 4.3 Suspended sediment concentration (SSC)

The suspended sediment concentration (or an indicator thereof) was measured by the LISST-100X (as volume concentration), Aquadopp (as acoustic backscatter), YSI (as turbidity), and in water samples during the 6-hour calibration campaigns, as described in section 2.3.3. The volume concentration and acoustic backscatter were calibrated as described in sections 3.2 and 3.2, respectively. The resulting 6-hour time series of SSC from all techniques are shown in Figure 43 and Figure 44 for day 1 and day 2, respectively.

On day 1, all measurement techniques are in general agreement about the trends in SSC, especially those collected after the campaign was moved to Lillo (around HW – 450 minutes). The measurements at the SOD6 location (before the time gap), show some discrepancies between the water samples and the calibrated time series. SSC samples at this location varied between 135 and 380 mg/L, while the calibrated time series report SSC values between 60 and 240 mg/L. The measurements at Lillo, which start just after slack tide, start with SSC measurements up to 240 mg/L, but quickly drop below 150 mg/L around HW – 420 minutes. Low tide is at HW – 320 minutes, and at this point the concentrations continue to decrease, to as low as ~50 mg/L. The concentrations then increase again as the water level begins rising more rapidly (around -200 minutes).

Figure 43. Suspended sediment concentrations as measured by the LISST-100X, Aquadopp, OBSs, and YSI during day 1 (29/1/2016), calibrated using the intermittent water samples (black circles/Xs). Aquadopp measurements are for the first cell of the down-looking Aquadopp

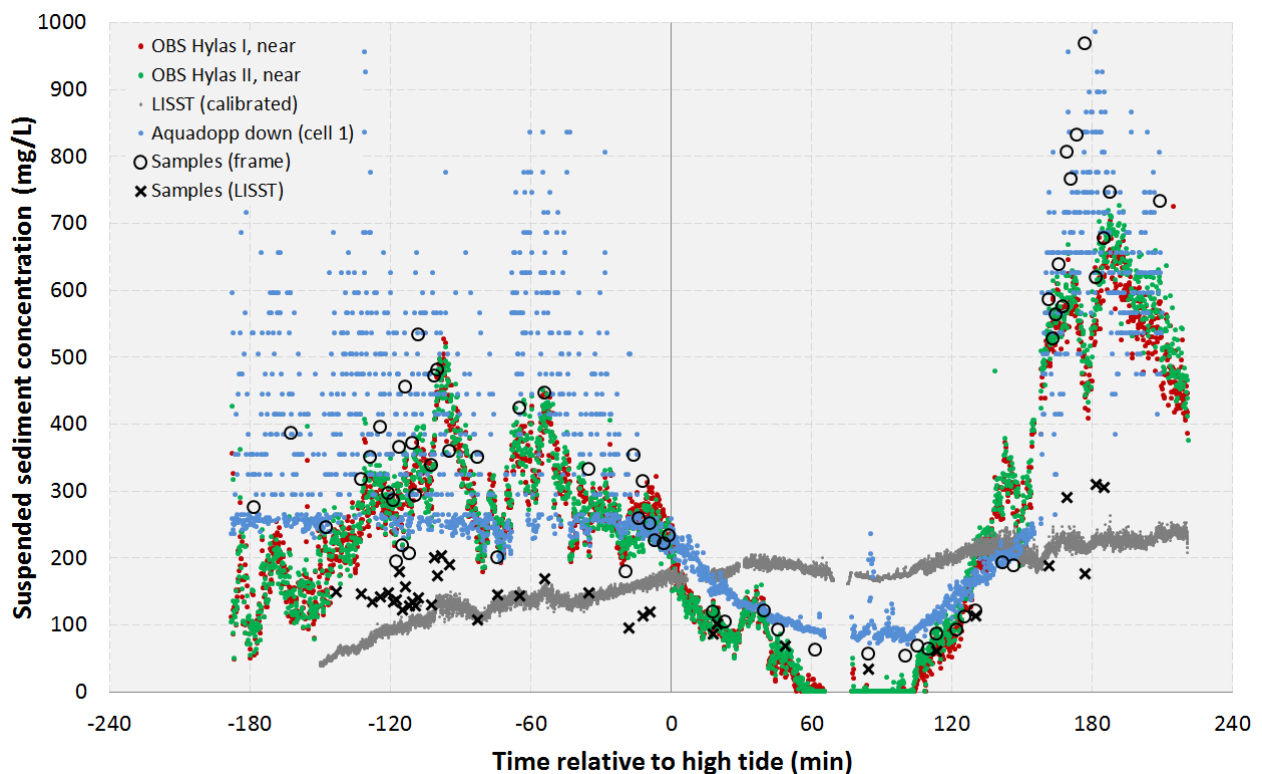


On day 2 there is a different story. Figure 44 plots the time series of water samples and calibrated LISST-100X and Aquadopp SSCs. The samples collected on the Aquadopp frame show much higher SSCs than those collected on day 1, with values peaking as high as 970 mg/L. The calibration for the Aquadopp backscatter (Figure 20) shows a clear “kink” in the trend around 80 dB. That change in slope of the calibration curve is the reason for the cloud of SSC estimates derived from the Aquadopp.

The Aquadopp backscatter (Figure 19) and measured water samples show somewhat similar trends (higher SSC/backscatter at the start and end of the measurement campaign, and a low point around 90 minutes after high tide (Figure 44)). The LISST-100X, however, shows a completely different trend. This is a result of an insufficient calibration curve derived for the LISST-100X, as described in section 3.3.

One clear discrepancy that appears during day 2 of the campaign is the difference in SSC for the water samples collected on the Aquadopp frame compared to those collected next to the LISST-100X. Since the LISST-100X was generally about 2-3 meters higher in the water column than the Aquadopp frame (Figure 15), this is in agreement with the expectation that SSC would be higher near the bed. This difference in SSC measured at the LISST-100X/Aquadopp does not appear on day 1, but that can be explained by the fact that the LISST-100X and Aquadopp were closer together in the water column (Figure 14).

Figure 44. Suspended sediment concentrations as measured by the LISST-100X, Aquadopp, and OBSs during day 2 (5/2/2016), calibrated using the intermittent water samples (black circles/Xs). No YSI data was recorded on day 2. Aquadopp measurements are for the first cell of the down-looking Aquadopp



#### 4.4 Grain size distribution

The median grain size (D50) and sand fraction (% >63  $\mu\text{m}$ ), as measured by the LISST-100X, are plotted in Figure 45 or day 1 and Figure 46 for day 2 of the calibration campaign. Overlaid are the median grain size and sand fraction of the water samples collected adjacent to the Aquadopp and LISST-100X frames.

The two sets of water samples are generally in agreement. On day 1 the median grain size does not change substantially throughout the measurement period, varying between 8 and 11  $\mu\text{m}$ . The grain size of samples collected near the LISST-100X are slightly smaller than those collected near the Aquadopp. The sand fraction decreases gradually from 10% to 3%. Around HW-200 minutes it increases slightly again to 6%. The LISST-100X and Aquadopp samples follow the same trend in sand fraction.

Day 2 experiences more variation in grain size distribution (Figure 46 and Figure 47). The beginning and end of the day are characterized by larger grain size (D50: 20 – 30  $\mu\text{m}$ ) and sandier composition (25 – 36%). Values drop gradually until about 1 hour after high tide, when grain sizes of 10 $\mu\text{m}$  and sand fractions of 4% are observed. The samples collected near the LISST-100X and Aquadopp show the same trends, though the magnitude of the variation is greater for the samples collected on the Aquadopp frame, which is to be expected as this frame was closer to the bed.

In general, the samples collected during this calibration campaign were less sandy compared to the those found at Hansweert (multiple samples with D50 of  $\sim 170 \mu\text{m}$ , Vandebroek *et al.*, 2017).

An immediate difference is apparent between the values measured by the LISST-100X and the water samples. One possible hypothesis for this is that the LISST-100X tends to record flocs as large grains of sediment, while the actual grain size is much smaller. Therefore, the LISST-100X may show a trend that is inverse what is collected in the water samples. This is particularly apparent on day 2 (Figure 46), when lab samples show higher grain sizes in the beginning and end of the campaign, while the LISST-100X shows largest grain size in the middle of the campaign. A closer look at the period between HW + 120 minutes to HW + 200 minutes (Figure 47) appears to support this theory:

- HW + 120': Flocs, which register as large grain size by the LISST-100X but small in the lab-samples are being transported at the lower velocities.
- HW + 160': The lab samples show an increase in sand fraction, while the LISST-100X grain size continues to decrease.
- HW + 175': Sand fraction increases in both the LISST-100X and lab samples, which could be explained by a large increase in volume concentration (LISST-100X) and transport of sand (lab samples).

Figure 45. Median grain size (D50) and sand fraction (% >63  $\mu\text{m}$ ) in time as measured by water samples and the LISST-100X on day 1 of the calibration campaign

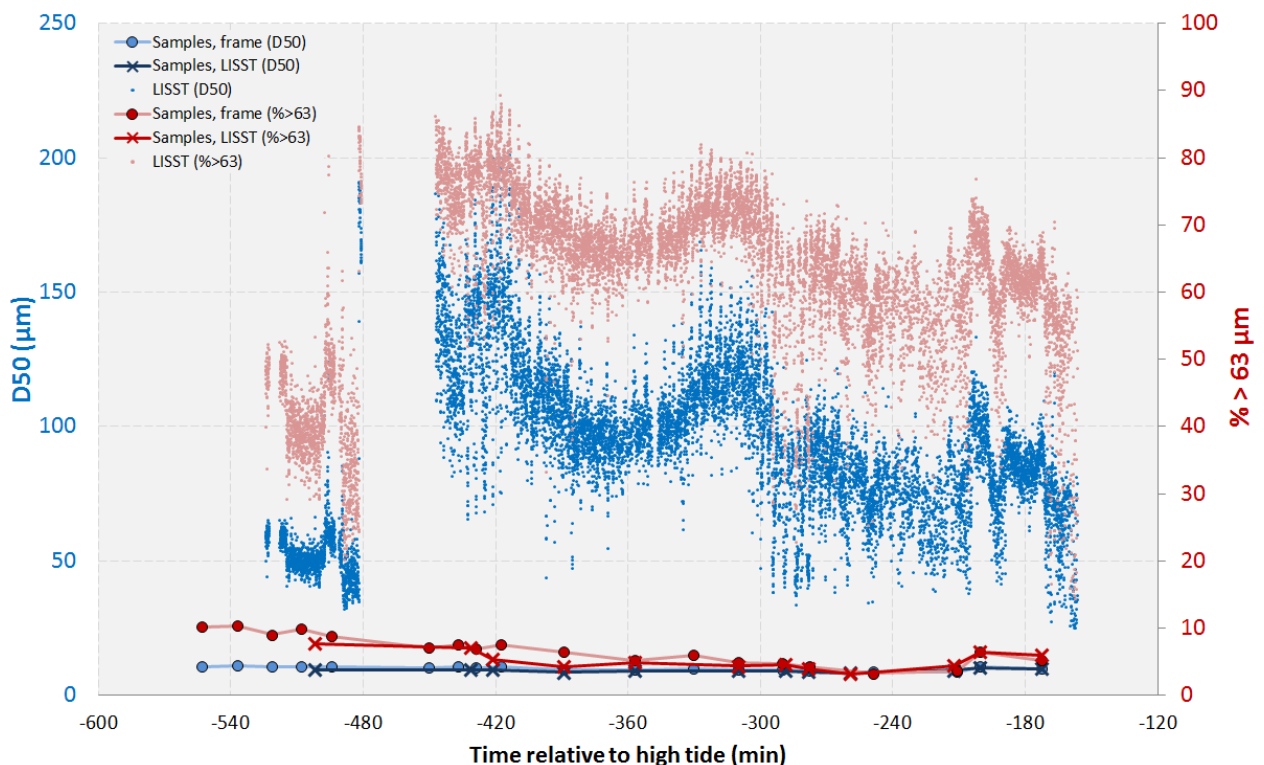


Figure 46. Median grain size (D50) and sand fraction (% >63  $\mu\text{m}$ ) in time as measured by water samples and the LISST-100X on day 2 of the calibration campaign

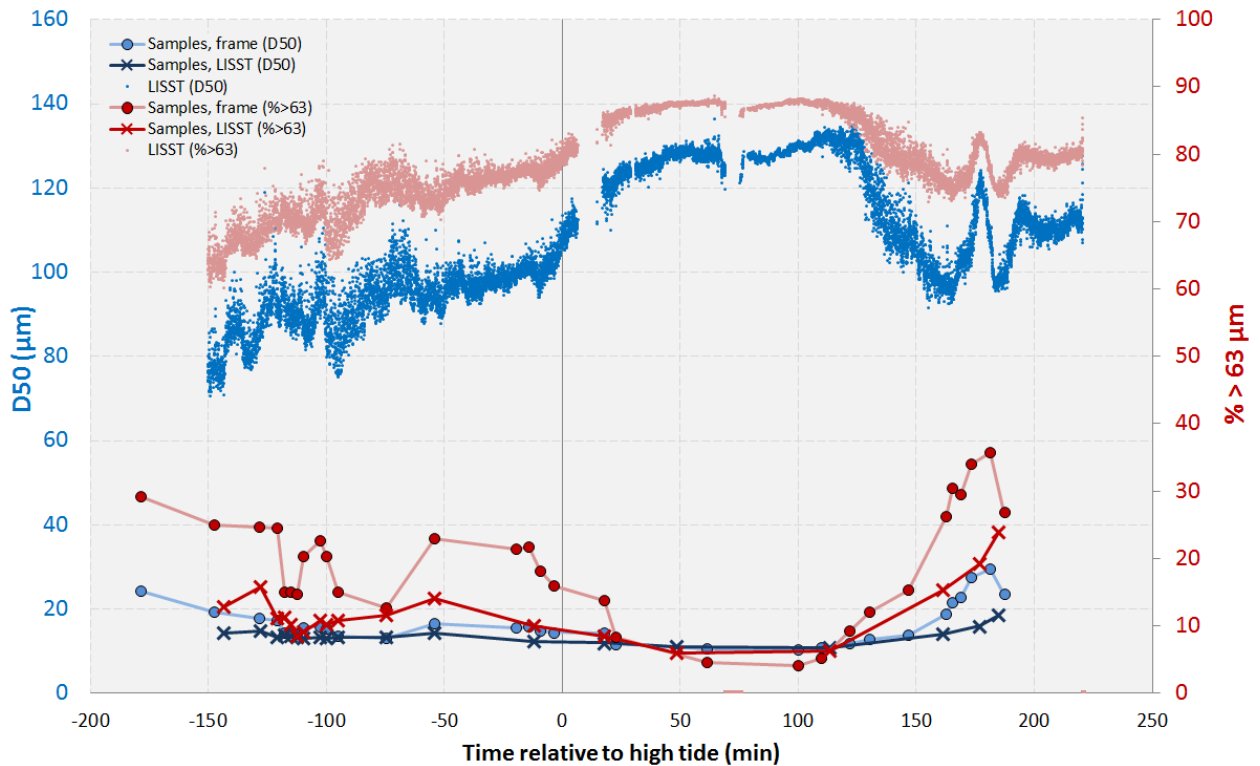
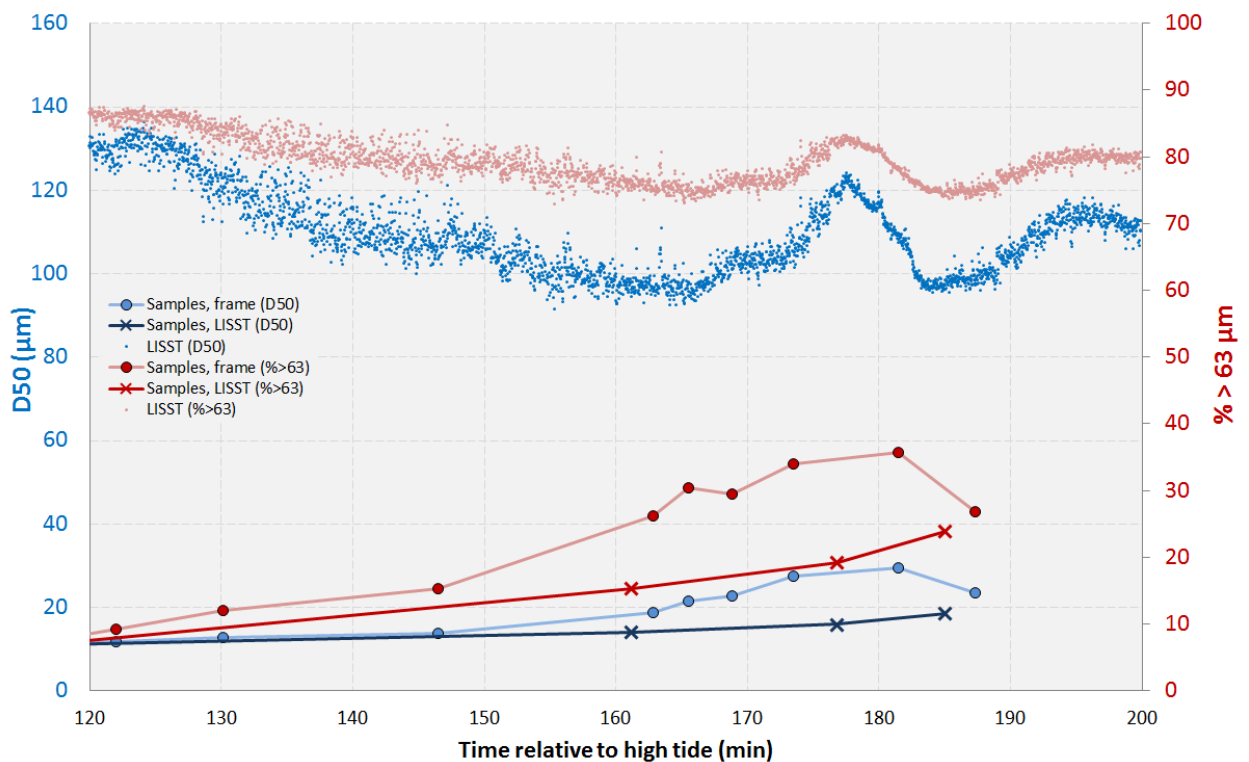


Figure 47. Median grain size (D50) and sand fraction (% >63  $\mu\text{m}$ ) in time as measured by water samples and the LISST-100X on day 2 of the calibration campaign, zoomed into 120 to 200 minutes after high water



## 5 Results: Measurement Frames

This section presents the results of the long-term measurement campaigns, after post-processing as described in section 3.

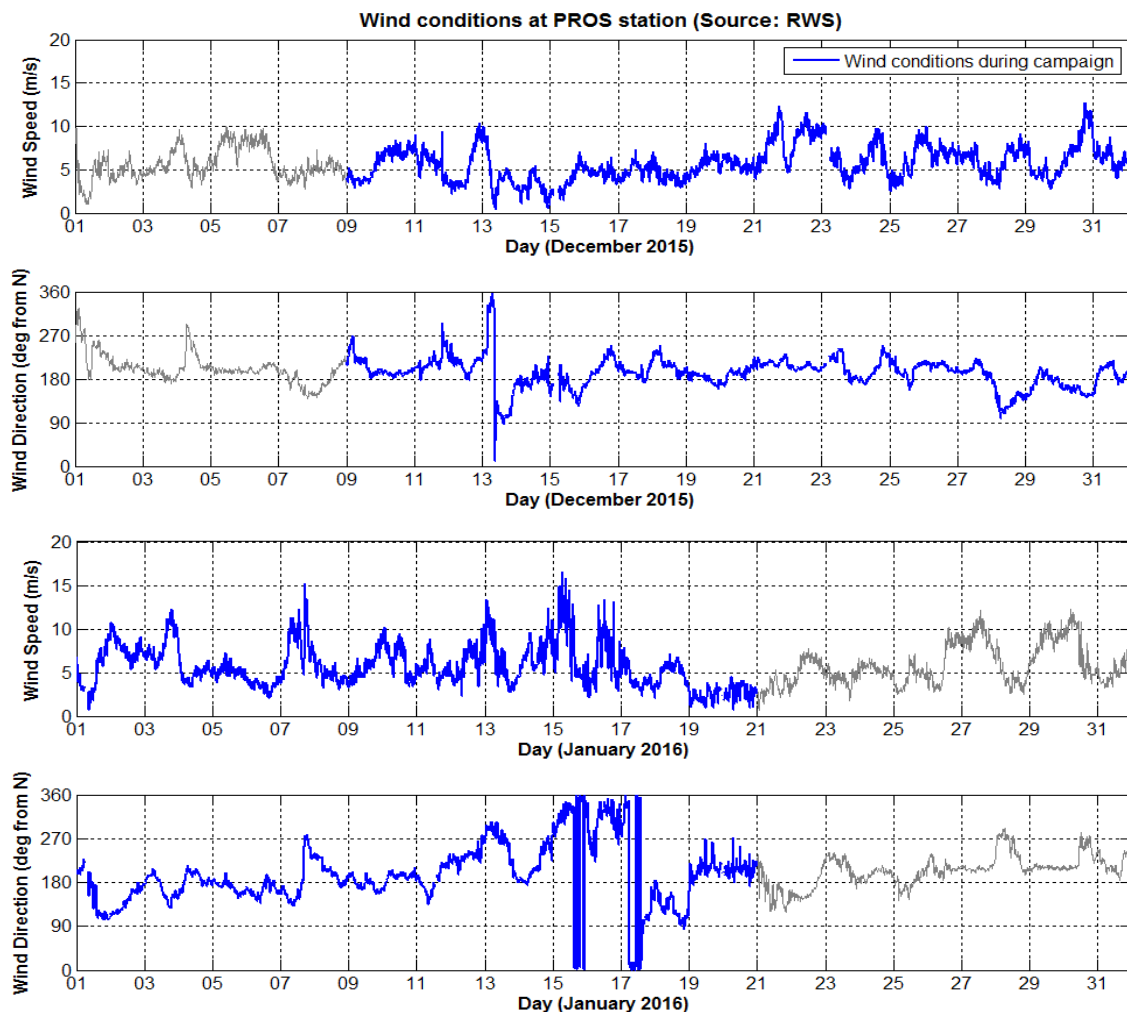
### 5.1 Ambient Conditions

The following sections present ambient conditions (wind and water levels) observed for the duration of the monitoring frame deployment at the PROS station (Figure 2).

#### 5.1.1 Wind

Wind conditions (speed and direction) at the PROS station are plotted in Figure 48 for the duration of the campaign. Winds were fairly consistent in December 2015, but turned towards the north and increased in magnitude towards the middle of January 2016.

Figure 48. Wind conditions at the PROS station during campaign #1 at Schaar Ouden Doel



(top: December 2015, bottom: January 2016)

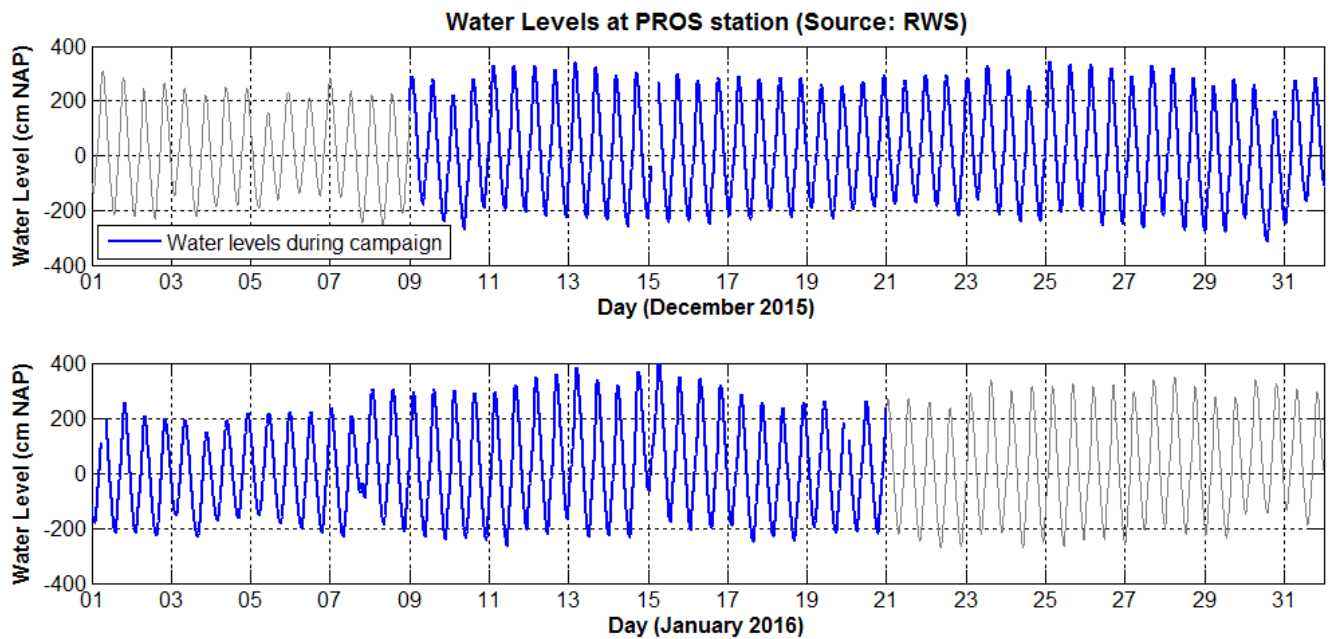
### 5.1.2 Water Levels

Figure 49 presents the measured water levels at the PROS station for the duration of the campaign. The highest observed water level of 412 cm NAP occurred at the PROS gauge on the morning of January 15<sup>th</sup>, 2016.

---

Figure 49. Water levels at the PROS station during campaign #1 at Schaar Ouden Doel

---



## 5.2 Currents

Figure 50 through Figure 55 show the depth averaged velocity overlaid with the measured water level at the PROS station for the HYLAS I and HYLAS II frames. Figure 56 through Figure 61 show the complete current profile over time. The depth time series collected by the AWAC was used to remove data beyond the water surface. Figure 62 and Figure 63 plots the two depth-averaged velocity magnitude on a single plot.

Figure 50. Depth averaged magnitude, direction, and water levels (as measured by the ADCP) for frame HYLAS I, weeks 1 and 2

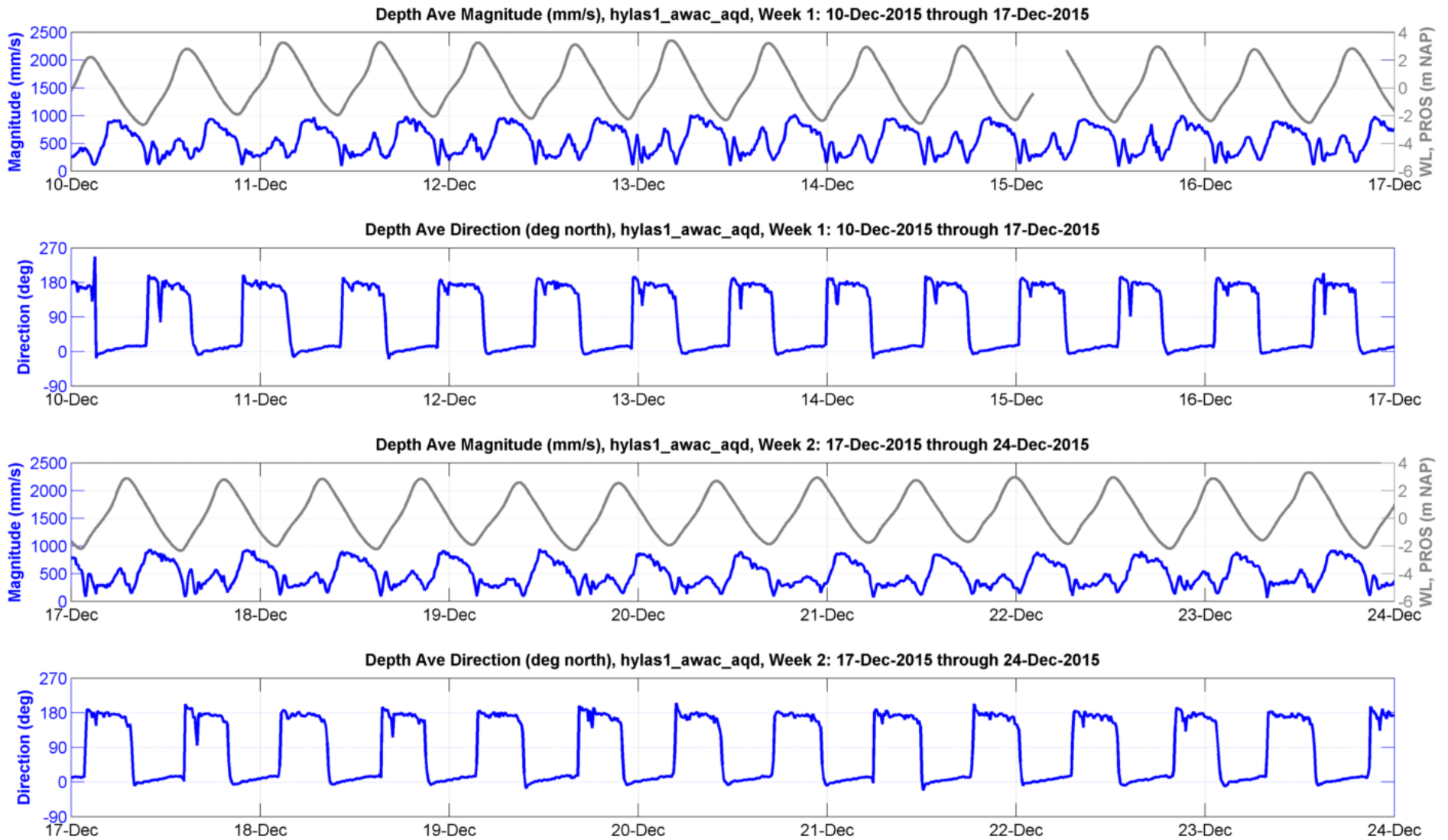


Figure 51. Depth averaged magnitude, direction, and water levels (as measured by the ADCP) for frame HYLAS I, weeks 3 and 4

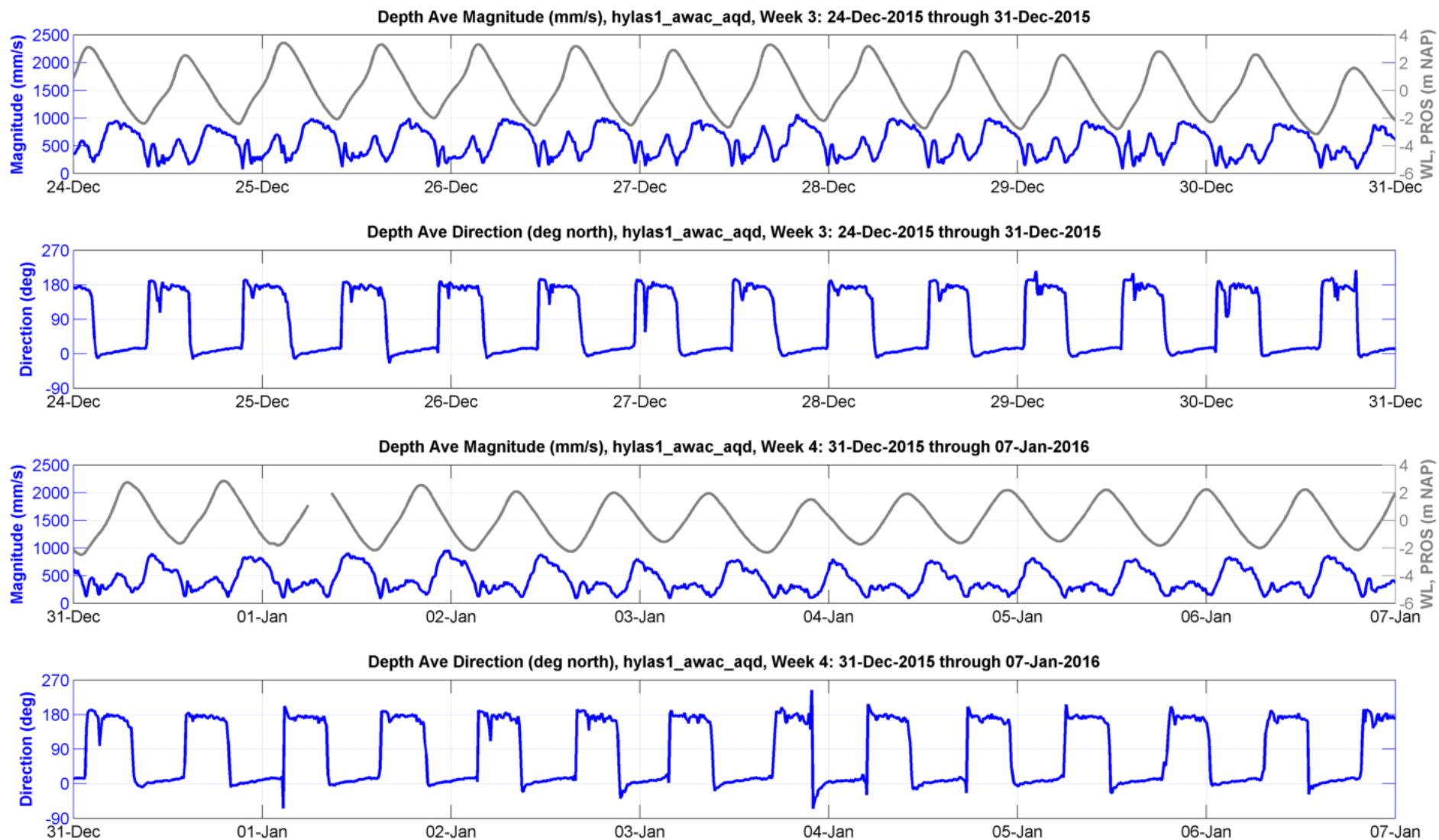


Figure 52. Depth averaged magnitude, direction, and water levels (as measured by the ADCP) for frame HYLAS I, weeks 5 and 6

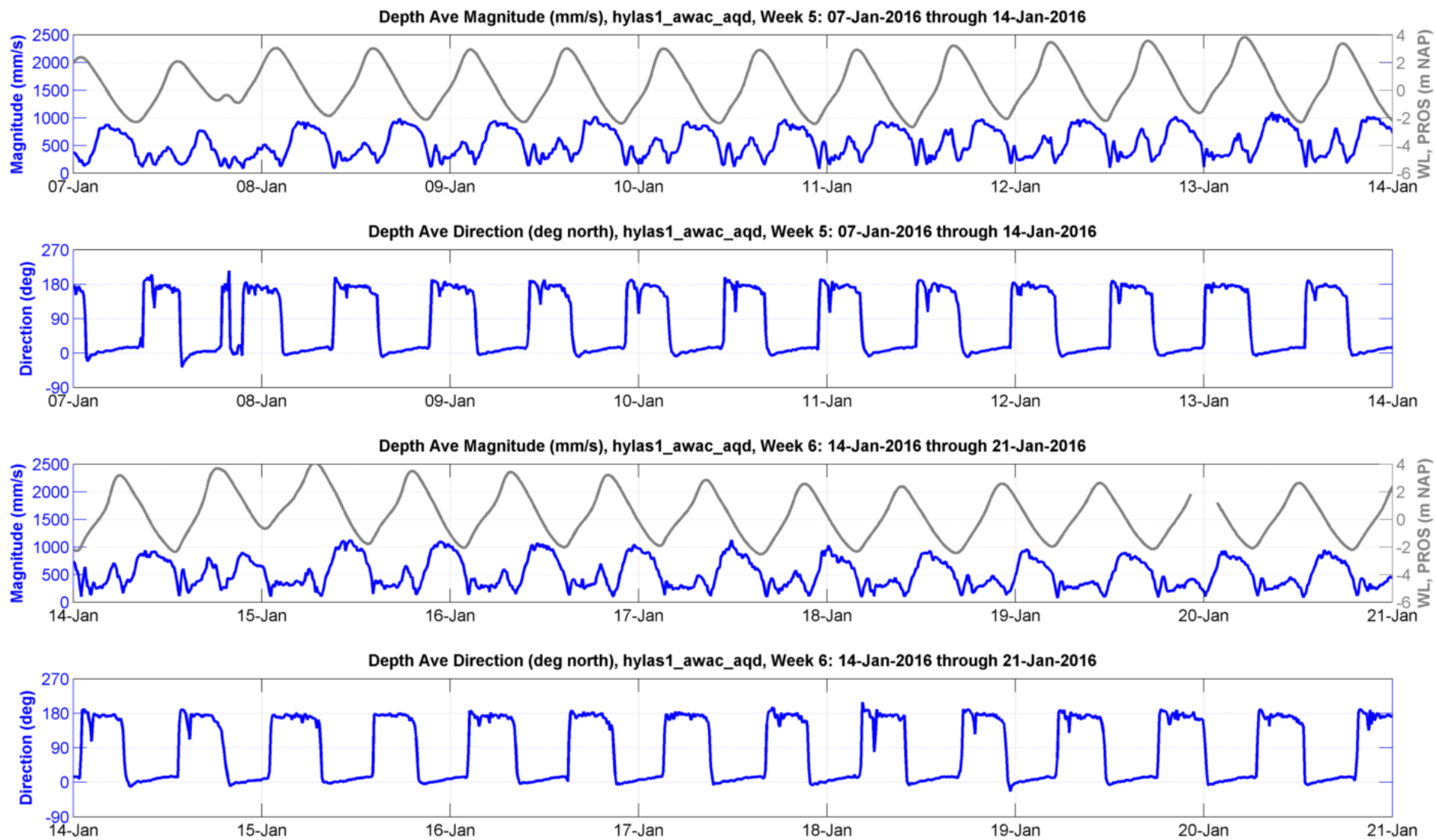


Figure 53. Depth averaged magnitude, direction, and water levels (as measured by the ADCP) for frame HYLAS II, weeks 1 and 2

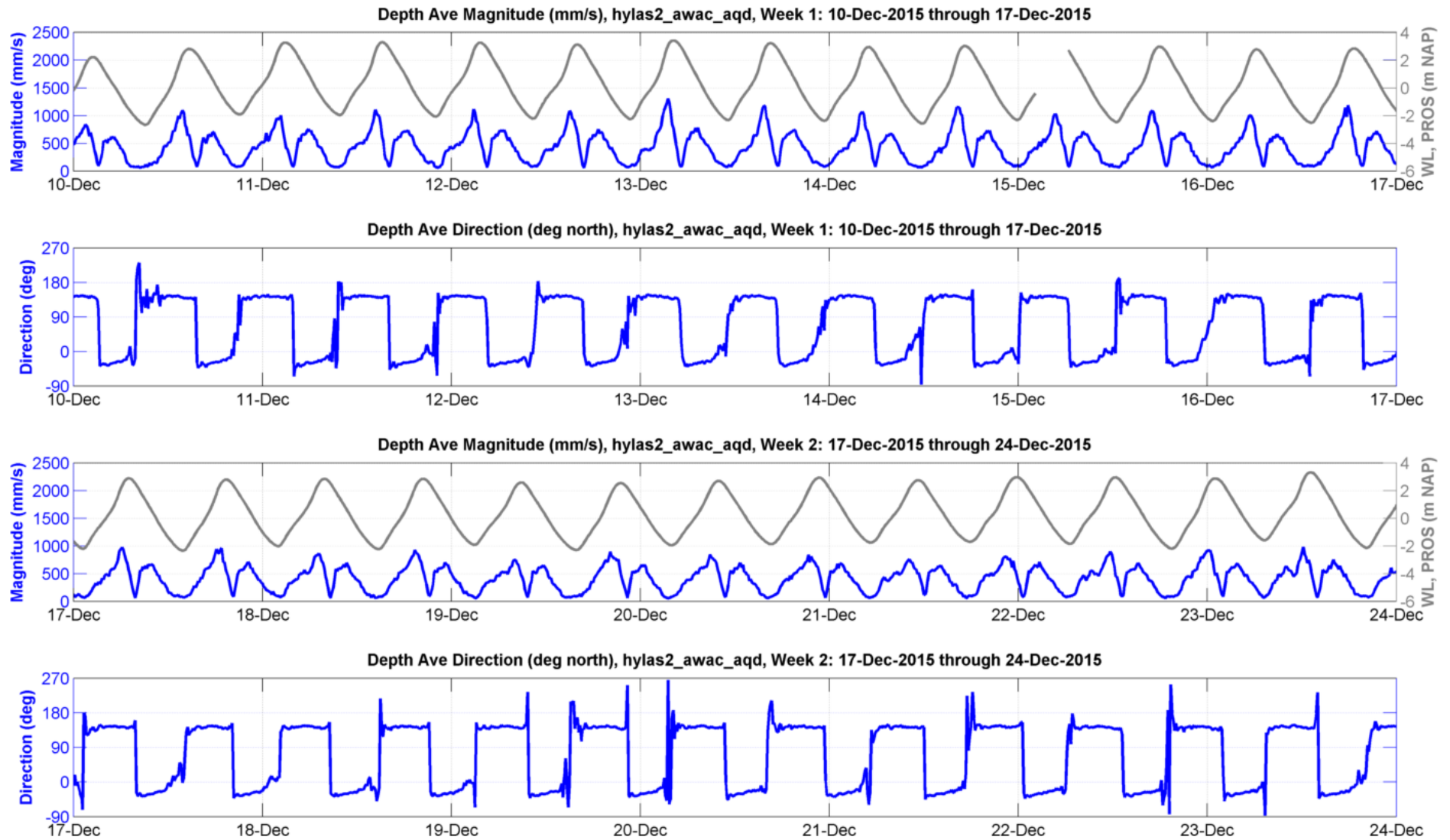


Figure 54. Depth averaged magnitude, direction, and water levels (as measured by the ADCP) for frame HYLAS II, weeks 3 and 4

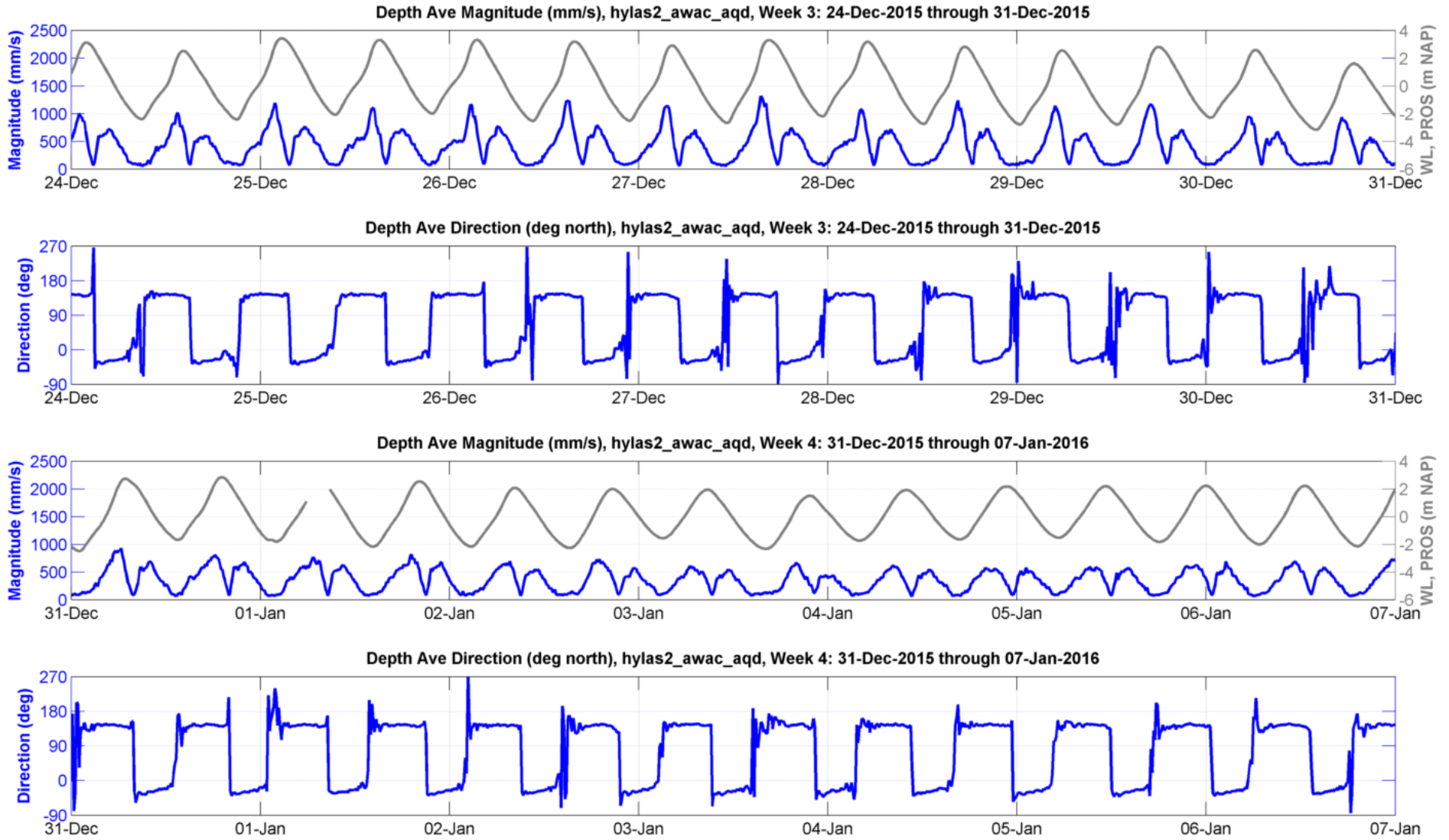


Figure 55. Depth averaged magnitude, direction, and water levels (as measured by the ADCP) for frame HYLAS II, weeks 5 and 6

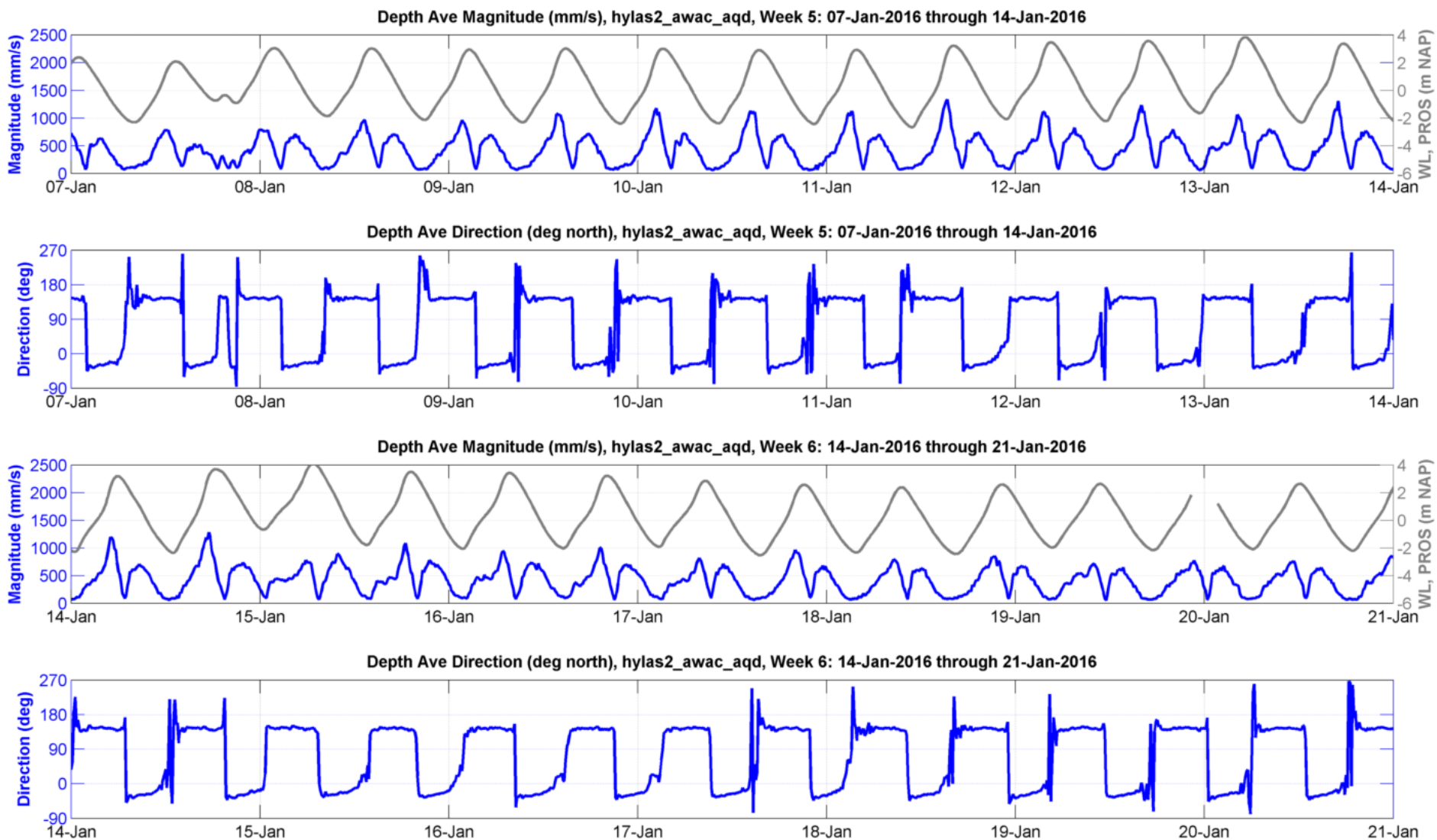


Figure 56. Current magnitude and direction for frame HYLAS I, weeks 1 and 2

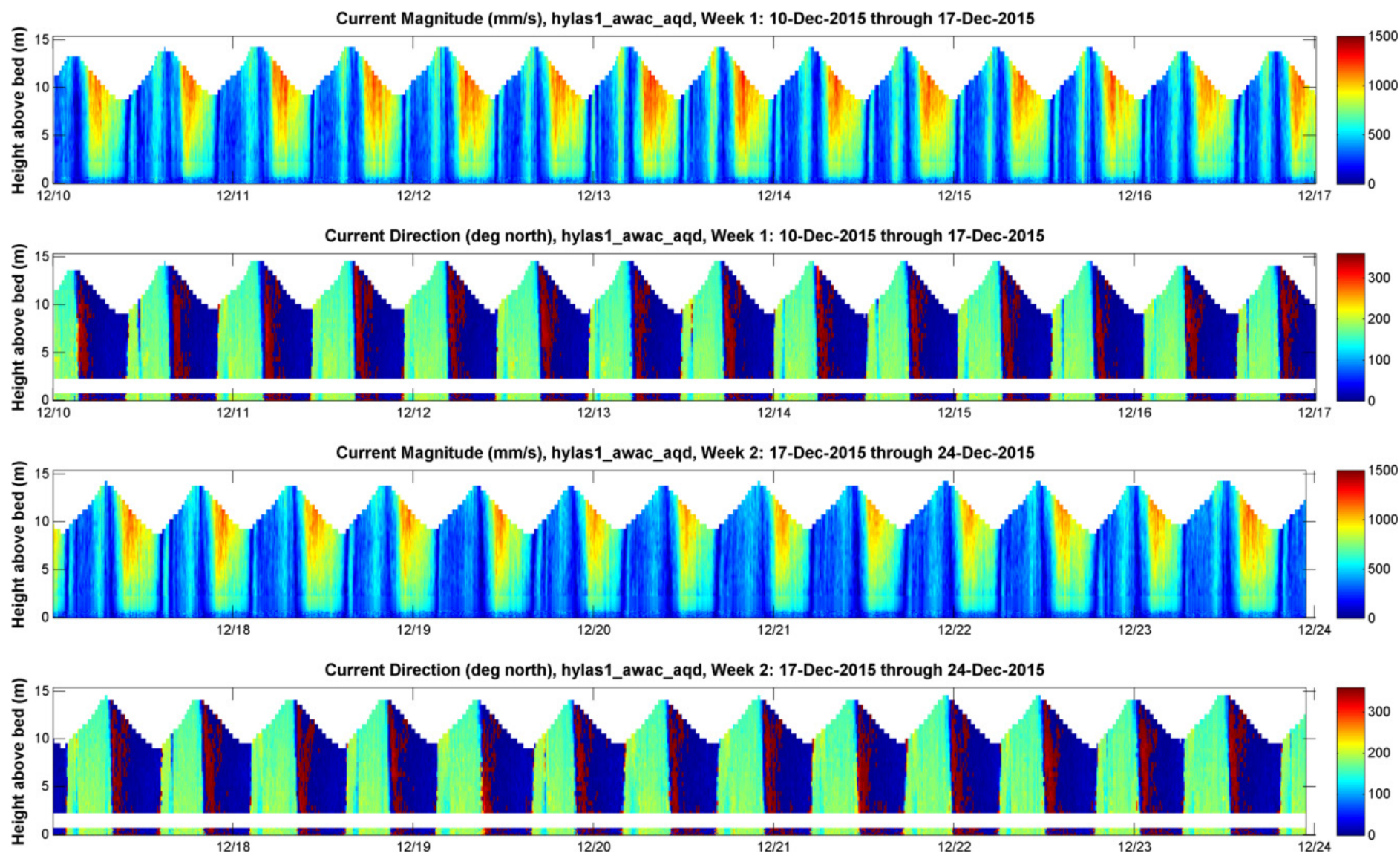


Figure 57. Current magnitude and direction for frame HYLAS I, weeks 3 and 4

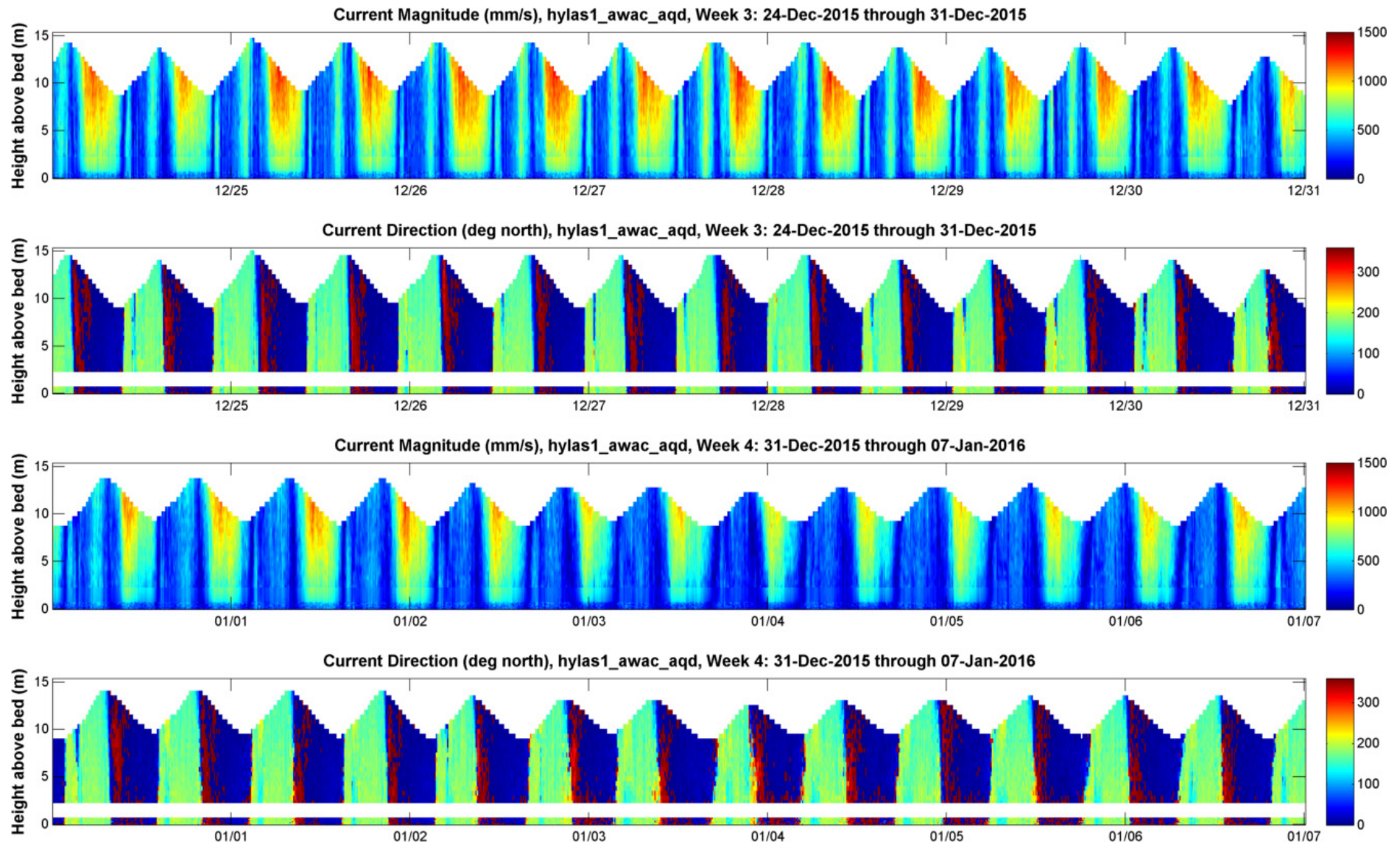


Figure 58. Current magnitude and direction for frame HYLAS I, weeks 5 and 6

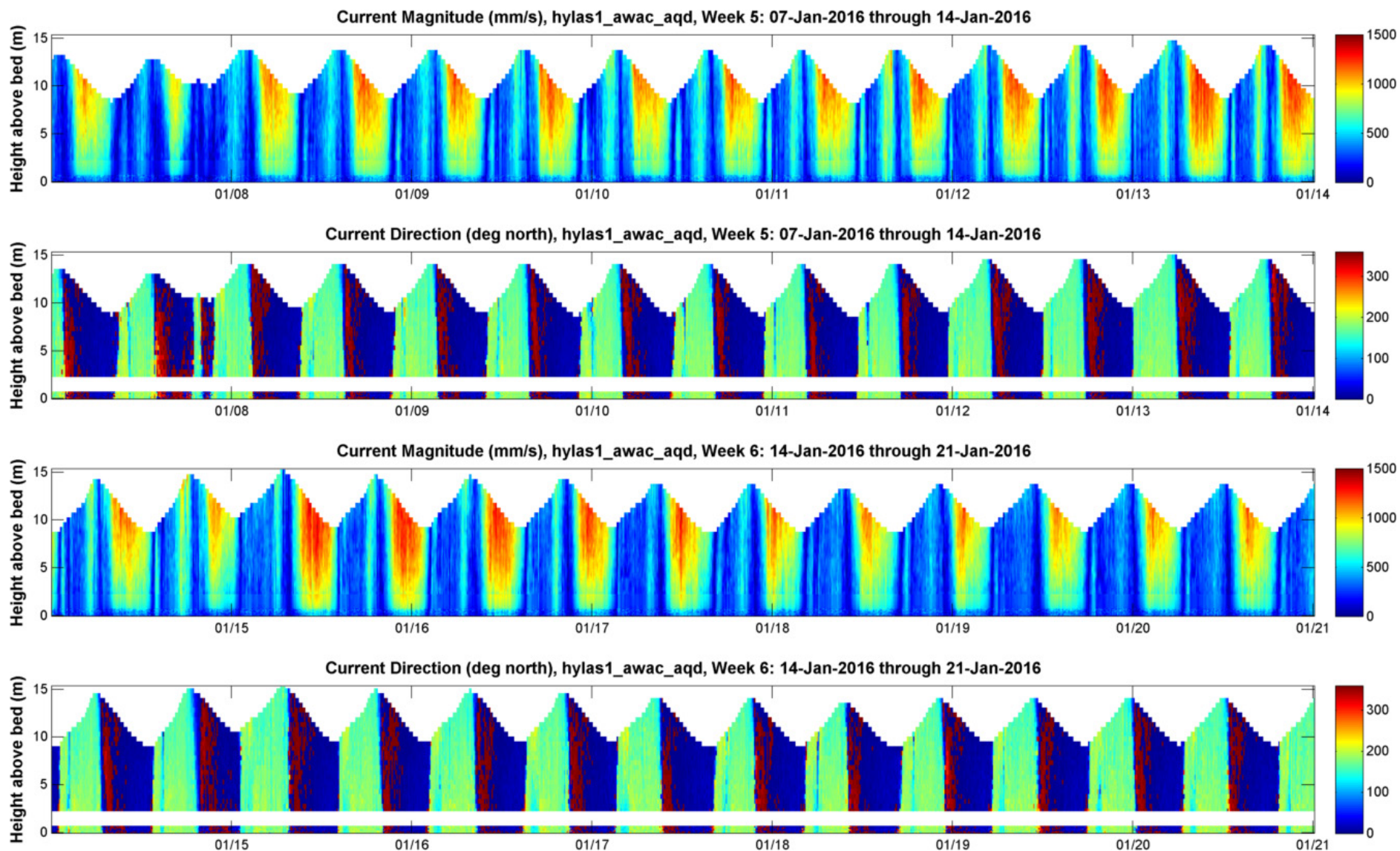


Figure 59. Current magnitude and direction for frame HYLAS II, weeks 1 and 2

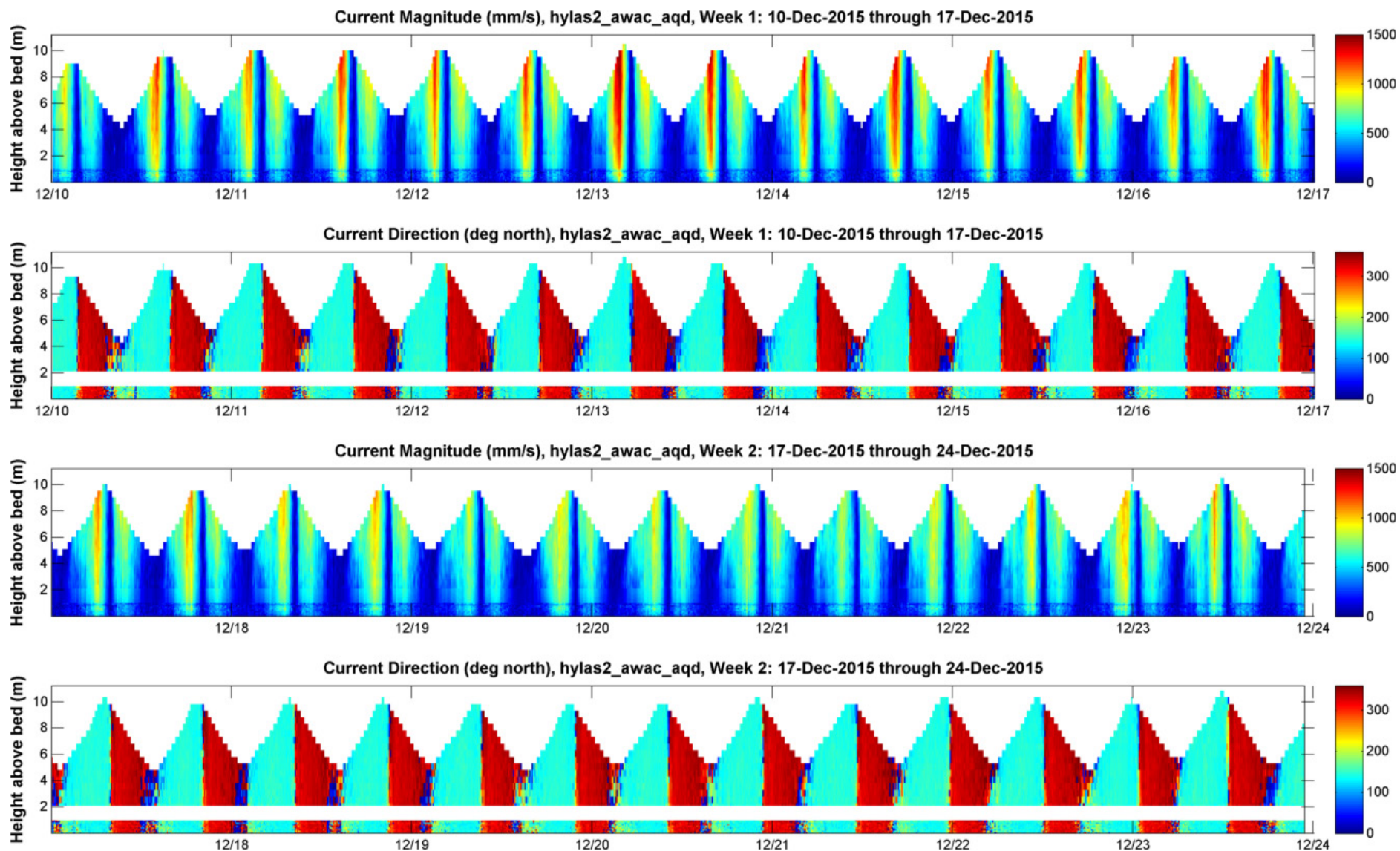


Figure 60. Current magnitude and direction for frame HYLAS II, weeks 3 and 4

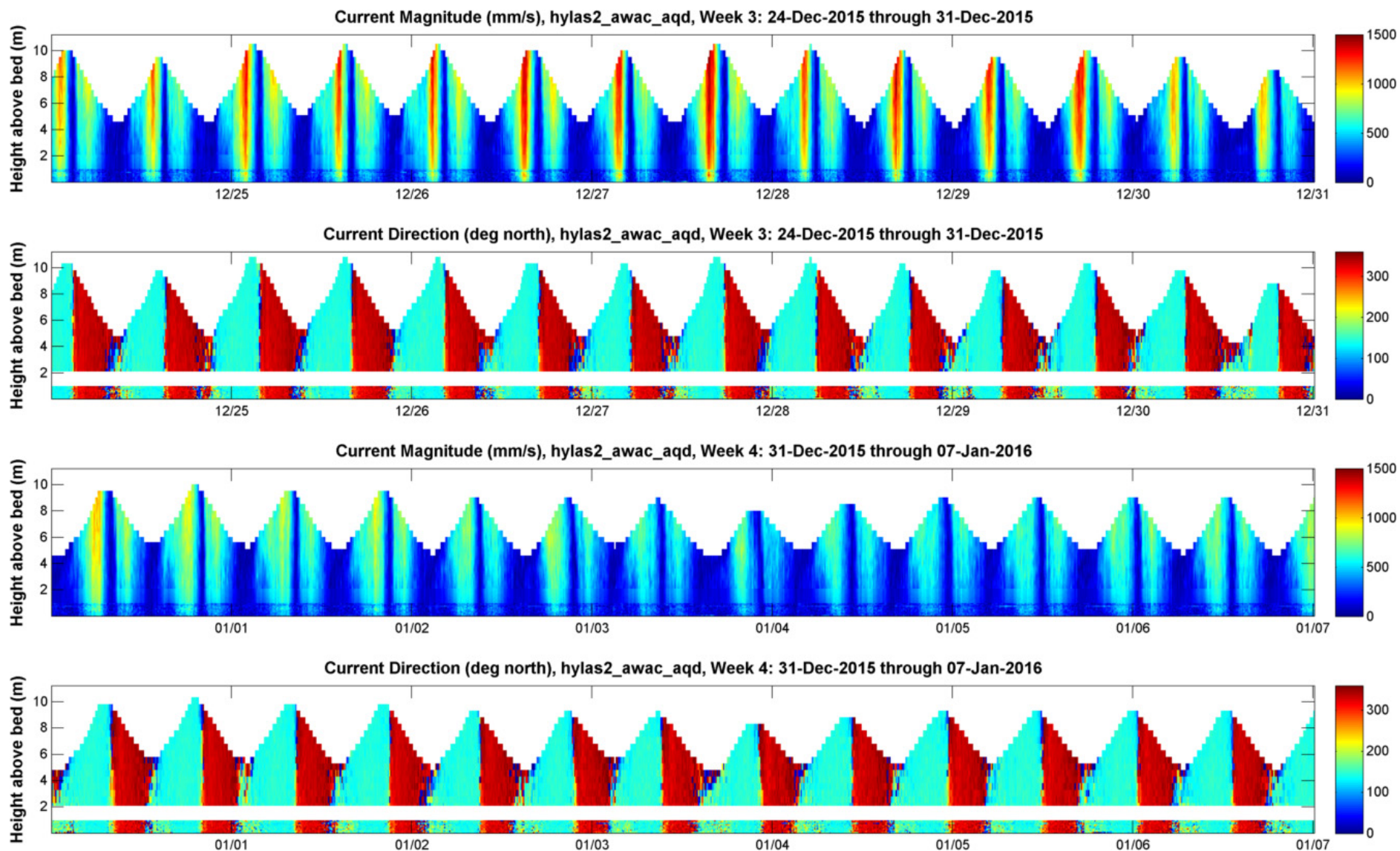


Figure 61. Current magnitude and direction for frame HYLAS II, weeks 5 and 6

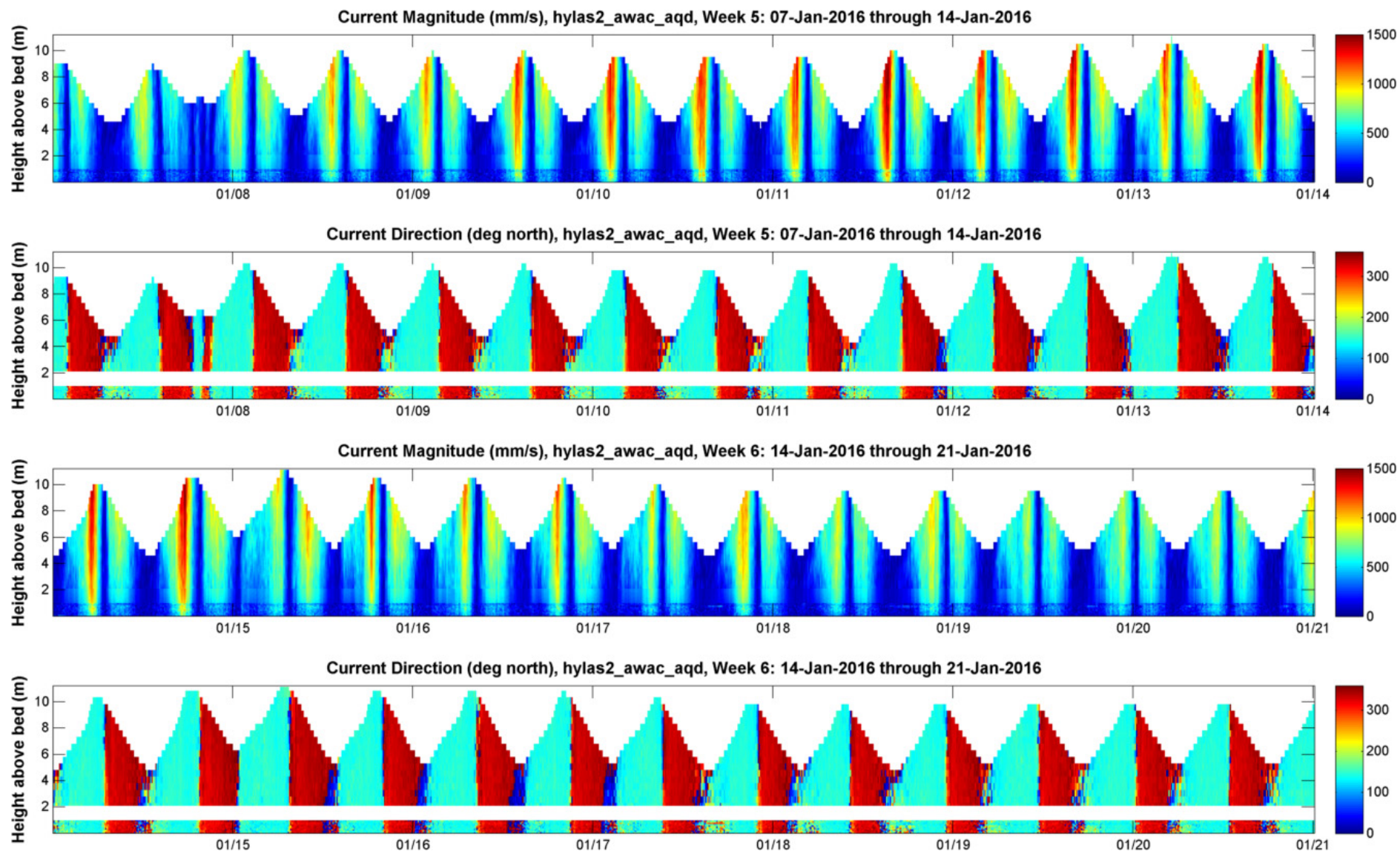


Figure 62. Depth averaged current magnitude for both frames HYLAS I & II, weeks 1 through 4

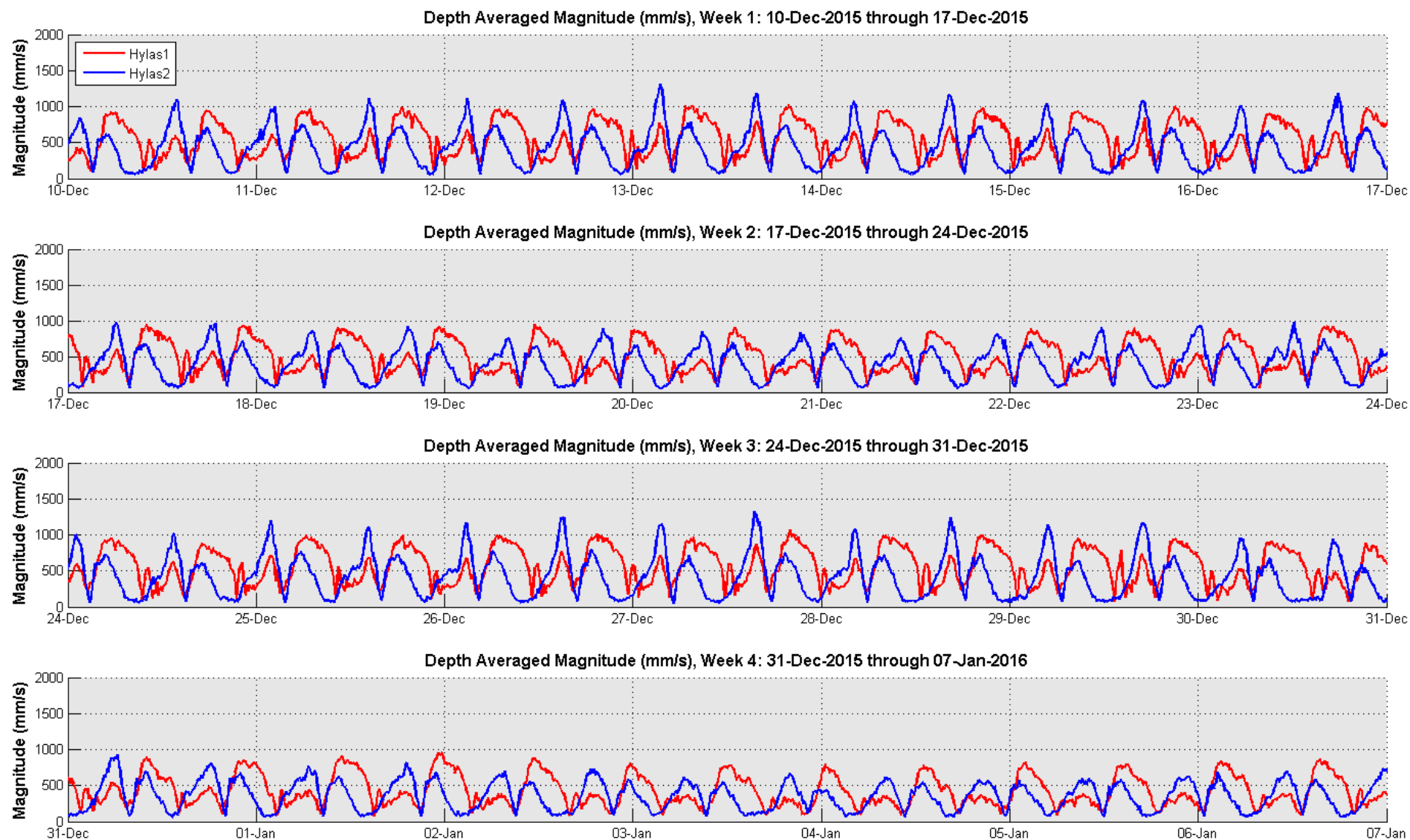
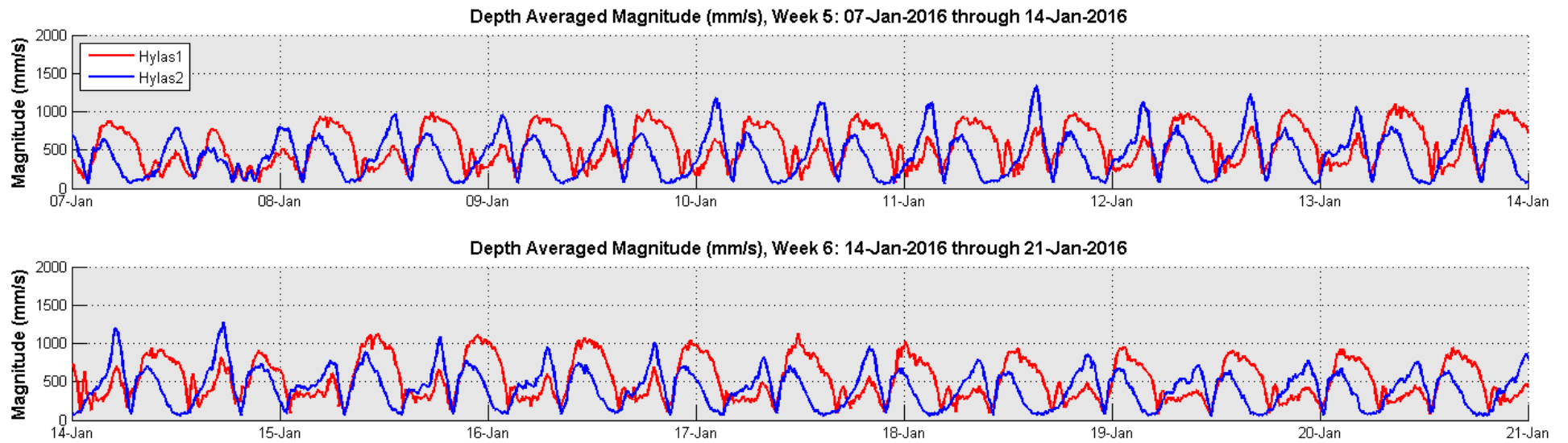


Figure 63. Depth averaged current magnitude for both frames HYLAS I & II, weeks 5 and 6



## 5.3 Sediment Transport

Figure 64 to Figure 73 present the sediment transport rates for the long-term measurement frames (HYLAS I and HYLAS II). The data for each frame is split onto four figures, to show 1 week of data in each figure. These rates were calculated according to the methods outlined in section 3.7. The uncertainty bands shown in the bottom pane of each figure reflects the 95% confidence intervals from the AWAC SSC calibration (described in section 0). No other uncertainties have been accounted for in these limits. Horizontal pink lines show space where interpolation was done in the gap between the Aquadopp and AWAC data, as described in section 3.6.

Figure 64. Suspended sediment concentration and sediment transport rate profiles and total sediment transport rate for HYLAS I frame, week 1.

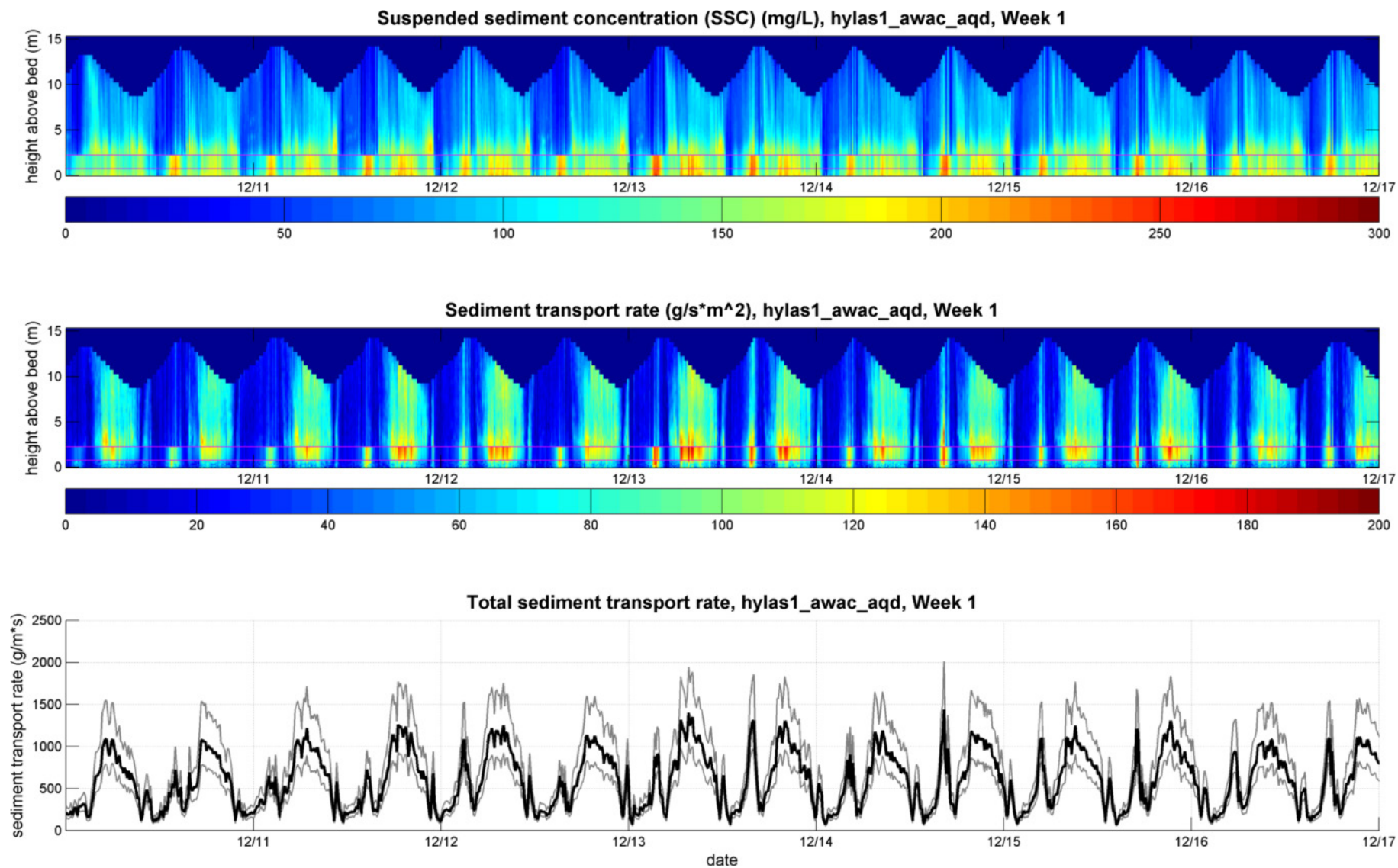


Figure 65. Suspended sediment concentration and sediment transport rate profiles and total sediment transport rate for HYLAS I frame, week 2

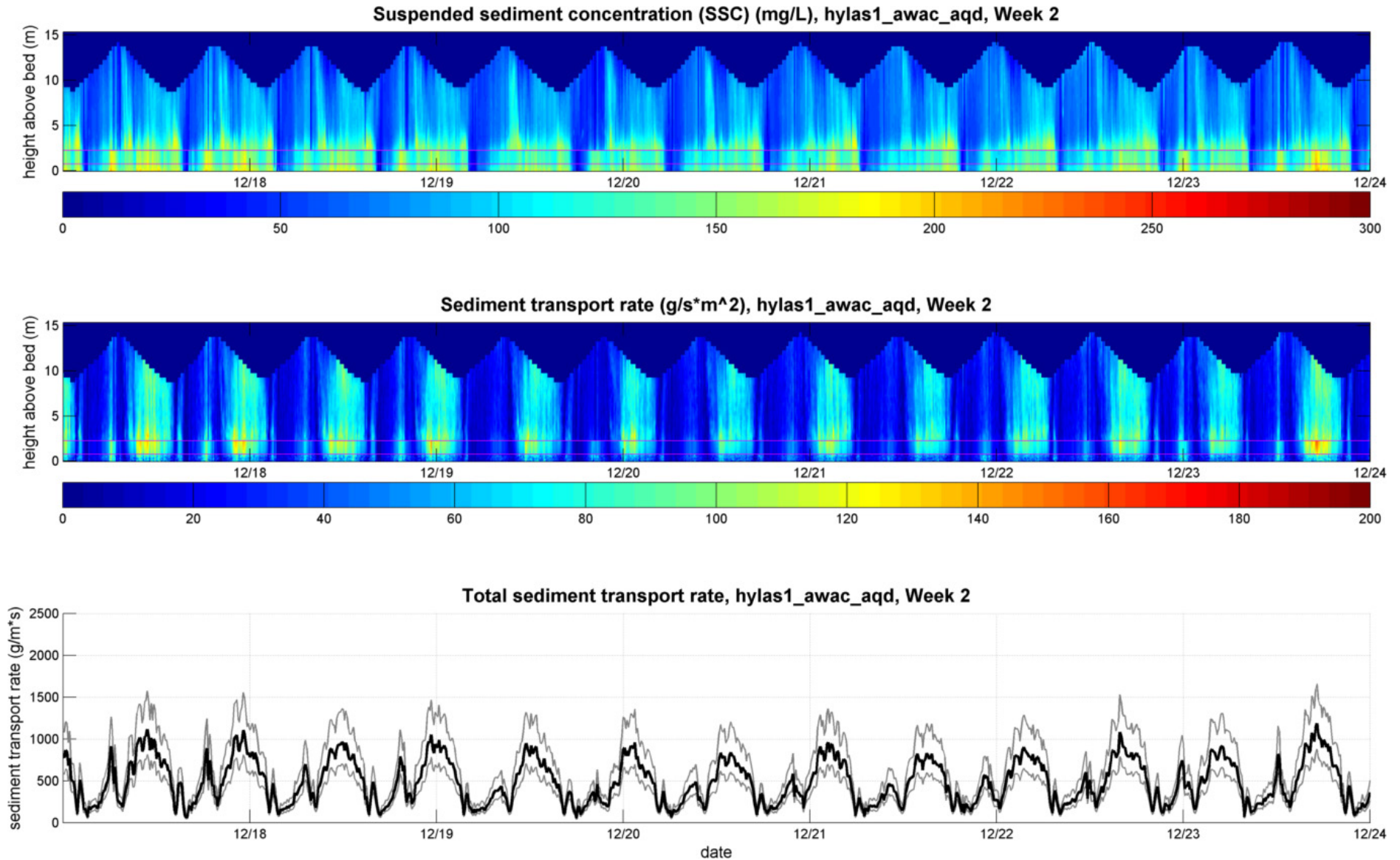


Figure 66. Suspended sediment concentration and sediment transport rate profiles and total sediment transport rate for HYLAS I frame, week 3

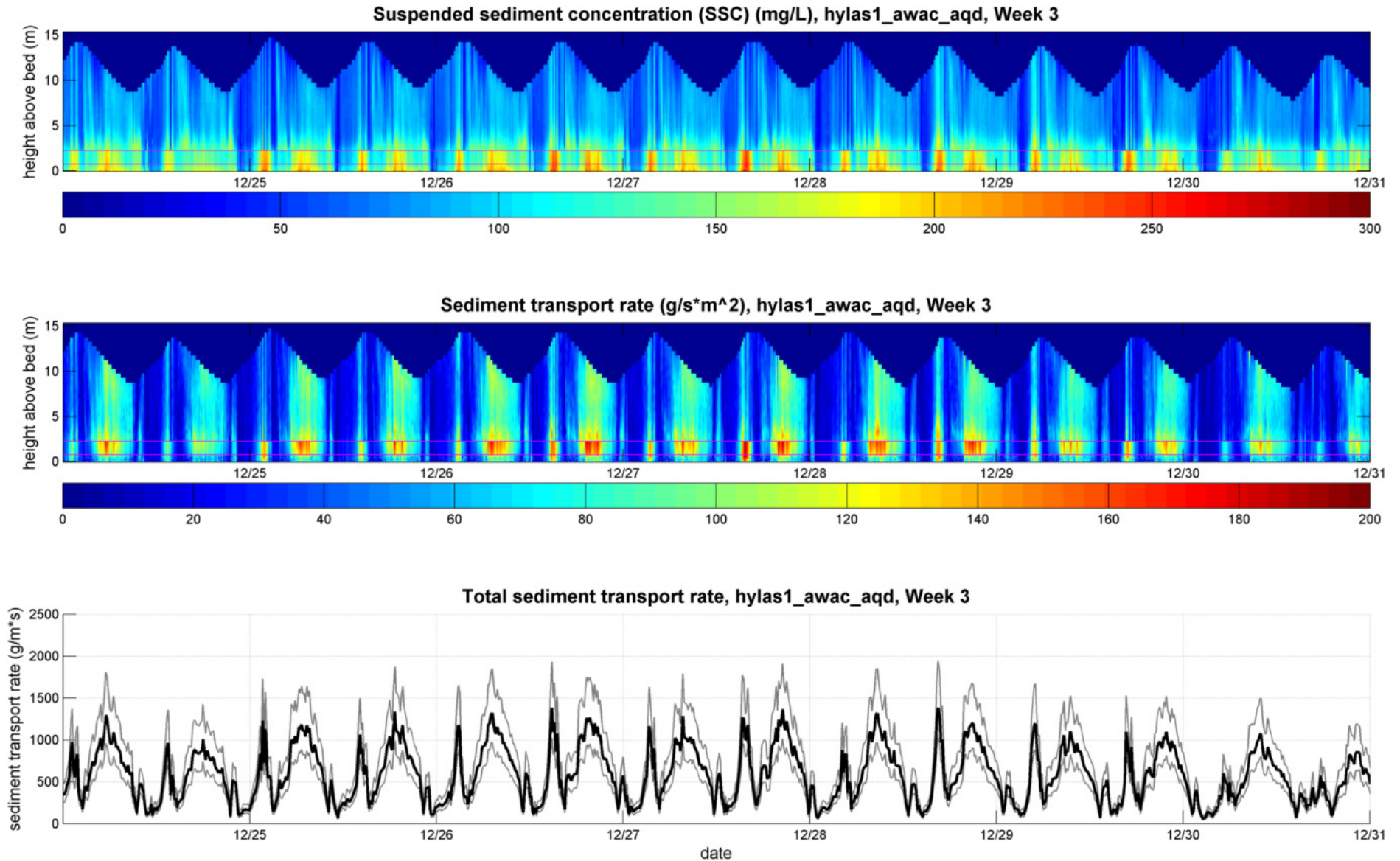


Figure 67. Suspended sediment concentration and sediment transport rate profiles and total sediment transport rate for HYLAS I frame, week 4

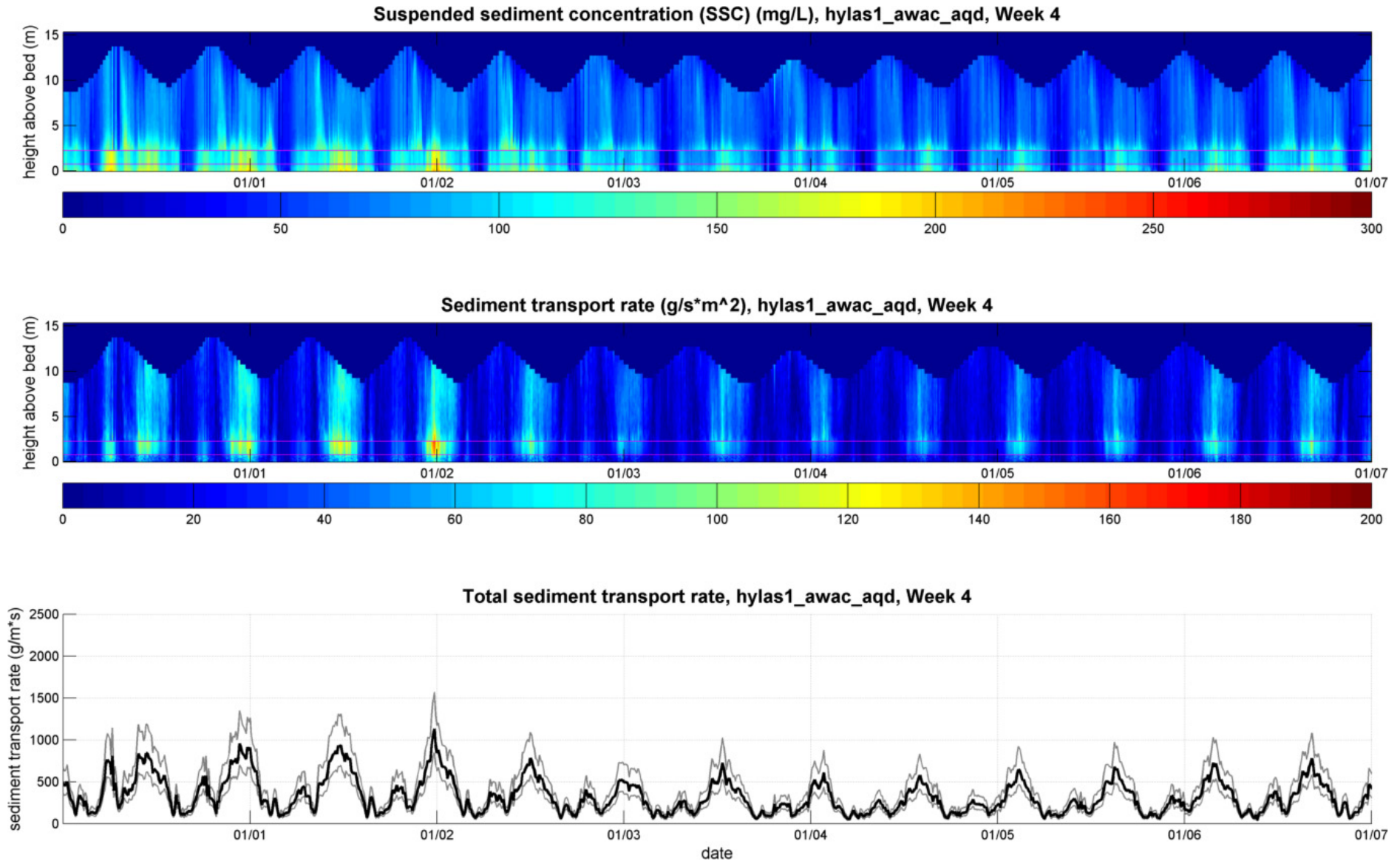


Figure 68. Suspended sediment concentration and sediment transport rate profiles and total sediment transport rate for HYLAS I frame, week 5

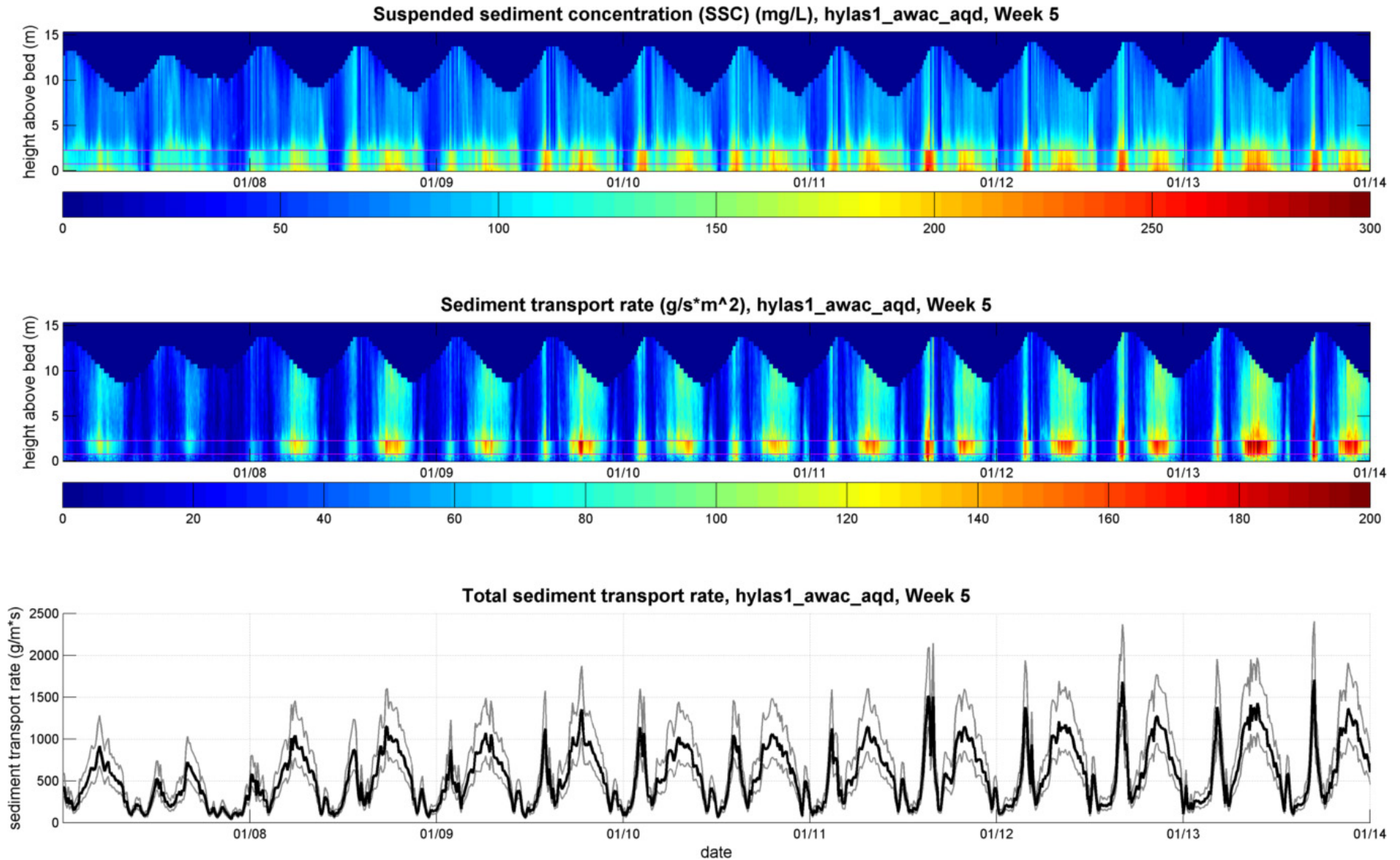


Figure 69. Suspended sediment concentration and sediment transport rate profiles and total sediment transport rate for HYLAS I frame, week 6

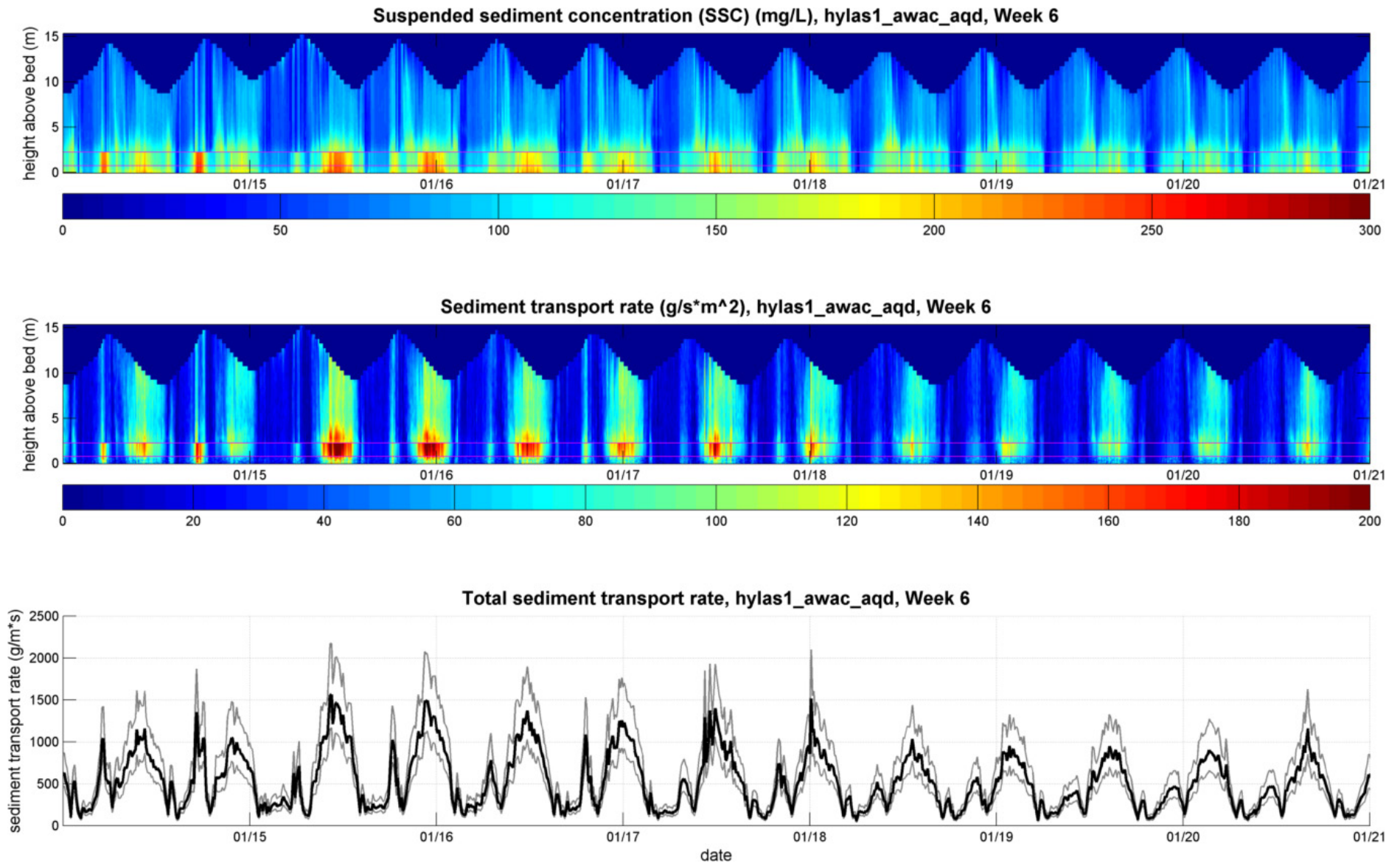


Figure 70. Suspended sediment concentration and sediment transport rate profiles and total sediment transport rate for HYLAS II frame, week 1

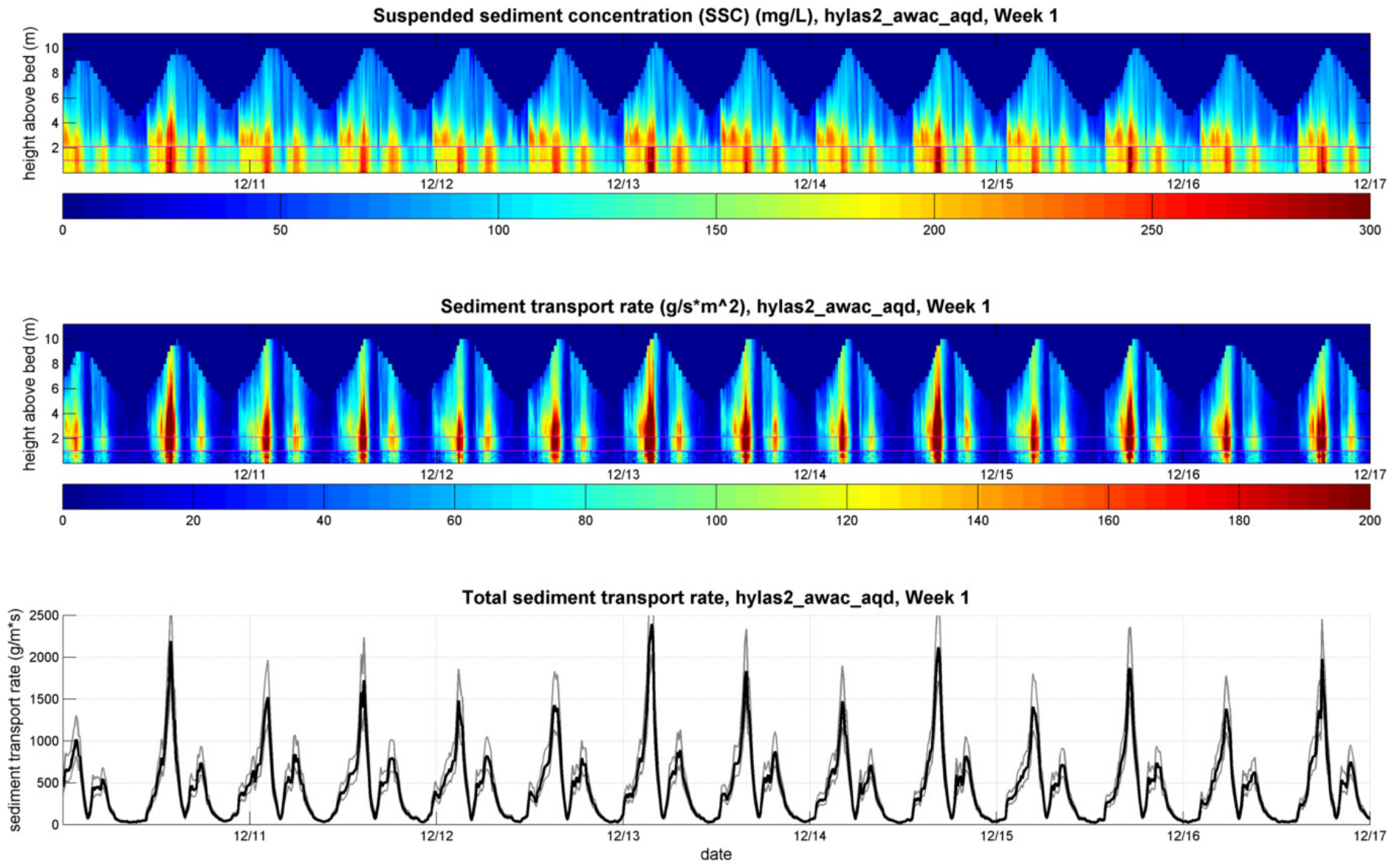


Figure 71. Suspended sediment concentration and sediment transport rate profiles and total sediment transport rate for HYLAS II frame, week 2

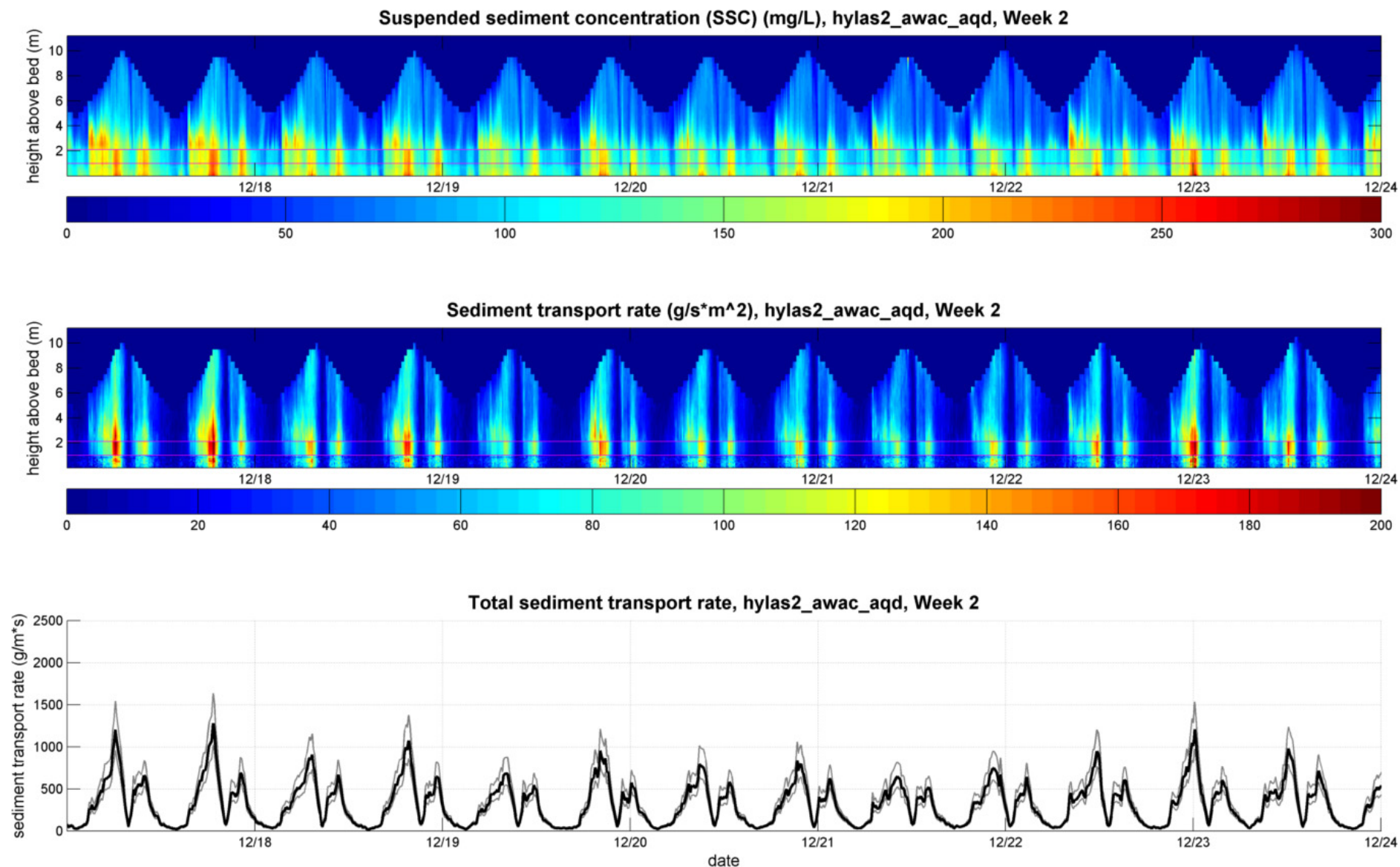


Figure 72. Suspended sediment concentration and sediment transport rate profiles and total sediment transport rate for HYLAS II frame, week 3

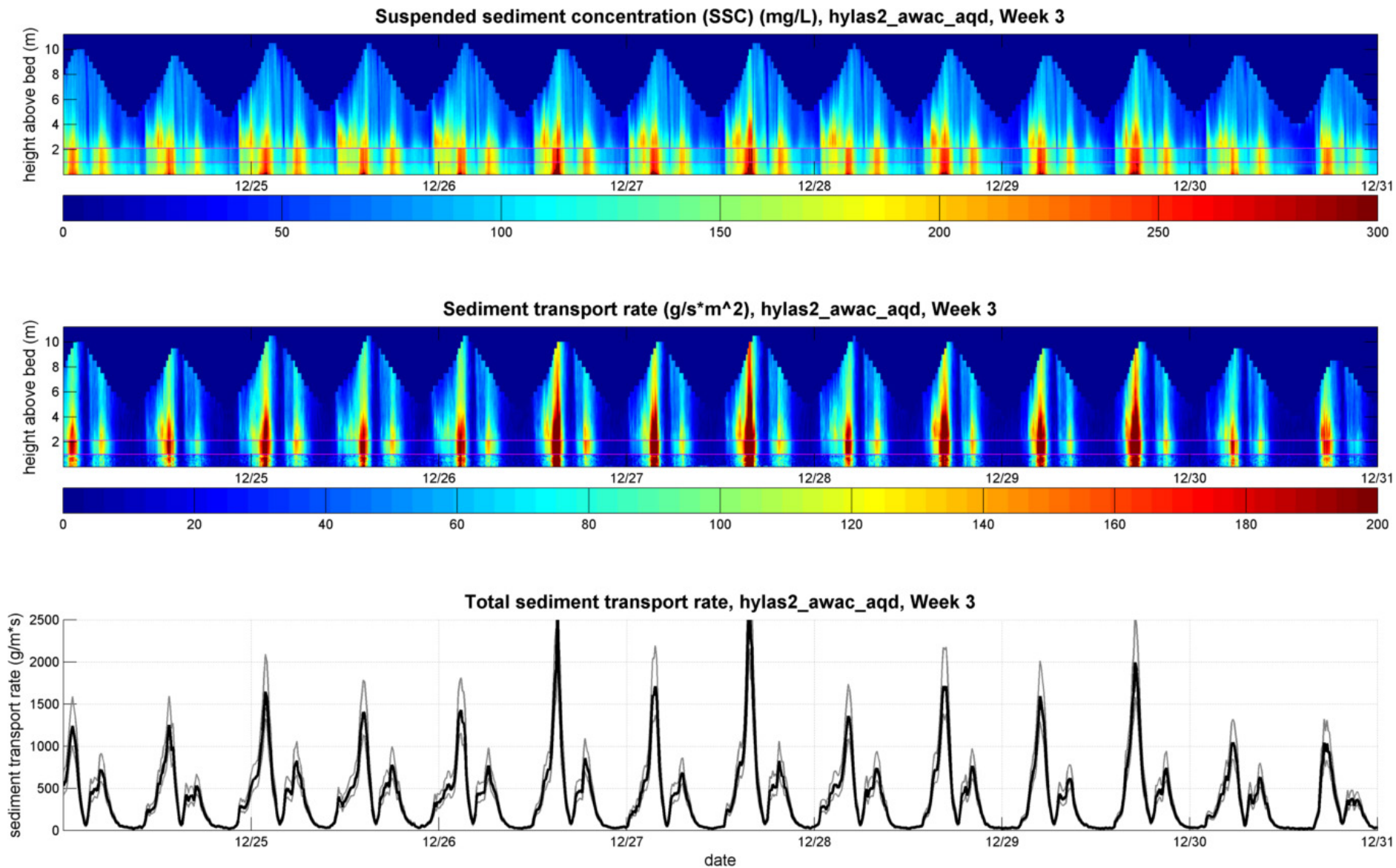


Figure 73. Suspended sediment concentration and sediment transport rate profiles and total sediment transport rate for HYLAS II frame, week 4.

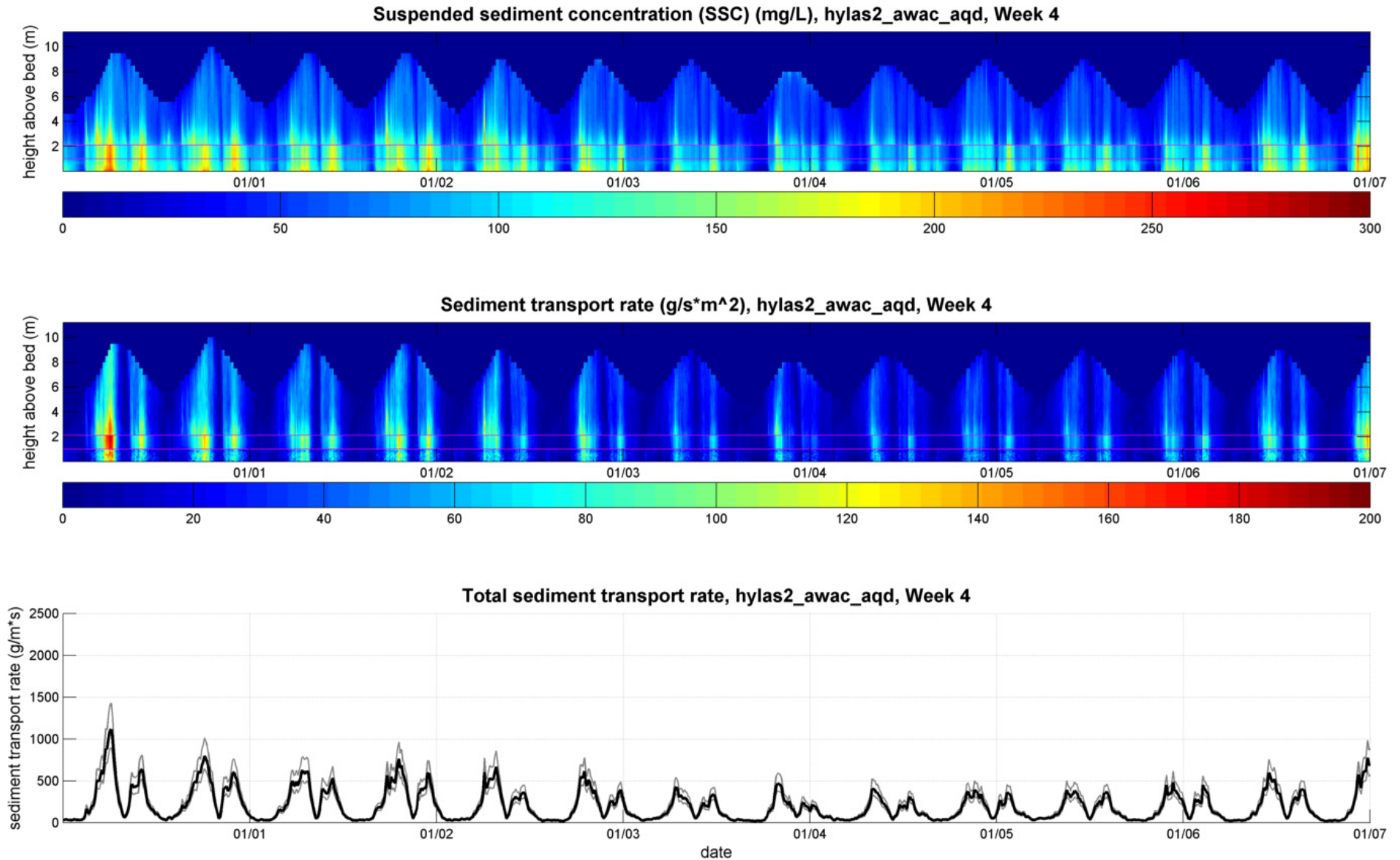


Figure 74. Suspended sediment concentration and sediment transport rate profiles and total sediment transport rate for HYLAS II frame, week 5

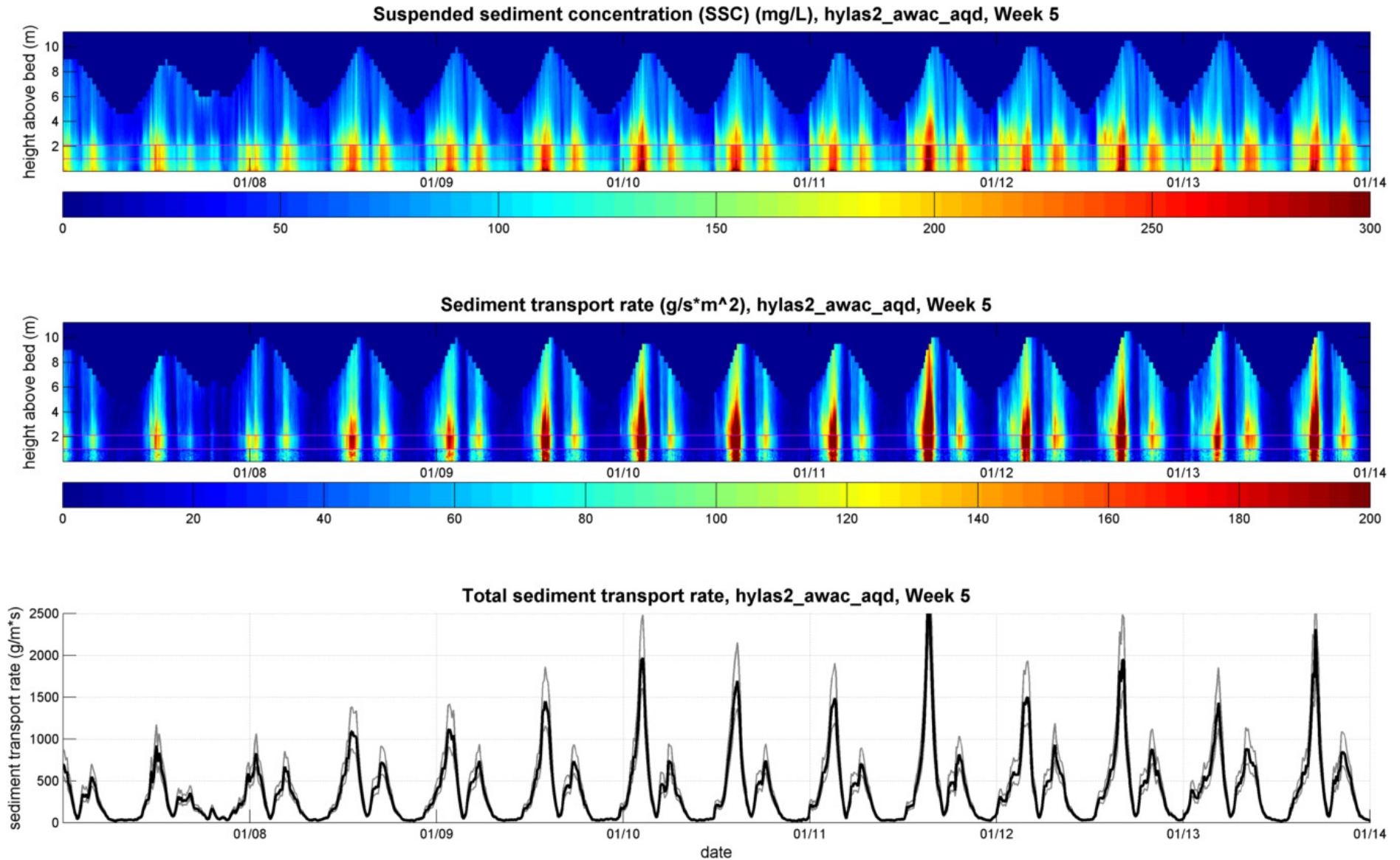
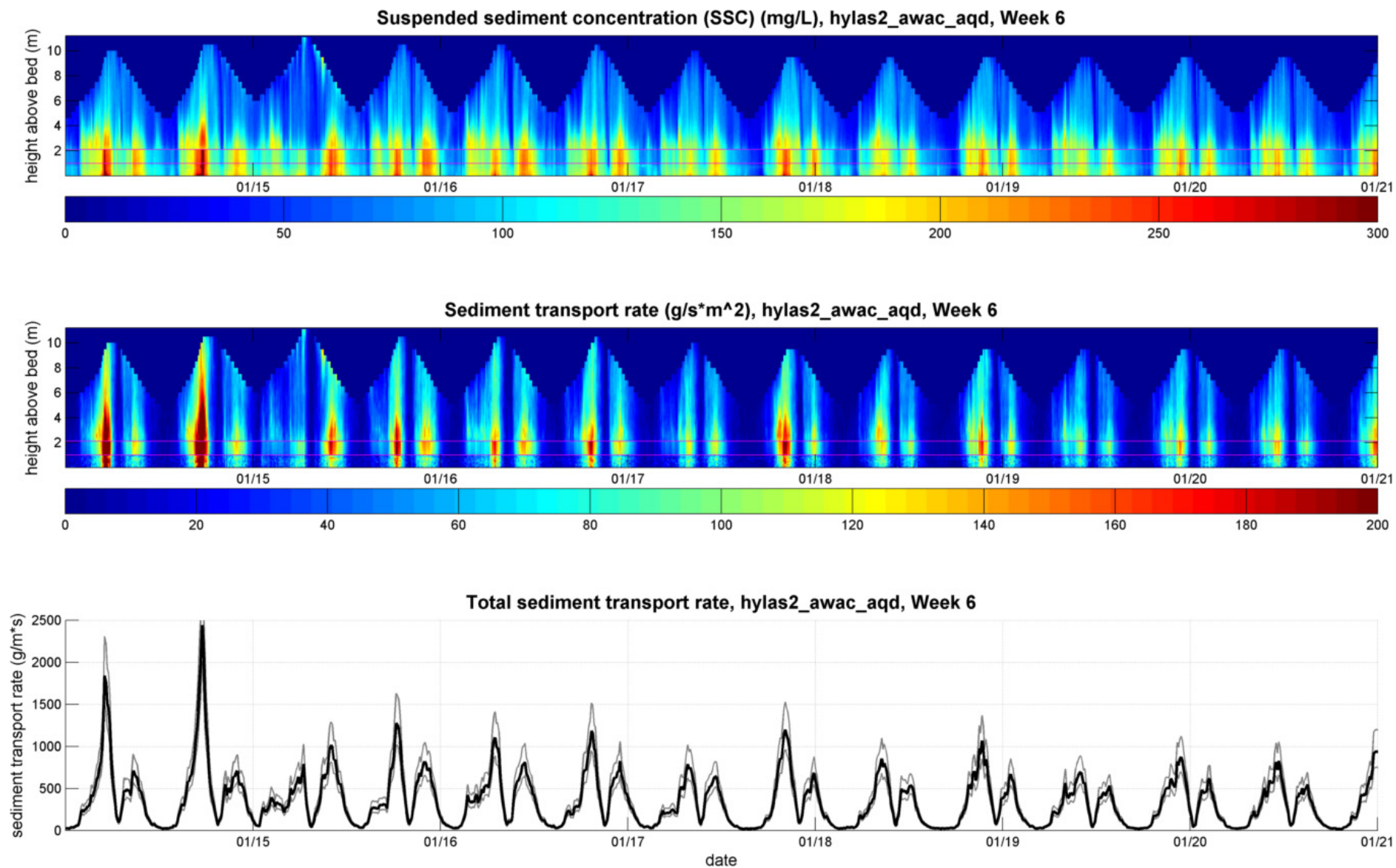


Figure 75. Suspended sediment concentration and sediment transport rate profiles and total sediment transport rate for HYLAS II frame, week 6





## 6 References

- Aardoom, J.H.** (2006). Quantification of sediment concentrations and fluxes from ADCP measurements, in: Evolutions in hydrography, 6th - 9th November 2006, Provincial House Antwerp, Belgium: Proceedings of the 15th International Congress of the International Federation of Hydrographic Societies. Special Publication (Hydrographic Society), 55: pp. 166-171.
- Gartner, J.W.; Cheng, R.T.; Wang, P.-F.; Richter, K.** (2001). Laboratory and field evaluations of the LISST-100 instrument for suspended particle size determinations. *Mar. Geol.* 175(1): 199–219. doi:10.1016/S0025-3227(01)00137-2
- Gartner, J.W.** (2005). Estimating suspended solids concentrations from backscatter intensity measured by acoustic Doppler current profiler in San Francisco Bay, California. *Marine Geology* 2011, 169-187.
- International Marine and Dredging Consultants (IMDC); Waterbouwkundig Laboratorium (WL)** (2007). Deelrapport 3: valsnelheid slib - INSSEV. Versie 2.0. Waterbouwkundig Laboratorium: Borgerhout. VI, 86 + 97 p. Appendices pp.
- Lohrmann, A.** (2001). Monitoring sediment concentration with acoustic backscattering instruments. Nortek AS Technical Note No. 003.
- Nortek (2001). Monitoring Sediment Concentration with acoustic backscattering instruments.
- Plancke, Y. and K. Paridaens** (2012). Comparison of measurement techniques for monitoring sediment transport, under field conditions, in the Scheldt estuary. Hydraulic Measurements and Experimental Methods 2012 Conference (HMEM 2012), Snowbird, Utah, August 12-15, 2012. pp. [1-8].
- Rouse, H.** (1937). Nomogram for the settling velocity of spheres. In: Division of Geology and Geography, Exhibit D of the Report of the Commission on Sedimentation, 1936-37, National Research Council, Washington, D.C., pp. 57-64.
- Thant, S.; Plancke, Y.** (2016). Sediment transport measurements in the Schelde-estuary: How do acoustic backscatter, optical transmission and direct sampling compare?, in: Erpicum, S. et al. (Ed.) Proceedings of the 4th IAHR Europe Congress, Liege, Belgium, 27-29 July 2016: Sustainable Hydraulics in the Era of Global Change. pp. 193-200.
- Vandebroek, E.; Plancke, Y.; Verwaest, T.; Mostaert, F.** (2017). Hydrodynamics and Sediment Dynamics in the Schelde Estuary: Factual data report for measurements at Drempe van Hansweert in May/June 2016. Version 4.0. WL Rapporten, 14\_024. Flanders Hydraulics Research & Antea Group: Antwerp, Belgium.
- Whipple, K.** (2004). 12.163/12.463 Surface Processes and Landscape Evolution, IV. Essentials of Sediment Transport, Course Notes, MIT Open Courseware. [https://ocw.mit.edu/courses/earth-atmospheric-and-planetary-sciences/12-163-surface-processes-and-landscape-evolution-fall-2004/lecture-notes/4\\_sediment\\_transport\\_edited.pdf](https://ocw.mit.edu/courses/earth-atmospheric-and-planetary-sciences/12-163-surface-processes-and-landscape-evolution-fall-2004/lecture-notes/4_sediment_transport_edited.pdf) Accessed: 26 January 2017.



# 7 Appendices

## 7.1 Appendix A – Aquadopp Profiler Technical Specifications

Technical Specifications

Water velocity measurement				
Acoustic frequency:	0.4MHz	0.6MHz	1.0MHz	2.0MHz
Maximum profiling range*:	80–90m	30–40m	12–20m	4–10m
Cell size:	2–8m	1–4m	0.3–4m	0.1–2m
Beam width:	3.7°	3.0°	3.4°	1.7°
Minimum blanking:	1m	0.50m	0.20m	0.05m
Number of beams:	3			
Maximum # cells:	128			
Velocity Range:	±10m/s (Inquire for extended range)			
Accuracy:	1% of measured value ±0.5cm/s			
Max. Sampling rate:	1Hz			
Velocity uncertainty:	Consult software program			
*) The Aquadopp profiler measures the current profile in a user specified number of cells from the instrument out to a maximum range that depends on the acoustic scattering conditions. The lower range should be expected with clear water and small cells and the higher range with large cells and acoustically turbid water.				
Cell zero (optional for 0.6MHz and 1MHz transducers)				
Cell zero acoustic frequency:	2Mhz			
Maximum profiling range*:	0.4–0.9m			
Number of beams:	3			
Echo intensity				
Sampling:	Same as velocity			
Resolution:	0.45dB			
Dynamic range:	90dB			
Standard sensors				
Temperature:	Thermistor embedded			
Range:	–4°C to 30°C			
Accuracy/resolution:	0.1°C/0.01°C			
Time response:	10 min			
Compass:	Magnetometer			
Accuracy/resolution:	2°/0.1° for tilt <20°			
Tilt:	Liquid level			
Accuracy/resolution:	0.2°/0.1°			
Maximum tilt:	30°			
Up or down:	Automatic detect			
Pressure:	Piezoresistive			
Range:	0–100m (standard)			
Accuracy/resolution:	0.5%/0.005% of full scale			
Analog inputs				
Number of channels:	2			
Voltage supply:	Three options selectable through firmware commands: •Battery voltage / 500 mA •+5V / 250 mA •+12V /100 mA			
Voltage input:	0–5V			
Resolution:	16 bit A/D			
Data communication				
I/O:	RS232, RS422. Software supports most commercially available USB–RS232 converters			
Communication Baud rate:	300–115200 (baud)			
Recorder download baud rate:	800/1200 k.Baud for both RS232 and RS422			
Data recording				
Capacity:	9 MB, can add 32/176/352/MB & 4GB Prolog			
Data record:	32 bytes + 8xNoells			
Mode:	Stop when full (default) or wrap mode			
Software:	AquaPro			
Operating system:	Windows®XP, Windows® 7			
Functions:	Deployment planning, data retrieval, ASCII conversion, online data collection, and graphical display			

Power			
DC Input:	9–15VDC		
Peak current:	3A		
Max average consumption at 1Hz:	0.2–1.5W		
Sleep consumption:	0.0003 mW (RS232), 0.005 mW (RS422)		
Transmit power:	0.3–20W, 3 adjustable levels		
Real time clock			
Accuracy:	+/- 1min/year		
Backup in absence of power:	4 weeks		
Internal batteries			
Type/capacity:	18 AA Alkaline cells/50Wh		
New battery voltage:	13.5VDC		
Duration (10-minute avg.):	80 days for 2MHz, 0.5m cells 50 days for 1MHz, 1.0m cells		
Exact battery consumption and velocity uncertainty are complex functions of the deployment configuration. Please consult the AquaPro software for more exact predictions.			
Materials			
Standard:	Delrin and polyurethane plastics with titanium screws		
Intermediate and deepwater models:	Titanium and Delrin plastics		
Connectors			
Bulkhead (Impulse):	MCBH-8-F5		
Cable:	PMCIL-8-MP on 10-m polyurethane cable		
Environmental			
Operating temperature:	–5°C to 35°C		
Storage temperature:	–20°C to 80°C		
Shock and vibration:	IEC 721–3–2		
Depth rating:	300m		
Dimensions			
	0.4MHz	0.6MHz	1MHz/2MHz
Weight in air:	3.4 kg	2.9 kg	2.2 kg
Weight in water:	0.2 kg	0.4 kg	0.2 kg
Length:	see dimensional drawings		
Diameter:	see dimensional drawings		
Options			
Batteries:	Lithium, Li-Io rechargeable		
External batteries:	Alkaline, Lithium or Lithium Ion. See battery brochure for details		
Transducer head:	Right angle head for 1 or 2MHz. Inquire for special configurations		
Deep water systems:	Inquire for 3000m & 6000m versions		
Communication:	Request special harness for RS422		





<b>NortekMed S.A.S.</b> Z.I. Toulon Est BP 520 83 078 TOULON cedex 09 FRANCE Tel: +33 (0) 4 94 31 70 30 Fax: +33 (0) 4 94 31 25 49 E-mail: info@nortekmed.com	<b>NortekUK</b> Mildmay House, High St. Hartley Wintney Hants. RG27 8NY Tel: +44- 1428 751 953 E-mail: inquiry@nortekuk.co.uk	<b>NortekUSA</b> 222 Severn Avenue Building 14, Suite 102 Annapolis, MD 21403 Tel: +1 (410) 295-3733 Fax: +1 (410) 295-2918 E-mail: inquiry@nortekusa.com	<b>青岛诺特克海洋仪器有限公司</b> 地址: 中国青岛香港中路66号 邮编: 266011 Tel: 0532-85017570, 85017270 Fax: 0532-85017570 E-mail: inquiry@nortek.com.cn
<b>Nortek B.V.</b> Schipholweg 333a 1171 PL Badhoevedorp Nederland Tel: +31 20 6543600 Fax: +31 20 6599830 email: info@nortek-bv.nl			

## 7.2 Appendix B – AWAC Technical Specifications

### Technical Specifications

<b>System</b>		
Acoustic frequency:	1MHz, 600kHz or 400kHz	
Acoustic beams:	4 beams, one vertical, three slanted at 25°	
Vertical beam opening angle:	1.7°	
Operational modes:	Stand-alone or online monitoring	
<b>Current Profile</b>		
Maximum range:	30m (1MHz), 50m (600 kHz), 100m (400kHz) (depends on local conditions)	
Depth cell size:	0.25 – 4.0m (1MHz) 0.5 – 8.0m (600kHz) 1.0 – 8.0m (400kHz)	
Number of cells:	Typical 20–40, max. 128	
Maximum output rate:	1Hz	
<b>Velocity measurements</b>		
Velocity range:	±10 m/s horizontal, ±5 m/s along beam	
Accuracy:	1% of measured value ±0.5 cm/s	
<b>Doppler uncertainty</b>		
Current profile:	1cm/s (typical)	
<b>Wave measurements</b>		
Maximum depth:	35m (1MHz), 60m (600 kHz), 100m (400kHz)	
Data types:	Pressure, one velocity along each beam, AST*	
Sampling rate (output):	2 Hz velocity, 4 Hz AST* (1MHz), 1 Hz velocity, 2Hz AST* (600kHz), 0.75 Hz velocity, 1.5Hz AST* (400kHz)	
No. of samples per burst:	512, 1024, or 2048. Inquire for options	
<b>Wave estimates</b>		
Range:	-15 to +15m	
Accuracy/resolution (Hz):	<1% of measured value/1cm	
Accuracy/resolution (Dir):	2° / 0.1°	
Period range:	0.5-100s (1MHz), 1 - 100s (0.6MHz), 1.5 - 100s (0.4MHz)	

Depth(m)	cut-off period (Hz)	cut-off period (dir)
5	0.5 sec	1.5 sec
20	0.9 sec	3.1 sec
60	1.5 sec	4.2 sec
100	2 sec	5.0 sec

<b>Sensors</b>	
Temperature:	Thermistor embedded in housing
Range:	-4°C to 40°C
Accuracy/ Resolution:	0.1°C/0.01°C
Time constant:	<5 min
<b>Compass</b>	
Accuracy/Resolution:	2°/0.1° for tilt <15°
Tilt:	Liquid level
Maximum tilt:	30°, AST* requires <10° instrument tilt
Up or down:	Automatic detect
<b>Pressure:</b>	
Standard range:	0-50 m (1MHz) / 0-100m (0.6MHz) / 0-100m (0.4MHz)
Accuracy:	0.5% of full scale. Optional 0.1% of full scale.
Resolution:	0.005% of full scale
<b>Transducer configurations</b>	
Standard:	3 beams 120° apart, one vertical
Platform mount:	3 beams 90° apart, one at 5°
<b>Materials</b>	
Standard:	Delrin and polyurethane plastics with titanium screws

<b>Connectors:</b>	
Bulkhead (Impulse):	MCBH-2-FS
Cable:	PMCIL-8-MP
<b>Environmental</b>	
Operating temperature:	-4°C to 40°C
Storage temperature:	-20°C to 60°C
Shock and vibration:	IEC 721-3-2
Depth rating:	300m
<b>Dimensions:</b>	
	See drawing on front page
Weight in air:	7.3 kg (0.4MHz), 6.2 kg (0.6MHz), 6.1 kg (1MHz)
Weight in water:	3.6 kg (0.4MHz), 2.9 kg (0.6MHz & 1MHz)
<b>Analog Inputs</b>	
Number of channels:	2
Supply voltage to analog output devices:	Three options selectable through firmware commands: • Battery voltage/500mA • +5V/250mA • +12V/100mA
Voltage Input:	0-5V
Resolution:	16 bit A/D
<b>Data Recording</b>	
Capacity(standard):	2 MB, can add: 32/178/352MB or 4GB
Profile record:	Ncells×9 + 120
Wave record:	Nsamples×24 + 1KB
<b>Data Communication</b>	
I/O:	RS 232 or RS 422
Communication baud rate:	300-115200
Recorder download baud rate:	600/1200 kBaud for both RS232 and RS422
User control:	Handled via «AWAC» software, or Activex® controls. «SeaState» for online systems.
ProLog:	Provides NMEA ASCII or Binary output formats for processed wave and current data.
<b>Power</b>	
DC Input:	9-18 VDC
Peak current:	3A
Power consumption:	Transmit power: 1-30W, 3 adjustable levels
Sleep consumption:	0.3 mW (RS232) 5 mW (RS422)
<b>Real time clock</b>	
Accuracy:	± 1min/year
Backup in absence of power:	1 year
<b>Offshore Cable</b>	
The Nortek offshore cable can, when properly deployed, withstand tough conditions in the coastal zone. In RS 422 configuration, cable communication can achieved distances up to 5 km.	
<b>Online Projects</b>	
Nortek can provide long cables, radio/telephone communication equipment, acoustic modems, etc., that can meet the requirements of your specific project.	

\*) AST = Acoustic Surface Tracking





**TRUE INNOVATION MAKES A DIFFERENCE**

<p><b>NortekMed S.A.S.</b> Z.I. Toulon Est BP 520 83 078 TOULON cedex 09 FRANCE Tel: +33 (0) 4 94 31 70 30 Fax: +33 (0) 4 94 31 25 49 E-mail: info@nortekmed.com</p>	<p><b>NortekUK</b> Tresanton House Bramshott Court Bramshott Hants GU30 7RG Tel: +44-1428 751 953 E-mail: inquiry@nortekuk.co.uk</p>	<p><b>NortekUSA</b> 222 Severn Avenue Building 14, Suite 102 Annapolis, MD 21403 Tel: +1 (410) 295-3733 Fax: +1 (410) 295-2918 E-mail: inquiry@nortekusa.com</p>	<p><b>青島諾特海洋測量設備有限公司</b> 地址：中國青島市香港路45號 江蘇分廠1302 郵政：266071 Tel: 0532-85017570, 85017270 Fax: 0532-85017570 E-mail: inquiry@nortek.com.cn</p>	<p><b>Nortek B.V.</b> Schipholweg 333a 1171PL Badhoevedorp Nederland Tel: +31 20 6543600 Fax: +31 20 6599830 email: info@nortek-bv.nl</p>
--	--	--	--	---

## 7.3 Appendix C – OBS 3+ Technical Specifications

Section 5. Specifications

### Section 5. Specifications

**Features:**

- Measures suspended solids and turbidity for up to 4000 NTUs
- Provides a compact, low-power probe that is field proven
- Compatible with all Campbell Scientific dataloggers (including the CR200(X) series)
- Stainless-steel body allows use down to 500 m in fresh water
- Titanium body allows use down to 1500 m in fresh or salt water
- Fitted with MCBH-5-FS, wet-pluggable connector—multiple mating cable length options available
- Accurate and rugged

**Compatibility**

**Dataloggers:**

CR200(X) series  
 CR800 series  
 CR1000  
 CR3000  
 CR5000  
 CR9000(X)  
 CR7X  
 CR510  
 CR10(X)  
 CR23X  
 21X

**Operating Temperature:** 0° to 40°C

**Ranges**

Turbidity (low/high): 250/1,000 NTU; 500/2,000 NTU; 1,000/4,000 NTU  
 Mud<sup>1</sup>: 5,000 to 10,000 mg l<sup>-1</sup>  
 Sand<sup>1</sup>: 50,000 to 100,000 mg l<sup>-1</sup>  
<sup>1</sup> Range depends on sediment size, particle shape, and reflectivity.

**Accuracy**

Turbidity<sup>2</sup>: 2% of reading or 0.5 NTU  
 Mud<sup>2</sup>: 2% of reading or 1 mg l<sup>-1</sup>  
 Sand<sup>2</sup>: 4% of reading or 10 mg l<sup>-1</sup>  
<sup>2</sup> Whichever is larger.

**Height**

OBS-3+: 14.1 cm (5.56 in)  
 OBS300: 13.1 cm (5.15 in)

**Diameter:**

2.5 cm (0.98 in)

5-1

**Weight:** 181.4 grams (0.4 lb)

**Power**  
 Voltage output: 5 to 15 Vdc/15 mA (Volts outputs)  
 4-20 mA transmitter: 9 to 15 Vdc/45 mA max. (4-20 mA output)

**Operating wave length:** 850 ± 5 nm

**Optical power:** 2000 µW

**Drift:** <2% per year

**Daylight rejection:** -28 dB (re -48 mW cm<sup>-2</sup>)

**Maximum data rate:** 10 Hz

**Maximum depth**  
 Stainless-steel body: 500 m (1640.5 ft)  
 Titanium body: 1500 m (4921.5 ft)

5-2

## 7.4 Appendix D – LISST-100X Technical Specifications

### Parameters Measured

- Particle size distribution
- Particle volume concentration
- Volume scattering function
- Optical transmission
- Depth
- Temperature

### Sediment size distribution and scattering angles

- 32 log-spaced size classes
- 1.25 – 250 or 2.5 – 500  $\mu\text{m}$  size range (equivalent to scattering at 0.08-15° or 0.04-7.5° in water, respectively)

### Sediment concentration

- Range: 1 – 800  $\text{mg l}^{-1}$  for standard 50 mm optical path (actual range depends on grain size )
- Resolution: < 1  $\text{mg l}^{-1}$

Material	SSC [mg/l] @ 98% optical transmission	SSC [mg/l] @ 30% optical transmission	D10[ $\mu\text{m}$ ]	D50[ $\mu\text{m}$ ]	D90[ $\mu\text{m}$ ]	SMD[ $\mu\text{m}$ ]
ISO Fine (ISO 12103-1,A2)	1	70	1.5	7	41	3
ISO Coarse (ISO 12103-1,A4)	5	150	4	38	99	10
Whitehouse 20-30 $\mu\text{m}$ glass beads	8	445	19	24	34	24
Sieved sand 75-125 $\mu\text{m}$	13	810	85	122	175	112

- With a 50% PRM in place, all SSC values in the table above should be multiplied by 2.
- With an 80% PRM in place, all SSC values in the table above should be multiplied by 5.
- With a 90% PRM in place, all SSC values in the table above should be multiplied by 10.

### Technology

- Solid state diode laser @ 670 nm, 1mW
- 32-ring custom photodiode detector
- Sample rate programmable, up to 25 Hz internally, 1Hz saving to data logger
- Optical path length @ 50 mm standard; bolt-on path reduction modules are available for higher concentration environments.

### Mechanical and electrical

- Dimensions: 13.3 cm diameter x 87 cm long (5.25' x 34.25')
- Weight: 11 kg (25 lbs) in air; 3.6 kg (8 lbs) in water
- 300 m depth rating
- Serial interface: RS232C @ 9600 baud; high-speed offload at 115K baud
- Alkaline battery pack: Custom 9V nominal, 42 Ah
- External power input (optional): 12VDC nominal, 10-24VDC
- CF memory card: 128Mb standard (1,600,000 size distributions)
- Battery current drain: 146mA/8mA/128 $\mu\text{A}$  (measuring/quiescent/sleeping)

## 7.5 Appendix E – YSI Technical Specifications

### Environmental

Operating Temperature	-40 to 60°C (-40 to 140 °F)
Enclosure	33 x 38 x 15.2 cm (13 x 15 x 6 in), fiberglass
Enclosure Rating	NEMA 4X
Pollution Degree	II (per UL3101)
Installation Category	III (per EN61010-1)

### Data Acquisition

6200 DCP (standard)	64 KB RAM, 56 KB required for run-time memory 8 KB (logging memory)
---------------------	--

Memory Options	256 KB, 200 KB (logging memory) 1 MB, 968 KB (logging memory)
----------------	--

### User-Interface

Software	YSI EcoWatch DCP™ featuring autoconfigurable sensors, real-time data displays, powerful reporting and plotting options Compatibility: Windows® 3.1, 95, 98 and NT.
Computer Hardware	Minimum: PC 386 (4 MB RAM, 4 MB hard disk space) Recommended: PC 486DX or higher, (8 MB RAM, 4 MB hard disk space)

### Power Information

Battery Type	Lead-acid, gel type, sealed (Power Sonic PS-12120 L)
Battery Rating	12 VDC, 5 A max current, 12 Ah capacity
Battery Fuse Type/Rating	Type 3AG (fast blow), 5 amps, 32 volts
I/O Interface Fuse Type/Rating	Type 3AG (slow blow), 5 amps, 32 volts

#### *When applicable...*

Line Power (nominal)	100/120//220/230-240 V~, 50/60 Hz, 0.8A//0.4A
Maximum Current	1.0 A @ 120 V~, 0.5 A @ 240 V~
AC Fuse Type/Rating for 100/120 V~ operation:	Type 3AG (slow blow), 1.0 A @ 120 V
AC Fuse Type/Rating for 220/240 V~ operation:	5 x 20mm IEC127 (time delay), 0.5 A(T), 250 V
	Fuses may be purchased from any YSI Factory Service Center.
Solar Panel	10 watt, 20 VDC (no load), 0.6 A max current
Electrical Safety	CE (pending)

### Communication Options

Direct cable	3 m (10 ft) RS-232 cable
Radio	2 watt, 2-way (no license required), 467.8 MHz
Telephone modem	Hayes-compatible
Cellular modem	Wireless phone modem, uses PSTN through cellular network

### Connectors/Access

Power (AC or solar)	1/2" non-metallic, water tight conduit or feed through gland AC, 3-prong male; Solar, 2-wire interface cable
Phone or direct	1/2" non-metallic, water tight conduit or feed through gland Phone, standard 3-wire cable; Direct RS-232, DB-9 male
RF (radio or cellular)	N-type
Sonde	MS-8 pin with tethered cap
Meteorological Suite	MS-17 pin with tethered cap
Rain Gauge	MS-4 pin with tethered cap
Solar Radiation Sensor	MS-5 pin with tethered cap
Ground	Standard Ground Lug

### Sensor Compatibility

Sonde Compatibility	YSI 600, 600R, 600XL, 600XLM, 6820, 6920.
Met Suite (WS, WD, RH, AT)	YSI MAZ6213, w/ 4.6 m (15 ft) cable
Met Suite (WS, WD, RH, AT)	YSI MAZ6219, w/ 13.7 m (45 ft) cable
Pyranometer (solar radiation)	YSI MAZ6214, w/ 3 m (10 ft) cable, leveling base
Pyranometer (solar radiation)	YSI MAZ6212, w/ 3 m (10 ft) cable, leveling base, CE approved
Rain Gauge (tipping bucket)	ISCO 674, w/ 4.6 m (15 ft) cable
Rain Gauge, with heater	YSI MAZ6216, w/ 4.6 m (15 ft) cable (also requires AC power)
Barometer	YSI MAZ6217, (located inside NEMA enclosure)

DEPARTMENT **MOBILITY & PUBLIC WORKS**  
Flanders hydraulics Research

Berchemlei 115, 2140 Antwerp

**T** +32 (0)3 224 60 35

**F** +32 (0)3 224 60 36

[waterbouwkundiglabo@vlaanderen.be](mailto:waterbouwkundiglabo@vlaanderen.be)

[www.flandershydraulicsresearch.be](http://www.flandershydraulicsresearch.be)